Numerical Simulation of Water-Alternating-Gas (WAG) Injection – Best Practices

Hassan Ali Alzayer

Submitted for the degree of Doctor of Philosophy

Heriot-Watt University

EGIS-IPE

APRIL 2019

ABSTRACT

To reliably predict the water-alternating-gas (WAG) injection performance, a transformational shift in the modelling of the WAG process is needed. Therefore, this thesis focused on identifying the shortcomings of the current reservoir simulators and suggesting a new methodology to improve the simulation prediction of WAG injection performance. To achieve this, several core-scale WAG injection experiments were analysed to identify trends and behaviours. Furthermore, these experiments were simulated using ECLIPSE-100 to identify the limitations of the current commercial simulators. Based on these exercises, a new methodology to improve the modelling process of WAG injection cycles using the current simulation capabilities were suggested.

The results of five unsteady-state water-alternating-gas injection experiments performed by various researchers, from Heriot-Watt University, at different conditions were used in this simulation study. These WAG injection core-flood experiments were analysed and simulated using the new approach. The simulation of the five different WAG injection experiments confirmed the positive impact of updating the WAG-hysteresis parameters in the later WAG injection cycles. This change significantly improved the match between simulation and WAG experimental results.

Therefore, a systematic workflow to acquire the relevant data and analyse them to generate the input parameters required for WAG injection simulation has been suggested. In addition, a logical procedure was suggested to update the simulation model after the third injection cycle as a workaround to overcome the limitation in the current commercial simulators. This guideline can be incorporated in the numerical simulators to help the industry in improving the accuracy of WAG injection simulation using the current simulation capabilities.

DEDICATION

I dedicate this thesis to my parents whom without their prayers and guidance I wouldn't achieve what I have achieved in my life.

أهدي هذا البحث إلى **أمي و أبي**

فهذا أقل ما يمكن أن أضعه بين يديكم

فبدعائكم وتوجيهاتكم أنرتم لي طريق النجاح

أسأل الله أن يديمكم وأن يرزقني البرّ بكم

Acknowledgement

First, I would like to thank Saudi Aramco for sponsoring my study and supporting me and my family in all aspects during this journey. Also, I would like to thank my family especially my parents for supporting me throughout the writing of this thesis and life in general. I have been blessed with their love and patience which motivated me every day.

Second, I would like to thank my academic supervisor Prof Mehran Sohrabi for his support and guidance throughout my PhD. Also, I would like to express my gratefulness to Dr Amir Jahanbakhsh who mentored me during my first year and helped me a lot to shape the direction of this research. Throughout my PhD program, I have received tremendous support from many PhD students, too many to list, and I would like to thank them all as well and wish them all the best. Finally, special thanks to Schlumberger and Weatherford Petroleum Consultants for donating their software Eclipse and Sendra, respectively to Heriot-Watt University which I used extensively to do my research.

DECLARATION STATEMENT

(Research Thesis Submission Form should be placed here)

Nomenclature:

ΔP	:	The change in pressure
ΔS	:	The change in saturation
ΔSo	:	The change in oil saturation
°C	:	Degrees Celsius
°F	:	Degrees Fahrenheit
1-D	:	One dimension
2-D	:	Two dimensions
a	:	The residual oil modification factor
α	:	Gas secondary drainage reduction exponent
a’	:	The residual oil modification factor for the first run
a’’	:	The residual oil modification factor for the second run
b	:	An exponent introduced by Jerald to adjust gas-trapping
β	:	The combined saturation term in STONEI equation
bbl	:	Oil barrel – an oil volume unit
C	:	Land’s gas-trapping constant
C’	:	Land’s gas-trapping constant for the first run
C’’	:	Land’s gas-trapping constant for the second run
C1	:	Methane
$CaCl_2$	:	Calcium chloride
CO_2	:	Carbon dioxide
cp	:	Centipoise – a unit for viscosity
DP	:	Pressure drop usually across a rock core sample
DPg^{2ph}	:	Pressure drop during two-phase gas injection
DPg^{3ph}	:	Pressure drop during three-phase gas injection
DPw^{2ph}	:	Pressure drop during two-phase water injection
DPw^{3ph}	:	Pressure drop during three-phase water injection
DX	:	Grid dimension in the x-direction
DY	:	Grid dimension in the y-direction
DZ	:	Grid dimension in the z-direction
EOR	:	Enhanced Oil Recovery
FOPT	:	Field Oil Production Total
FWL	:	Free-water-level
GAW	:	Gas-alternating-water injection
GOR	:	Gas-oil-ration

η	:	STONEI Exponent
HWU	:	Heriot-Watt University
IFT	:	Interfacial tension
IHRRS	:	Total's In-House Research Reservoir Simulator
iWAG	:	Immiscible water-alternating-gas injection
kr	:	Relative permeability
krg (Sg^{start})	:	Gas relative permeability at the gas saturation start
krg^{input}	:	The input gas relative permeability
krg^{input} (Sg^{start})	:	The input gas relative permeability at the gas saturation start
krgo	:	Gas relative permeability to oil
$krgo^{input}$	:	The input gas relative permeability to oil
krg^{sd}	:	The secondary drainage gas relative permeability
kro'	:	The end-point oil relative permeability
kro^{3ph}	:	Three-phase oil relative permeability
krog	:	Oil relative permeability to gas
krow	:	Oil relative permeability to oil
krw	:	Water relative permeability
krw'	:	The end-point of the water relative permeability
krw^{2ph}	:	Two-phase water relative permeability
krw^{3ph}	:	Three-phase water relative permeability
krw^{imb}	:	Imbibition water relative permeability
kv/kh	:	Vertical to horizontal permeability ratio
mD	:	Milli-Darcy – a unit to measure rock permeability
μg	:	Gas viscosity
MMP	:	Minimum Miscibility Pressure
MMstb	:	Million stock tank barrels
μo	:	Oil viscosity
μw	:	Water viscosity
mWAG	:	Miscible water-alternating-gas injection
N2	:	Nitrogen
NaCl	:	Sodium Chloride
nC4	:	Normal butane
NCFE	:	Numerical Core Flood Experiment
nmWAG	:	Near miscible water-alternating-gas injection

OOIP	:	Original Oil In Place
OWC	:	Oil-Water-Contact
Pc	:	Capillary Pressure
Pcwo	:	Water/oil capillary pressure
psi	:	Per square inch – a unit to measure pressure
PV	:	Pore-Volume
PVinj	:	Pore-Volume Injected
PVprod	:	Pore-Volume Produced
ρg	:	Gas density
ρo	:	Oil density
ρw	:	Water density
scf	:	Standard cubic foot – a unit to measure gas volume
Sg	:	Gas saturation
Sgc	:	Critical gas saturation
Sgi	:	Initial gas saturation
Sg^{max}	:	Maximum gas saturation
Sg^{start}	:	Gas saturation at the start of a cycle
Sgt	:	Trapped-gas saturation
Sn	:	An n-phase saturation
Sn^{i}	:	Initial n-phase saturation
Sor	:	Residual oil saturation
SOR^{3ph}	:	Three-phase residual oil saturation
Sorg	:	Residual oil saturation to gas
Sori	:	Initial residual oil saturation
Sorm	:	Minimum residual oil saturation
Sorw	:	Residual oil saturation to water
SS	:	Steady State
Sw	:	Water saturation
SWAG	:	Simultaneous-Water-And-Gas injection
Swc	:	Connate water saturation
Swi	:	Initial water saturation
SWI	:	Saturation Weighted Interpolation
USS	:	Unsteady State
WAG	:	Water-Alternating-Gas Injection
WAG-HYST	:	Hysteresis in water-alternating-gas injection

TABLE OF CONTENTS

LISTS OF TABLES AND FIGURES

List of Figures:

List of Tables:

LIST OF PUBLICATIONS

1. Alzayer, H. A., Jahanbakhsh, A., & Sohrabi, M. (2017, April). New Methodology for Numerical Simulation of Water-Alternating-Gas (WAG) Injection. In *IOR 2017-19th European Symposium on Improved Oil Recovery*.

2. Alzayer, H., Jahanbakhsh, A., & Sohrabi, M. (2017, May). The Role of Capillary-Pressure in Improving the Numerical Simulation of Multi-Phase Flow in Porous Media. In *SPE Reservoir Characterisation and Simulation Conference and Exhibition*. Society of Petroleum Engineers.

3. Alzayer, H., & Sohrabi, M. (2018, August). A New Approach to Simulate Near-Miscible Water-Alternating-Gas Injection for Mixed-Wet Reservoirs. In *SPE Kingdom of Saudi Arabia Annual Technical Symposium and Exhibition*. Society of Petroleum Engineers.

4. Alzayer, H., & Sohrabi, M. (2018, March). Water-Alternating-Gas Injection Simulation-Best Practices. In *SPE EOR Conference at Oil and Gas West Asia*. Society of Petroleum Engineers.

Chapter 1—Introduction to WAG Injection

1.1 Background

Hydrocarbons will continue to be the primary source of energy for countries with rising economies for at least the next 20 years; thus, the need for petroleum products will be maintained [1]. A considerable volume of oil (about 65 per cent of Original Oil in Place on average) is actually left unrecovered, whilst the industry is in demand of it. In fact, a 10 per cent increase in the current average oil recovery of 35 per cent would supply the globe with enough fuel for another 30 years [2]. Tremendous efforts and huge investments have been dedicated to improving and enhancing oil recovery in the past. However, there is now a range of technologies to target the remaining and residual oil in these only partially depleted oil reservoirs.

In the past two decades, the focus on enhancing oil recovery from existing oil reservoirs has been increasing. One of the key indicators of the industry's interest is the amount of published literature on certain technical subjects. For instance, onepetro.org contains hundreds of thousands of technical papers on various subjects related to the oil and gas industry. Figure 1-1 shows the number of technical papers published on onepetro.org about enhanced oil recovery (EOR) and water-alternating-gas (WAG) injections until December 2018:

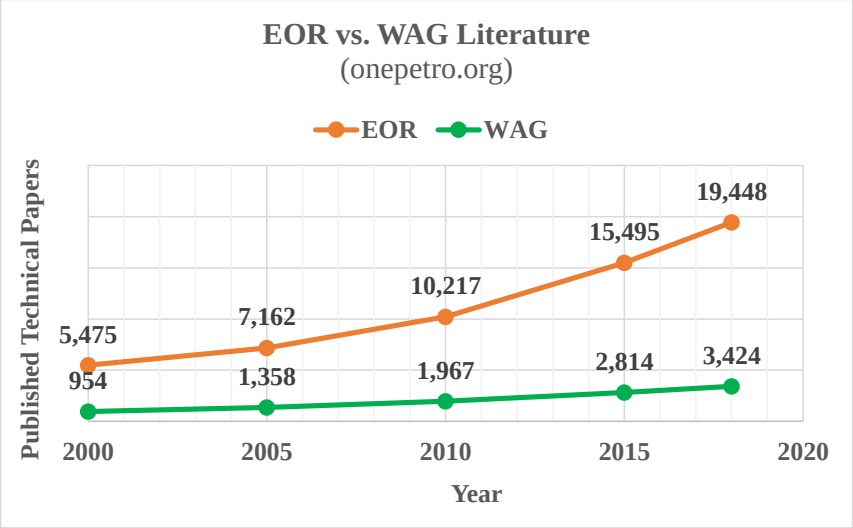

Figure 1-1: The number of technical papers published about enhanced oil recovery (EOR) and water-alternating-gas (WAG) injections until December 2018 (onepetro.org)

The total number of published technical papers about EOR by 2000 was 5,475, whilst the total number about WAG was less than 1,000. However, the number of publications on

these two subjects had increased more than 2.5 times by 2018, an indication that the EOR techniques are gaining more attention and will grow faster in the near future.

Even though interest in EOR technologies is rising, the simulation of EOR methods is still lagging behind. Water-alternating gas as an EOR method comprises about 18 per cent of the published literature on EOR, yet only about 3 per cent of these papers on WAG injections discuss the simulation of this method. However, the focus on simulation has been increasing lately, as shown in Figure 1-2:

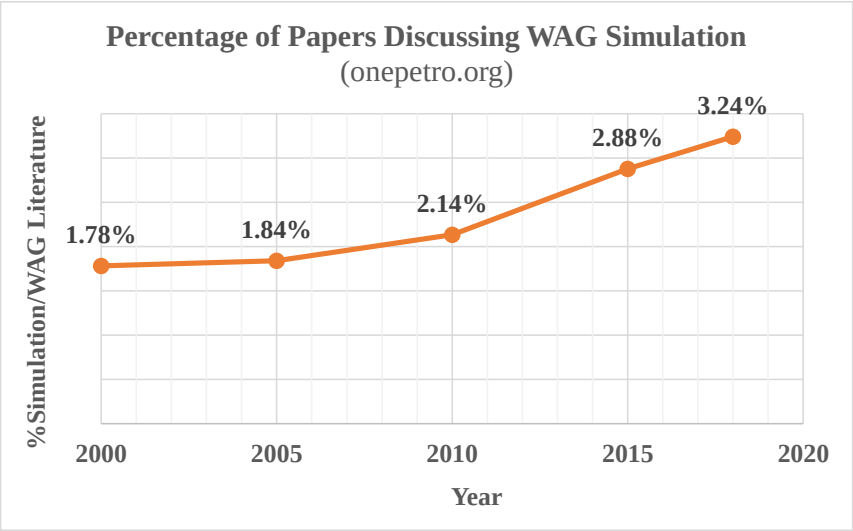

Figure 1-2: Percentage of publications that discuss WAG simulation compared to the total number of published papers on WAG injection (onepetro.org)

The percentage of published papers on WAG injection simulation has increased from 1.78 per cent in 2000 to more than 3 per cent in 2018 (Figure 1-2), a trend that is expected to increase as more WAG injection projects are tested in the industry. Numerical simulation of such a complex process is essential to reduce uncertainty and improve the outcome of any WAG injection project.

1.2 Water-Alternating-Gas Injection

Water-alternating-gas is the process of injecting water cycles in between gas cycles to control the mobility of the gas. This injection method is mostly applied in oil reservoirs after an extended period of water injection. Although there are several conventions, in this thesis, WAG usually refers to water-alternating-gas starting with a water injection cycle (when starting with gas injection, those injections are referred to in this thesis as GAW).

Water-alternating-gas injection is reported to add up to 20 per cent of oil recovery in some cases [3], depending on whether the WAG process is miscible (mWAG), near miscible

(nmWAG), or immiscible (iWAG). To clarify, the miscibility is the ability of two fluids to form a single phase when contacted. The near miscible process is when two fluids can form a single phase after multiple contacts as described later. The immiscible process, however, is when two fluids cannot form a single fluid regardless of being in contact. To achieve miscibility between the reservoir oil and the injected gas, the reservoir pressure must be greater than the minimum miscibility pressure (MMP). If the reservoir pressure is less than the MMP, the injected gas and reservoir oil will have higher interfacial tension, and no miscibility would be achieved [3]. One important mechanism attained by WAG is that the injected gas can access new pores and displace more oil, whilst the injected water can improve sweep efficiency. However, immiscible WAG injection is usually less effective in terms of additional oil recovery than the miscible process [4].

Research efforts have been ongoing in the past decades to understand the oil recovery process through WAG injection using micromodels, core-flood experiments, and numerical simulation [5-10]. Micromodels are physical models made by engraving discrete pore networks on transparent glass plates to visualize the oil recovery process. Core-flood experiments are usually made in laboratories using either reservoir rock samples or similar outcrop rock to understand the fluid/rock interactions. The observed behaviours from micromodels and core-flood experiments can be modelled using numerical simulation to further understand and analyse the collected information.

The current knowledge about the WAG recovery process resulting from such research has advanced the related technologies in today's practises. Several three-phase relative permeability models, to empirically estimate the three-phase oil relative permeability, have been developed since the 1960s. However, the complete physics to understand this concept and the hysteresis in relative permeability and capillary pressure are still lacking to reliably predict WAG injection performance. The term hysteresis is used to describe the irreversibility of a physical process and its dependence on saturation path and history; for example, the water relative permeability during imbibition process (water saturation is increasing) is different than the water drainage relative permeability (water saturation is decreasing). The details from published research in this area are reviewed in the next chapter.

There are several ways to refer to each cycle in the WAG injection. In this thesis, a different convention is used for each injection cycle. W is used to indicate water injection

cycles and G for gas injection cycles. Each cycle is then numbered, regardless of the phase type, starting from 1; for example, in the WAG injection process, the first cycle is referred to as W1 and then the gas injection cycle after that as G2 because it is a gas phase but a second cycle to be injected. In GAW injection, the first injection cycle is referred to as G1, followed by W2, and so forth. The reason for this is to avoid having the same references for different processes.

1.2.1 Immiscible WAG Injection

If the reservoir pressure is less than the MMP, the injected gas and reservoir oil will have higher interfacial tension, and no miscibility would be achieved [3].

If the injected gas cannot develop miscibility with the oil phase, then the WAG process is considered immiscible (iWAG). The main objective of the gas injection cycle is to improve displacement efficiency at the pore scale. However, if the gas is immiscible, then the oil displacement at the pore level would be lower in the case of iWAG if compared to mWAG [11].

Based on the micromodels visualisation of iWAG, the first gas injection cycle (G1) will establish a single path through the porous media, and as more gas is injected, it will follow the same path with no more oil recovery. Then, as the three-phase water is injected into the system (W2), it will fragment the oil and gas to reshuffle the saturations inside. As a result, the second gas injection cycle (G3) establishes a new path which would recover more oil [11-15].

Regardless of the gas/oil miscibility, the three-phase water relative permeability (krw^{3ph}) would be lower than the two-phase relative permeability due to the presence of free gas saturation. As the water enters a system with free gas saturation, it would tend to redistribute the gas saturation and trap some of the gas [11].

1.2.2 Miscible WAG Injection

For oil reservoirs, there are two common miscibility conditions: first and multi-contact miscibility. Hydrocarbon gases such as propane and butane, in addition to some liquid hydrocarbons like gasoline, are considered first contact solvent. Those are very expensive solvents for continuous injections in the reservoir and could be used as additives to enhance other low-cost multi-contact miscible solvents. The most commonly used multi-contact miscible solvents in EOR are methane, carbon dioxide (CO_2), and nitrogen (N2).

When lean gas or compressed CO_2 is injected into the reservoir, it starts to vaporise components from the reservoir oil, which will enrich the solvent until it becomes miscible. Then heavier components from the reservoir oil will start condensing into the solvent stream, which is called condensing-gas drive. Miscibility of such solvents is greatly dependent on the reservoir pressure, temperature, and fluid composition. Reservoir pressure must be greater than the MMP to achieve miscibility [16].

For first contact miscible solvents, the MMP can simply be determined by increasing the pressure inside a cell that contains the two fluids until the interface between the two fluids disappears. For multi-contact miscible solvents, the most common way to measure MMP is the slim-tube displacement apparatus [16]. The slim-tube apparatus, as the name indicates, is a device with a long thin-tube filled with glass beads or pre-designed special sand to measure miscibility between two fluids in porous media.

Miscible displacement is a complex process to be modelled as it combines the complexity of three-phase relative permeability, hysteresis, and fluid composition. There are several important changes that may occur as the system reaches miscibility [11]:

1. The displacement path
2. The three-phase wetting order
3. Near-miscible relative permeability

1.2.3 Near-Miscible WAG Injection

For the near-miscible gas injection (nmWAG), the first gas cycle (G1) would establish a single path through the porous media. As the first gas injection cycle is continuous, the single gas path would expand as more mass transfer happens between the oil and the injected gas, resulting in additional oil recovery (lower Sor). Then, as the water is injected into the system (W2), it will reshuffle the saturations inside. The second gas drainage (G3) in the near-miscible WAG would follow the same initial path, unlike the immiscible gas injection. However, in this case, the gas phase will start swelling and displacing more and more oil within the three-phase zone [11-15, 17].

Cyclic hysteresis, sometimes known as three-phase hysteresis or WAG hysteresis, is a phenomenon occurring in many recovery processes, including the WAG injection. Hysteresis means that a phase's relative permeability is dependent on the saturation path

and saturation history. Recently, researchers highlighted the important role of cyclic-hysteresis in the oil recovery by WAG injection [18-23]

1.3 Scope of Work

The focus of this thesis is on the cyclic-hysteresis role in the additional oil recovery from WAG injection. Therefore, the miscibility component of the additional oil recovery is not discussed in detail or included in the simulation models. The core-flood experiments presented and utilised in this thesis were designed to account for the effect of hysteresis at near-miscible conditions (not fully developed miscibility) and exclude any mass transfer between fluids during the experiment. To eliminate the mass transfer during any core-flood experiments, fluids (gas, oil, and water) were pre-equilibrated by conducting two-phase and three-phase mixings [19].

1.3.1 Problem Statement

The primary reason for the low recovery factors from oil reservoirs are the poor displacement and sweep efficiency due to interfacial tension (IFT) and reservoir heterogeneity. Enhanced oil recovery refers to methods whereby more oil can be recovered after secondary recovery. Therefore, extensive efforts in the oil industry have been directed towards understanding and optimising EOR technologies. Currently, chemical, thermal, gas, and several other EOR methods are being investigated. The methods most commonly applied in the industry are thermal and gas EOR [24]. In this thesis, however, the emphasis is on WAG injection.

Water-alternating-gas injection is a promising EOR technique to unlock some of the remaining oil in the half-full reservoirs, and WAG flooding is a proven technology applied in several fields. However, it is complex and expensive, requiring careful planning and efficient development. Currently, numerical reservoir simulation is the most applicable tool to guide reservoir engineers and managers to determine the optimum means for maximising oil recovery yet having three different phases coexist in the reservoir at the same time complicates the physics of oil recovery. The current capabilities of reservoir simulators are not sufficient to model the key mechanisms of oil recovery by WAG [21, 25-27]. Undoubtedly, though, any WAG injection project needs extensive reservoir simulation studies to optimise the field development plan and predict reservoir performance. Therefore, accurate numerical simulation is needed to guide future field implementations of WAG EOR.

The three main enablers for accurate WAG injection simulation are technology, the modelling process, and experience. The technology can be leveraged to maximise the outcome of WAG injection through accurate modelling software, advanced techniques to maximise three-phase regions in the reservoir and reducing the cost of WAG operations. However, the main challenge in terms of WAG injection simulation is not the technology alone but mainly the understanding of the process to be modelled. Consequently, much must be done for accurate prediction of any three-phase flow system. Thus, the question is: can the desired level of speed and accuracy be achieved with the current technology, modelling process, and experience?

To efficiently predict WAG injection performance, a transformational shift in the WAG modelling process is needed. Therefore, this thesis focusses on identifying the shortcomings of the current reservoir simulators and providing a guideline for more efficient WAG injection simulations. The aim is to reduce the simulation prediction error and develop more efficient future WAG injection projects.

1.3.2 Thesis Overview

As the objective of this thesis is to provide a guideline for a more reliable WAG injection simulation, the shortcomings in the numerical simulation must be adjusted through a better modelling process. Therefore, the thesis starts by reviewing the historical evolution of the published literature about the three-phase relative permeability and hysteresis models. Chapter 2 summarises the main models of three-phase flow and hysteresis from 1968 to 2000. Then the various efforts to improve the understanding of WAG injection's oil recovery process over the past 18 years is reviewed, including models which have shaped the understanding of the three-phase flow in porous media and become well-known in the current oil and gas industry. There are some major modifications to the commercially available three-phase hysteresis models which are also discussed. Finally, some published simulation studies at core and reservoir scales are reviewed.

To characterise the rock and fluids in the oil reservoirs, a common practise in the oil and gas industry is to perform experiments and analyses on reservoir core samples with the objective to understand the rock and fluid properties as well as the flow dynamics. In this thesis, the emphasis is on the rock-fluid properties such as relative permeability (kr), capillary pressure (Pc), and cyclic-hysteresis (WAG-HYST) parameters. These properties are usually estimated from core-scale experiments with the help of numerical simulation.

Therefore, Chapter 3 discusses the required experiments and the analyses necessary to obtain the key parameters for the WAG injection process. Since the numerical simulation accuracy is only as good as the input parameters, Chapter 3 establishes the required data for a more accurate WAG injection simulation.

Chapter 4 explains the analysis and simulation process of a series of unsteady-state WAG experiments performed at Heriot-Watt University to identify the shortcomings of the commercially available cyclic-hysteresis models. Therefore, the required simulation parameters to model the physical process of WAG injection are discussed. The outcomes of this chapter can provide a clear direction to improve the accuracy of WAG injection simulation for future projects.

Reservoir heterogeneity and anisotropy, as well as the gravity effect, make the simulation of WAG injection at reservoir scale more challenging. Therefore, chapter 5 first evaluates the effect of relative permeability and capillary pressure using a two-dimensional cross-section simulation model with homogenous properties. Then since WAG injection involves injection of gas into the reservoir, the role of vertical permeability is investigated. The common understanding in the industry is that vertical permeability is usually lower than horizontal permeability; thus, many simulation engineers would assume that vertical permeability is about 10 per cent of horizontal permeability. However, this is not accurate in most cases, especially with fine grid models. Therefore, Chapter 5 provides a sensitivity study to understand the role of vertical permeability in WAG injection performance compared to waterflooding. A quarter five-spot sector model is utilised to illustrate the effect of vertical permeability on WAG injection performance.

Various rock types can exist in a small volume of a reservoir rock. When gridding the rock section to make a numerical simulation model, often more than one rock type must be represented in each grid cell. Geologists usually work on averaging static properties and distribute them along the geological model grids. However, for the dynamic simulation model, sometimes only one average set of relative permeability functions can be used in the simulation models due to the lack of such data in most reservoirs. This could have a severe effect on WAG injection performance, and thus it is discussed in Chapter 5 along with the effect of cyclic-hysteresis on WAG injection performance at the reservoir scale.

Finally, a systematic workflow to acquire the relevant data and analyse them to generate the input data for WAG injection simulation is suggested in Chapter 6. The first part of the chapter is about the ideal set of experiments to collect enough data to build the simulation model. Then a sequence of actions to analyse the experimental data and extract information on cyclic-hysteresis is discussed. Finally, the procedure to simulate the WAG injection process on any scale is introduced. The last chapter, Chapter 7, concludes this thesis and provides recommendations for future work.

Chapter 2—Three-Phase Relative Permeability and Hysteresis

This chapter contains a critical literature review of the historical evolution in the three-phase relative permeability and hysteresis models. These models have shaped the understanding of the three-phase flow in porous media, which has become a common practise in the oil and gas industry recently. The first part of the chapter reviews the major three-phase flow and hysteresis model in relative permeability, followed by a summary of the various efforts to improve understanding of the WAG process. Finally, the major modifications to the commercially available three-phase hysteresis models are reviewed, and publications on the simulation of WAG injection at core and reservoir scales are discussed.

2.1 The Major Three-Phase Flow Models (1968–2000)

The efforts to understand the processes of three-phase flow and hysteresis have been ongoing for more than fifty years. Having three different phases coexist in the reservoir and flow at the same time complicates the physics of oil recovery. Therefore, the oil and gas industry has been actively researching this area, resulting in the widely accepted models below.

2.1.1 Land Model

In 1968, Land [28] introduced a calculation method of imbibition relative permeability for water-wet sand, based on pore-sized distribution and the relationship of residual to initial non-wetting phase saturation. He proposed the following relationship to approximate trapped gas saturation during imbibition:

$$C = \frac{1}{Sgt'} - \frac{1}{Sgi'} \qquad \textit{Equation 2-1}$$

where [C] is the gas-trapping parameter, which is sometimes called Land's parameter. [Sgt'] is the residual or trapped-gas saturation, and [Sgi'] is the initial gas saturation at the start of the imbibition process. Even though Land's work was not experimentally proven for three-phase flow, it is used in some current three-phase hysteresis models [29-31].

2.1.2 Stone's Three-Phase Oil Relative Permeability Models

Around the same time, Stone contributed to the knowledge of three-phase flow by proposing two empirical models to estimate three-phase relative permeability from measured two-phase data. These two models (STONE I and STONE II) are widely used

in the oil industry. To apply Stone's methods, accurately measured water-oil and gas-oil relative permeability curves must be available to interpolate between them [32].

Several years after the first three-phase oil relative permeability model, a new model, known as STONE II, was proposed [33] to account for hysteresis by using the appropriate saturation direction relative permeability curve. In other words, if both water and gas are increasing in the system (W↑G↑), then the imbibition water-oil curve and the drainage gas-oil relative permeability are used to estimate the three-phase oil relative permeability (kro^{3ph}). The STONE II model was also able to estimate a new residual oil saturation in the three-phase region (SOR^{3ph}), which was expected as input in STONE I. However, there were still some limitations in these models, as reported by Stone, especially in the regions of low gas and high water saturation [33].

Between 1973 and 1988, several researchers tried to modify Stone's models, for example, Dietrich and Bondor (1976), Aziz and Settari (1979), and Fayers and Mathews (1984) [34-36]. These modifications improved the usability and applicability of Stone's three-phase oil relative permeability model.

2.1.3 Conventional Hysteresis Models

In 1976, Killough [37] developed a capillary pressure and relative permeability hysteresis model for water-wet systems to be used in reservoir simulation. His proposed model allows for smooth scanning curves to be calculated between drainage and imbibition, bounding curves for wetting and non-wetting phases (Figure 2-1 and Figure 2-2).

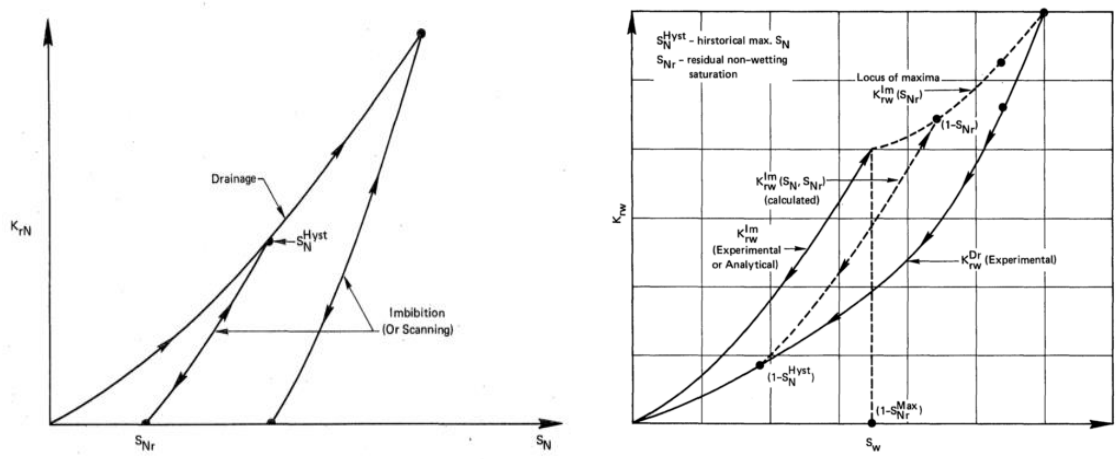

Figure 2-1: Non-wetting (left) and wetting (right) phases' hysteretic relative permeability as per Killough model [37]

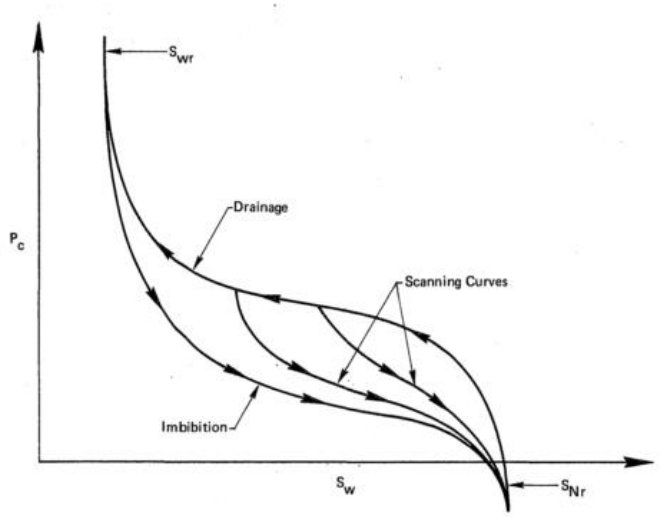

Figure 2-2: The capillary pressure hysteretic behaviour as per Killough model [37]

In 1981, Carlson [38] presented a method to simulate gas imbibition relative permeability by providing the drainage gas relative permeability, the historical maximum gas saturation, at least one point from an experimental imbibition curve (usually the first point to get the imbibition critical gas saturation), and Land's parameter (C) to calculate the trapped gas saturation, Sgt. Figure 2-3 shows an example where Carlson calculated the gas imbibition curve (dashed line) for a set of data from the San Andres formation in Texas:

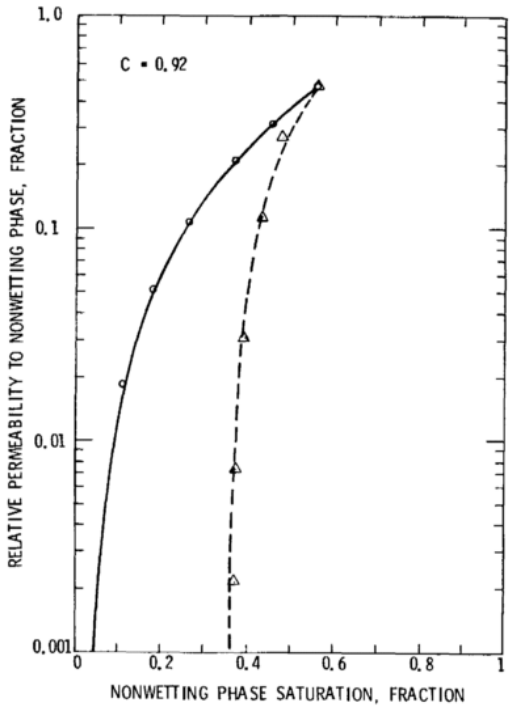

Figure 2-3: Calculation for the gas imbibition curve (dashed line) for data from San Andres formation, Texas [38]

2.1.4 Saturation-Weighted Interpolation Model

In 1988, Baker reviewed almost all the previous three-phase relative permeability models and proposed a new correlation. The model proposed by Baker, which is based on the saturation-weighted interpolation, assumes that there is some dependency amongst all three phases (oil, water, and gas). By testing the predictability of the model on some published three-phase data and comparing it with other three-phase oil-relative permeability models, Baker claimed that his saturation-weighted interpolation method was superior. This simple model was accepted by the industry and implemented in most commercial simulators [39].

2.1.5 Stone I Exponent Model

In 1992, Hustad and Holt modified Stone's first model by introducing an exponent term (η) to the combined saturations (β) [40].

$$kro = \frac{krow(Sw) * krog(Sg)}{krocw} * \beta^{\eta} \qquad \textit{Equation 2-2}$$

$$\beta = \frac{So^*}{(1 - Sw^*)(1 - Sg^*)} \qquad \textit{Equation 2-3}$$

For low oil saturation, a common situation in WAG applications, [β] should be closer to 0 by applying the appropriate value [η] to match the observed oil recovery. The STONE I Exponent [η] of 1.0 resembles STONE I's original form whilst it can be more or less than 1 to control the spreading of oil isoperms within the saturation space. More details and descriptions of this modification to the STONE I model can be found in the original reference [40].

2.1.6 Three-phase Correlation for Prudhoe Bay by Jerauld

In 1997, Jerauld [41] produced a three-phase correlation based on data from Prudhoe Bay, the largest oil field in North America, to be used in mixed-wet reservoirs where hysteresis and compositional effects are essential. In his published paper, he suggested a modification to Land's gas-trapping model by introducing an exponent term (b) between 0 and 1, where b=0 is the exact form of Land's equation:

$$Sgt(Sg^{max}) = \frac{Sg^{max}}{1 + (\frac{1}{Sgr} - 1)(Sg^{max})^{1+bSgr/(1-Sgr)}} \qquad \textit{Equation 2-4}$$

He also elaborated more on the gas-trapping behaviours in two phases, where he mentioned the following physical consistency:

- Trapped-gas saturation is usually less than the maximum gas saturation [$Sgt<Sg^{max}$].
- Trapped-gas saturation [Sgt] approaches the maximum gas saturation [Sg^{max}] at low Sg^{max}.
- Trapped-gas saturation [Sgt] does not depend on pressure, temperature, or scale of measurement.
- Trapped-gas saturation [Sgt] by oil is equal to trapped-gas saturation by water.

Founded on Prudhoe Bay gas trapping data published by Jerauld, the reduction in residual oil saturation based on trapped-gas saturation [$SOR \approx Som - 0.13*Sgt$] is less than what was suggested in the literature for water-wet rock [$SOR \approx Som - 0.5*Sgt$]. He indicated that the difference could be due to the wettability of the rock and, therefore, suggested that the residual oil [Sor] and trapped-gas [Sgt] saturations in mixed-wet rocks are independent because they have different flow paths.

2.1.7 WAG-Hysteresis Model by Larsen and Skauge

In 1998, Larsen and Skauge suggested that previous two-phase (conventional) hysteresis models (section 2.1.3) could not be used for WAG injection. Thus, they proposed a three-phase hysteresis model for the numerical simulation to allow gas trapping during WAG cycles. In this thesis, the Larsen and Skauge model is referred to as the WAG-HYST model, for which they used experimental data generated in the laboratory [29]. The WAG injection experiments they used were limited to one hysteresis loop, which can start with either water injection [**W1]** followed by gas injection [**G2]** and then a second water injection [**W3]** or gas injection [**G1]** followed by water injection [**W2]** and then a second gas injection [**G3**] [42]. There is evidence indicating that additional hysteresis cycles would exhibit different behaviours than the first hysteresis loop; therefore, this model has historically struggled to match repeated WAG injection cycles data in core-flood experiments [8, 43]. However, since this is the main WAG hysteresis model available in the numerical simulators, it is discussed in more detail in various sections of this thesis.

The WAG-HYST is composed of three models, namely, the gas model, oil model, and water model. The extensions and assumptions of those models are discussed in the following sections.

2.1.7.1 WAG-Hysteresis Gas Model

Gas is assumed to be the non-wetting phase, and it is responsible for a unique hysteresis behaviour in the WAG injection process. Larsen and Skauge reported cycle-dependent hysteresis for gas. Therefore, drainage gas relative permeability ($krgo^{input}$) would be significantly lower in the presence of mobile water saturation (Sw>Swc). To model this in the numerical simulation, they related the reduction of drainage gas relative permeability to the water saturation (Sw) and trapped-gas saturation (Sgt) during the hysteresis loops (Figure 2-4). The gas secondary-drainage relative permeability is calculated based on the following equation:

$$krg^{sd} = \left[krg^{input} - krg^{input}(Sg^{start})\right] * \left[\frac{Swc}{Sw^{start}}\right]^{\propto} + \left[krg^{i}(Sg^{start})\right]$$

Equation 2-5

where

krg^{sd}	is the calculated gas secondary-drainage relative permeability;
krg^{input}	is the input gas primary-drainage relative permeability;
$krg^{input}(Sg^{start})$	is the input relative permeability at the start of the secondary drainage;
Swc	is the connate water saturation;
Sw^{start}	is the water saturation at the start of the secondary drainage;
$krg^{i}(Sg^{start})$	is the imbibition relative permeability at the start of the secondary drainage process; and
$\propto$	is the reduction exponent input in the WAG-HYST model.

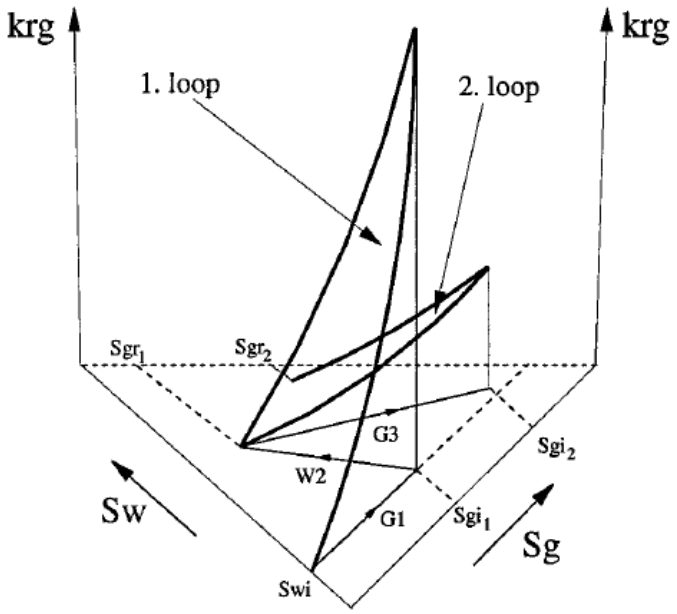

Figure 2-4: A plot to illustrate the gas-relative permeability reduction process during three-phase flow [29]

Therefore, the numerical simulation requires the following inputs for the gas phase:

- Primary-drainage gas relative permeability ($krgo^{input}$), obtained from a two-phase gas injection experiment into a core saturated with oil at Swc
- Land's gas-trapping parameter [C], which is a constant used to calculate trapped-gas saturation, as described in Equation 2-1 (Some commercial simulators would utilise trapped-gas saturation as input to calculate trapping parameter [C] using the same relationship.)
- The secondary-drainage gas relative permeability reduction exponent (α), which modifies $krgo^{input}$ based on the amount of mobile water present in the system

2.1.7.2 WAG-Hysteresis Oil Model

Oil is assumed to be the intermediate wetting phase; therefore, it depends on the saturation of the other phases as well. If the STONE 1 three-phase oil relative permeability model is activated in the simulation model, then the initial residual oil saturation (Sori) can be reduced in proportion to the trapped-gas saturation, as shown in Equation 2-6:

$$Sorm = Sori - aSgt \qquad \textit{Equation 2-6}$$

where (Sorm) is the minimum residual oil saturation by WAG injection. This is achieved by reducing the two-phase initial residual oil saturation (Sori) by the reduction fraction (a) of the trapped gas (Sgt). If (a) is equal to 1.0, then Sori will be reduced by the same amount as the trapped-gas saturation. However, if (a) is less than 1, then the reduction in Sori will be a fraction of Sgt.

2.1.7.3 WAG-Hysteresis Water Model

Water is assumed to be the wetting phase in the WAG-hysteresis model. In the three-phase zone, where gas has flooded the zone previously, the imbibition three-phase water-relative permeability (krw^{3ph}) should be lower than the imbibition two-phase water-relative permeability. The scale of reduction to the water-relative permeability depends on the amount of gas saturation in the system (Figure 2-5).

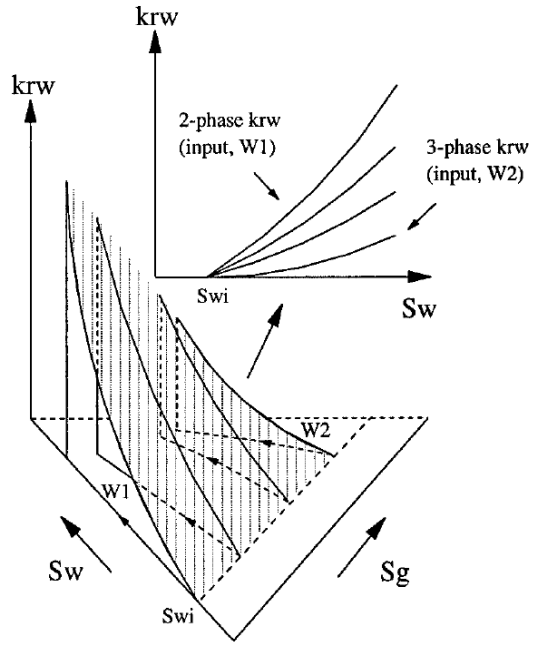

Figure 2-5: A plot to demonstrate the process of reducing the water-relative permeability in the three-phase zone based on the amount of gas saturation [29]

The WAG-HYST water model available in commercial numerical simulators does not automatically calculate (krw^{3ph}) from the input two-phase relative permeability curve. Therefore, the krw^{3ph} bounding curve must be directly specified in the simulation model. The bounding three-phase water-relative permeability can ideally be obtained by matching the data from appropriate three-phase water injection experiments (from the water injection cycle after the maximum gas saturation was introduced). The numerical WAG-HYST model can interpolate between the two bounding curves based on the amount of gas saturation in the grid cell (Equation 2-7) [44]:

$$krw^{imb} = krw^{2ph} * \left(1 - \frac{Sg^{start}}{Sg^{max}}\right) + krw^{3ph} * (\frac{Sg^{start}}{Sg^{max}}) \qquad \textit{Equation 2-7}$$

where

krw^{imb}	is the calculated water three-phase imbibition relative permeability;
krw^{2ph}	is the input two-phase water imbibition relative permeability;
krw^{3ph}	is the input three-phase water-relative permeability;
Sg^{start}	is the gas saturation at the start of the three-phase water imbibition; and
Sg^{max}	is the maximum historical gas saturation.

2.1.8 Three-Phase Model by Blunt

Blunt [45] extensively reviewed the available literature published before 1999 and analysed several experiments to extend Baker's saturation-weighted interpolation. His aim was to account for layer flow, different wettability conditions, and phase trapping (oil and gas) which was not accounted for previously. He claims that his model demonstrates a better oil-relative permeability prediction in three-phase flow on water-wet Berea sandstone cores. This model highlighted some important aspects of three-phase flow; however, the effect of gas-trapping, as well as wettability, was not incorporated.

2.1.9 Three-Phase Relative Permeability by Stanford University

Between 1998 and 2000, a research group at Stanford University [46] studied three-phase flow in sand packs at different wettability conditions: water-wet, oil-wet, mixed-wet, and fractionally wet sand packs. They then tried to measure three-phase relative permeability of each phase during gas gravity drainage of oil and water at different wettability conditions. Based on the results of their study, they reported the following observations:

- Water-relative permeability in the water-wet sand pack is similar to oil-relative permeability in the oil-wet sand pack.
- In the mixed-wet and intermediate-wet sand packs, a layer drainage regime is observed.
- Gas as the non-wetting phase shows a smaller three-phase relative permeability in the oil-wet than the water-wet sand pack.

- There is a noticeable difference in the intermediate wetting phase relative permeability at low saturation (So < Sor).

2.2 Advancements in Understanding the WAG Injection Process (2000–2018)

Several research centres including the centre for EOR and CO_2 solutions at Heriot-Watt University (HWU) have contributed to the understanding of the characterisation of three-phase flow and WAG injection since early 2000. They have extensively studied the oil recovery process by WAG injection from pore scale (high-pressure micromodel section 2.2.1) to the core scale (core-flood experiments section 2.2.2). The various studies documented in the literature to visualise and understand the process of oil recovery by WAG are discussed in the following sections:

2.2.1 High-Pressure Micromodel WAG Injection Tests

In 2004, a comprehensive study on the 'visualisation of oil recovery by WAG injection using high-pressure micromodels' at different wettability conditions was published by Sohrabi et al. [13] because visualising such a process would allow a deeper understanding of the flow physics. The description of the flow behaviour during WAG injection at different wettability micromodels is summarised in Table 2-1 below:

Table 2-1: Summary of the oil recovery process visualisation from micromodels performed by Sohrabi et al. and published in 2004 [13]

Wettability	Description of Flow Based on Micromodel Visualisation
Water-Wet	Water is the most wetting phase in the water-wet system; therefore, it flows as a continuous thin film which thickens as more water is injected against the corners of the etched pores. The oil phase will be displaced by water until it becomes discontinuous in the middle of the pore. When the first gas is injected into the system, the gas phase would enter the oil-filled pores first and start displacing the oil. During the secondary imbibition of water, the water phase would flow into the pores filled with gas and displace it and the oil until the gas phase becomes trapped. Then, during the gas secondary drainage, new pores that are filled with oil will be invaded by gas, leading to more oil recovery. This process can be repeated until no significant additional oil is recovered by WAG injection.

Oil-Wet	Water is the non-wetting phase in the oil-wet system; therefore, it flows into the middle of the etched pores. The oil phase will be displaced by water as a piston-like method. When the first gas is injected into the system, the gas/water IFT is greater than the gas/oil IFT, forcing the gas to enter the oil-filled pores and displace the oil. During the subsequent cycles of water injections, no significant oil recovery is observed. However, during the gas cycles, new oil-filled pores were invaded by gas, leading to additional oil recovery by WAG injection.
Mixed-Wet	Some pores in the mixed-wet systems are water-wet, and others exhibit oil-wet characteristics. Therefore, the process observed during WAG injections in a mixed-wet micromodel is a combination of the water-wet and oil-wet systems (Figure 2-6).

The results of the micromodel visualisation confirmed that oil recovery by WAG injection could lead to a significant increase in the oil recovery factor compared to waterflood or continuous gas injection. Also, the effect of rock wettability on the oil recovery by WAG injection was investigated and the results are shown in Figure 2-6:

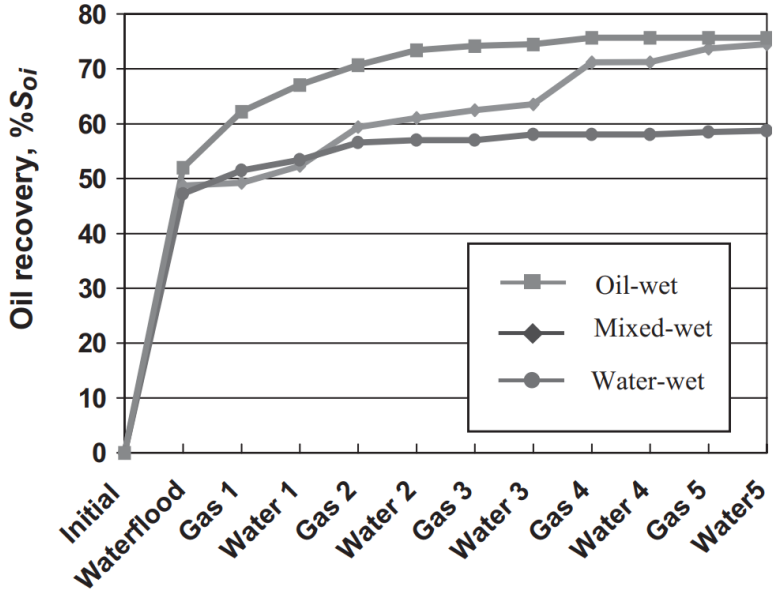

Figure 2-6: Oil recovery (% OOIP) by WAG injection observed from the different wettability micromodels published by Sohrabi et al. [13]

2.2.2 WAG Injection Core-Flood Experiments

To understand the oil recovery behaviour by WAG injection in real reservoir rocks, several core-flood experiments were conducted by various researchers. Each year more WAG core-flood experimental data are published by the leading research centres in this area. However, in this section, only a few examples of the extensive core-flood experiments were discussed.

WAG core-flood experiments on different wettability-state Berea sandstone-cores undertaken by Element et al. were published in 2003. Their experimental findings have supported the key hysteresis features used in the WAG-HYST model. They reported that hysteresis cycles are irreversible, and trapped-gas saturation should cause a reduction in water and gas-relative permeability in three-phase regions. Therefore, the residual oil saturation would be lowered as a result of the trapped-gas saturation inside the pores. Furthermore, they also reported that Land's gas-trapping parameter [C] could be different for each hysteresis cycle [47]. Figure 2-7 shows the variable Land's parameter for different water injection cycles [47]:

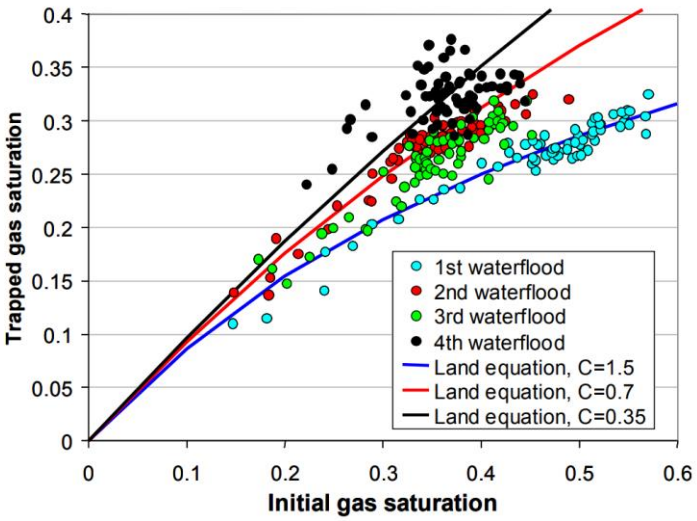

Figure 2-7: Land's parameter for different water injection cycles into water-wet cores (GAW) [47]

This particular observation came as more WAG cycles were implemented beyond a single hysteresis loop. Furthermore, their observation on the variable gas-trapping behaviour has been confirmed by several authors since 2003 [25, 27, 48].

Research efforts at HWU have been ongoing for the past decade to understand the oil recovery process by WAG injection, using micromodels, core-flood experiments, and

numerical simulation [5-10]. The current knowledge of the WAG recovery process resulting from such research has advanced the related technologies in current practises. An extensive set of experiments was conducted at different wettability and oil-gas interfacial tension conditions [6, 7], and by far, these experiments provide the most complete core-flood data to understand the oil recovery behaviour by WAG injection.

The main conclusion drawn from the extensive core-flood experiments is that hysteresis in WAG injection is important at most conditions; however, a less significant effect is observed in a higher permeability core (1000 mD). Also, the oil recovery by WAG in mixed-wet rocks is lower when starting with a gas injection cycle (GAW) [6]. The results of this study lead to more investigations on the role of the size and order of injection cycles as discussed next.

In 2015, the centre for EOR and CO_2 solutions at HWU published another set of WAG injection experimental results performed on oil-wet carbonate core samples. They studied the effect of injection schemes (GAW, WAG, or SWAG) on oil-wet carbonate rock and concluded that SWAG injection (simultaneous water-and-gas) performed better in terms of early oil recovery (six pore-volume injections), whilst WAG (starting with the water injection cycle) recovered more than 70 per cent of original oil in place (OOIP) after fourteen pore-volume injections (Figure 2-8). This study highlighted the impact of injection order on WAG performance which is of high importance to the industry.

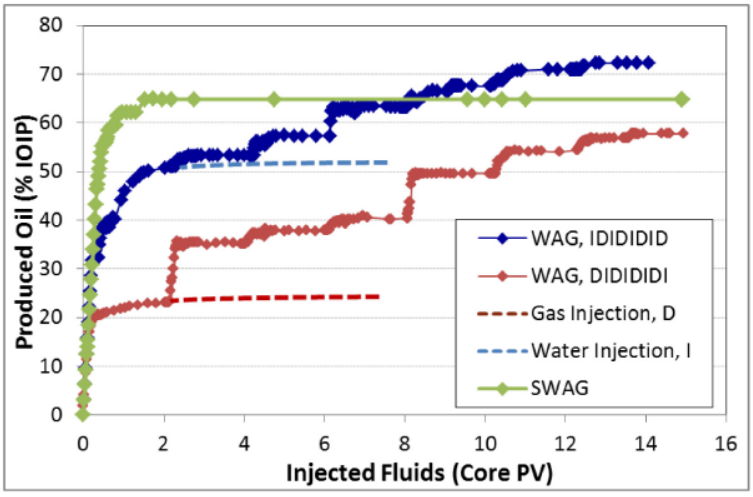

Figure 2-8: Oil recovery comparison for different WAG injection schemes in oil-wet carbonate rock [7]

The most recent set of experimental data which explored the effect of wettability on the WAG injection performance was published in 2018 by Alkhazmi et al. [19]. Various core-flood experiments performed on low-permeability sandstone rock samples at weakly water-wet, water-wet, and mixed-wet conditions were discussed. Based on their results,

shown in Figure 2-9, the ultimate recovery of mixed-wet sandstone rock is the highest regardless of the injection scheme. This observation indicated that the effect of rock wettability is stronger than the effect of the WAG injection order.

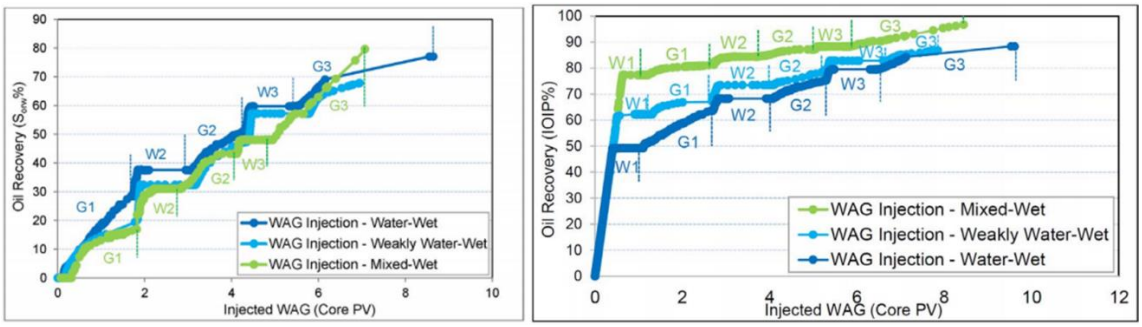

Figure 2-9: Oil recovery by WAG injection (right) and GAW injection (left) at near-miscible gas-oil IFT for three different wettability conditions published by Alkhazmi et al. [19]

Similar work by Alkhazmi et al. was also published in 2018 [10] to investigate the length and the order of immiscible WAG injection cycles on mixed-wet rock samples. Their experimental results showed that the long slugs starting with gas injection significantly outperformed the other injection schemes, as shown in Figure 2-10:

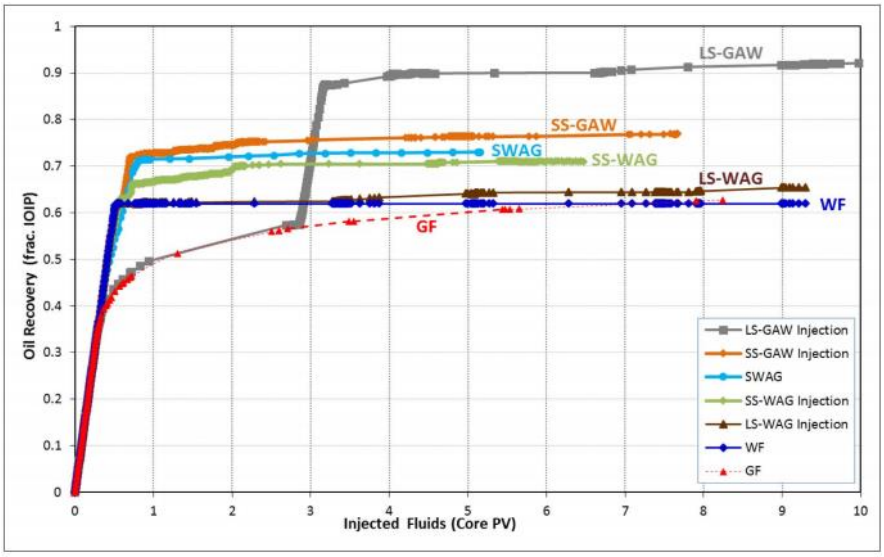

Figure 2-10: Oil recovery comparison for various WAG injection schemes at mixed-wet rock samples as published by Alkhazmi et al. [10]

2.2.3 WAG Injection Core-Scale Simulation

Numerical simulation is a practical tool to understand flow and oil recovery behaviours during WAG injection. Therefore, several attempts to model WAG core-flood experiments were published in the literature. This section highlights several of those attempts.

The various core-flood experiments performed and published by Heriot-Watt University have been utilised by different researchers to understand cyclic-hysteresis behaviour

during the WAG injection process. For instance, Shahverdi and Sohrabi [27] developed a core-flood simulator to directly estimate three-phase relative permeability curves from the unsteady-state WAG injection experiments. The trend of cyclic-hysteresis observed by historically matching the WAG injection experiments revealed some observations that differ from the existing hysteresis models. They concluded that both water and gas phases are functions of two independent saturations, which is different than what is found in most published literature. The following findings led them to make the previous conclusion:

- Three-phase gas-relative permeability exhibited more significant hysteresis during successive gas injection compared to the three-phase water injection cycles.
- Three-phase water-relative permeability showed less hysteresis in mixed-wet compared to the water-wet systems during gas injection cycles. However, it showed almost no hysteresis effect during water injection cycles. Furthermore, the three-phase water-relative permeability can be higher than the two-phase relative permeability in mixed-wet systems, as claimed by Shahverdi and Sohrabi [27].
- Three-phase oil-relative permeability demonstrated a noticeable hysteresis behaviour during water injection cycles, whilst there was almost no hysteresis effect during gas injection cycles for water-wet and mixed-wet systems.

In 2017, Mehzari and Sohrabi [25] suggested a methodology involving history-matching multiple core-flood experiments to define the WAG injection parameters, utilising a history-matching algorithm to approximate a reasonable representation of the WAG injection characterisation. Based on their suggested methodology, better representation of two-phase relative permeability curves can be obtained by matching the first two cycles of WAG injection core-flood experiments. These improved curves were used in a history-matching process of multiple core-flood experiments to obtain a set of parameters to characterise the cyclic-hysteresis for the particular reservoir system involved.

Although this approach appears attractive, the history-matching process using the current capability of the numerical simulations is not ideal. A similar approach was done by Duchenne et al. [21] to emphasise that a more dynamic procedure to estimate three-phase hysteresis parameters is essential for improved prediction of WAG injection performance.

2.2.4 New Proposed Three-Phase Hysteresis Models

In 2015, several scientists from the University of Texas at Austin proposed a new three-phase relative permeability and hysteresis applicable for various wettability conditions. Their hysteresis model modifies Land's non-wetting phase trapping model (1968) by introducing a dynamic coefficient and claims to overcome the limitations of the other three-phase hysteresis models based on their tests on experimental data obtained from non-water-wet rocks.

The proposed model by the University of Texas at Austin can supposedly estimate the hysteresis behaviour of all three phases and correct the cycle-dependent land coefficient in WAG cycles which characterise the amount of trapped-gas saturation. The published study reported that gas trapping is the major factor for the loss of injectivity observed in some WAG injection projects at the field scale. This updated model was incorporated into their numerical simulator [31].

In 2016, researchers from TOTAL SA [48] leveraged the WAG injection experiments at mixed-wet conditions published in the literature to better understand the WAG mechanism. Duchenne et al. suggested a modification to the three-phase WAG hysteresis model by Larsen and Skauge [29]. The main attribute altered is Land's gas-trapping model. The proposed general form of gas trapping accounts for the displacing phase of the gas. However, the extended three-phase hysteresis model by TOTAL was introduced to their in-house simulator (IHRRS) and used to history-match experimental data to estimate the hysteresis parameters and to achieve a good match to the WAG injection experimental data, accounting for a different trapped-gas saturation function when a significant oil bank is being displaced (oil displacing gas).

More recently, a 2018 study by the University of Texas at Austin [49] suggested a new three-phase hysteresis model be coupled with their compositional simulator. The new model accounts for the effect of hysteresis and fluid compositions for relative permeability [kr] and capillary pressure [Pc]. Using the Gibbs free energy (GEF) of oil, gas, and water at every time-step, the model would interpolate between reference values to define relative permeability and capillary pressure. Their suggested model uses an algorithm to integrate hysteresis and trapping number to simulate miscible WAG injection or similar processes; this algorithm showed good numerical stability and consistency of results and more efficient simulation time [49].

2.2.5 Reservoir-Scale WAG Injection Simulation

Although WAG injection has proved successful in several oil fields worldwide, there is a need to optimise this process. A robust forecasting method is required to reliably design the capacity of the surface facilities prior to the production start-up, which is sometimes the biggest bill in the development budget. However, the current capabilities of reservoir simulators are not sufficient to model the key components of oil recovery by WAG [23]. Enforcing three-phase flow in the reservoir by WAG injection complicates the physics of oil recovery. Certainly, extensive reservoir simulation studies are required to predict reservoir performance and optimise the field development plans.

In 1994, Guzman et al. evaluated the uncertainty of oil recovery predictions by three-phase flow techniques at reservoir-scale simulation by conducting a detailed simulation study to determine the variations in oil recovery predictions resulting from the choice of a three-phase relative permeability model. Their results showed that there is a considerable difference in oil recovery and GOR amongst different three-phase relative permeability models. Also, they suggested that the three-phase region in all of their simulations was significant, accounting for at least 20 per cent of the reservoir volume.

In 2004, Spiteri and Juanes [50] investigated the impact of relative permeability hysteresis on WAG injection simulation by using homogenous and heterogeneous reservoir-scale models to illustrate the effect of hysteretic-relative permeability in WAG injection. Their results confirmed that the use of proper hysteresis model is important to realistically predict the performance of the WAG injection process.

In 2007, Skauge and Dale [11, 51] investigated the effect of including capillary pressure in field-scale simulation when the WAG hysteresis option is used. The objective of the study was to enhance the description of the physics of a multiphase flow. When a WAG hysteresis model is used, the segregation of the gas and water is slower. Therefore, the breakthrough time for both fluids was delayed, and oil recovery was increased.

Based on their study, they reported a further delay to the predicted breakthrough time of the injected phases when capillary pressure is included. As a result of the capillary pressure used, the three-phase zone is larger, leading to higher oil recovery predictions.

The size of the three-phase zone depends on the following (based on Stone, 1982):

- injection rate
- vertical permeability
- density difference between fluids

However, the capillary pressure and three-phase relative permeability hysteresis are also important in defining the three-phase zone.

The simulation model used in this study was 1000mX100mX100m with a grid size of 10mX10mX10m. The static properties are summarised in Table 2-2:

Table 2-2: The static properties of the simulation model used in reference [11]

Porosity	Permeability X&Y	Permeability Z	Pressure	Swc
25%	500mD	50mD	300 bar	29%

A WAG injection every six months was implemented for a total duration of five years. The injection/production rate is assigned to be 1000 Rm3/d.

Five cases were evaluated, and the results are summarised in Table 2-3. The first case (case 1) ignored the three parameters (hysteresis, Pc, and kr+Pc effect) and showed the lowest total oil recovery (FOPT) after 5 years of WAG injection. As Pc effect is added to case 2, the model predicted slightly more oil recovery. A clear increase in the oil recovery prediction by cases 3, 4, and 5 was observed as a result of adding three-phase hysteresis effect. This study showed the influence of hysteresis and Pc in WAG injection performance.

Table 2-3: Summary of the five cases evaluated by reference [51]

Case	Hysteresis	Pc	Kr + Pc effect	FOPT (Rm^3)
Case 1	No	No	No	1040000
Case 2	No	Yes	No	1050000
Case 3	Yes	No	No	1220000
Case 4	Yes	Yes	No	1240000
Case 5	Yes	Yes	Yes	1320000

In 2010, Masalmeh and Wei [22] performed a simulation study to evaluate the impact of relative-permeability hysteresis, compositional effects, and interfacial tension for WAG injection by using different permeability profiles at various fine-grid sector models to

generalise the results for a wider range of carbonate reservoirs. They concluded that the three-phase hysteresis and compositional effects must be properly accounted for when WAG injection simulation is performed. They also suggested that a fit-for-purpose simulation study should guide the design of laboratory experiments to shift the focus towards the most sensitive parameters that affect the oil recovery.

In 2014, Lin Zuo [52] and his colleagues evaluated the most common three-phase relative-permeability models (STONE 1, STONE 2, Baker, and Linear) in simulating WAG injection at reservoir scale based on the high-uncertainty region concept. They concluded that the three-phase relative permeability model is more sensitive in simulating immiscible than miscible WAG injections. Also, they suspected that the error due to three-phase relative permeability prediction in field-scale miscible WAG is not significant compared to other uncertainties in the field.

Based on the literature review discussed here, the need for more accurate simulation process to match the observed data from the various WAG injection experiments is apparent. The efforts invested so far in understanding the oil recovery process by WAG injection has led to significant advancement in the current practices. However, the need for a systematic approach to acquire the relevant data and properly simulate the WAG injection process is noticeable. This thesis should unify the industry's approach to evaluate WAG injection projects and improve its performance using current modelling capabilities.

Chapter 3—Required Data for WAG Injection Simulation

It is a common practise in the oil and gas industry to perform experiments and analyses on reservoir core samples to understand the rock and fluid properties as well as the flow dynamics. The static and dynamic properties obtained from the core-scale sample (one- to four-inch core diameter) would be used to predict the performance of the larger-scale reservoirs. Similarly, for the WAG injection process, researchers use core-flood experiments and numerical simulation at core scale [6, 7, 18, 21, 25, 27, 53] to scale up the properties related to the WAG injection process to the reservoir-scale simulation grid blocks.

This thesis emphasises the rock-fluid properties such as relative permeability [kr], capillary pressure [Pc], and cyclic-hysteresis [WAG-HYST] parameters, which are usually estimated from core-scale data with the help of numerical simulation. Therefore, this section discusses the experiments required to estimate the simulation parameters and model the physical process of WAG injection.

3.1 Required Two-Phase Displacement Experiments

Two-phase relative permeability (kr) and capillary pressure (Pc) are often numerically estimated from history-matching steady-state (SS) or unsteady-state (USS) core-flood experiments [54]. For Pc, it is usually obtained from a separate experiment, such as mercury injection, porous plates, or centrifuge, and used as input for the relative-permeability estimation process. However, kr and Pc are often estimated simultaneously using commercial applications [55, 56]. Since hydrocarbon recovery is greatly controlled by both kr and Pc, their accuracy is crucial in any multiphase flow simulation [57].

Two-phase relative permeability is the parameter describing the simultaneous flow of two phases in the porous media. It can be estimated with the help of numerical simulation by matching the data from USS displacement experiments. Water and oil flow functions (kr and Pc) can be obtained from a water-displacing oil experiment, whilst the gas and oil flow functions (kr and Pc) can be acquired from a gas-displacing oil experiment at initial water saturation (Swi). The following two-phase displacement experiments are essential to estimate the required input for the numerical simulation.

3.1.1 Water-Oil Imbibition Experiment

The water-oil imbibition process starts by injecting water into an oil-saturated core at connate water saturation (Swc). The water is injected continuously to displace the oil down to the residual oil saturation after water injection (referred to as Sorw). The pressure and production data observed from this water injection cycle can be used to generate imbibition water-oil two-phase relative permeability (krw, krow). However, only when oil and water are simultaneously flowing at the core outlet can the water-oil relative permeability be estimated (the valid saturation range is only between the two dashed red lines in Figure 3-1).

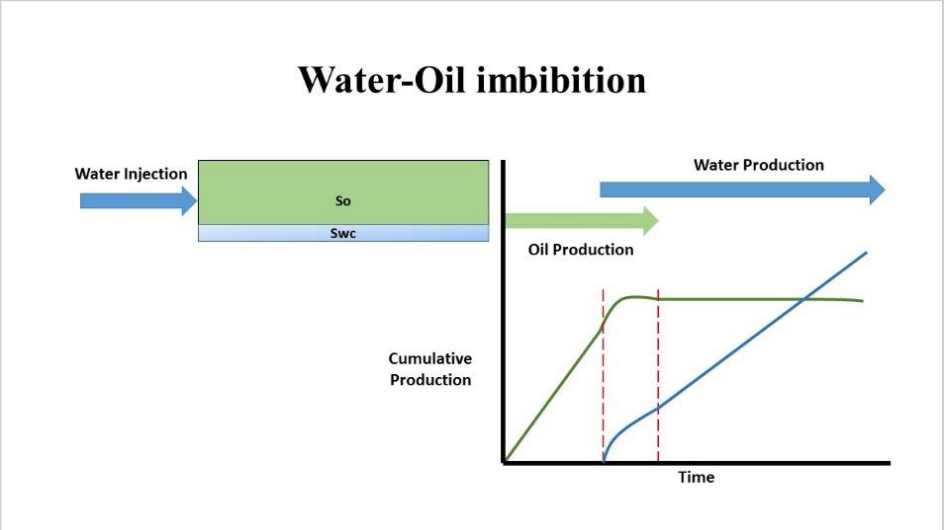

Figure 3-1: Water-oil imbibition process

3.1.2 Gas-Oil Drainage Experiment

The gas-oil drainage process starts by injecting gas into an oil-saturated core at Swc to displace oil down to the residual oil saturation by gas injection (Sorg). The gas-oil drainage relative permeability [krgo and krog] can be estimated from the experimental data (production and pressure). However, the saturation range is valid only when oil and gas are simultaneously flowing at the core outlet (between the two dashed red lines shown in Figure 3-2).

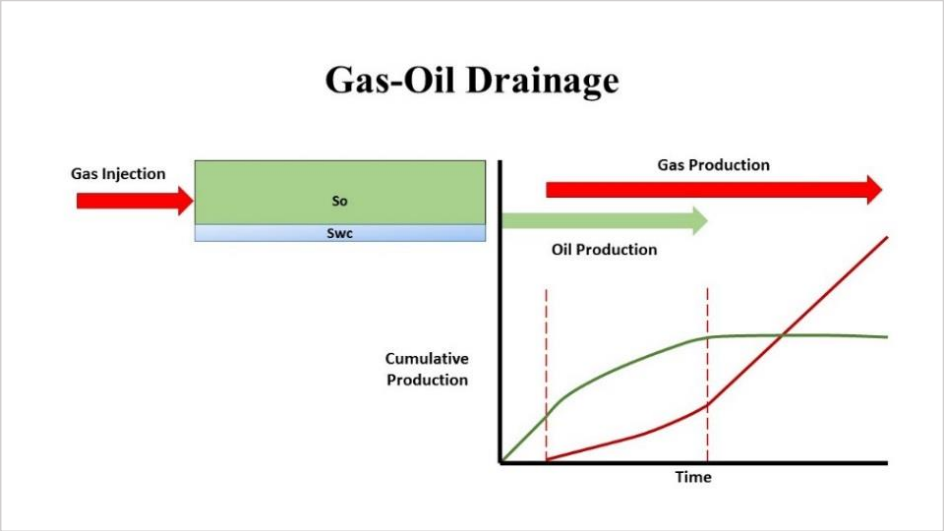

Figure 3-2: Gas-oil drainage process

3.1.3 Oil-Gas Imbibition Experiment

In some cases, the oil phase can displace the gas. Therefore, the oil-gas imbibition process should be defined in the simulation. An example of such a process is when an oil bank is formed and then accesses pores with the gas phase present. The oil phase would displace this gas, similar to the process highlighted in Figure 3-3.

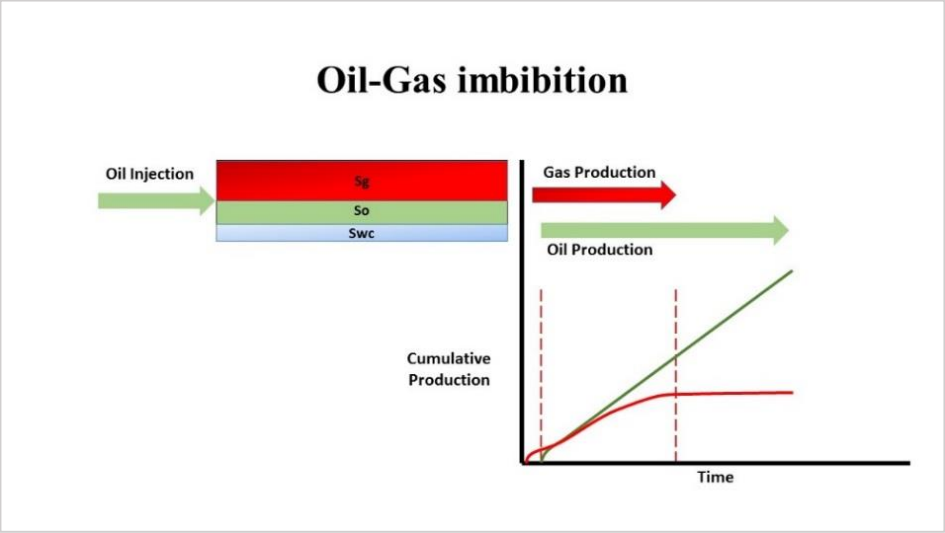

Figure 3-3: Oil-gas imbibition process

The oil-gas imbibition relative permeability can be estimated when oil and gas are simultaneously flowing at the core outlet.

The obtained data from these experiments are required to estimate the two-phase kr and Pc which are required for the numerical simulation. In the following section, the recommended estimation process is discussed.

3.2 Estimation of Two-Phase Relative Permeability and Capillary Pressure

Relative permeability (kr) and capillary pressure (Pc) are important physical parameters to describe multiphase flow in porous media. The Pc is a consequence of forces acting at the pore scale between two immiscible phases and is quantified as the pressure difference between the non-wetting and wetting phases. The drainage capillary pressure can be used to define the initial distribution of fluids within the reservoir model. For oil reservoirs with an oil-water contact (OWC), the two-phase drainage oil-water Pc is used to initialise the model with the fluid saturations above the free-water level (FWL). The Pc and kr curves for each rock type can be estimated from laboratory experiments and entered, in tabulated form, into the numerical simulators. Indeed, the kr and Pc input in the numerical simulation must be consistent.

However, the imbibition Pc where the water saturation is increasing as a result of water flooding or aquifer influx into the reservoir is often ignored or misused at reservoir-scale simulation because the pressure drop across coarse grids is often higher than the capillary pressure, which makes Pc negligible. In some cases, reservoir engineers try to capture the effect of imbibition Pc within the kr function itself. Yet this approach is somewhat questionable due to the possibility of viscous force dominating the flow in the USS core-flood experiments.

Sometimes in the oil and gas industry the imbibition Pc in the oil reservoir under water flooding is set to be zero whilst accounting for its effect within the kr function. However, capillary forces are very important in multiphase flow in porous media [58] and must be properly handled in simulating the reservoir performance.

To ensure that multiphase flow physics are correctly modelled in the numerical simulation, the balance amongst capillary, viscous, and gravity forces inside the porous medium must be understood. For example, the pressure drop across a low-permeability core sample during a core-flood experiment could be high enough to mask the effect of prevailing capillary force. Therefore, the kr obtained from such an experiment may have a capillary effect inherent in it. However, in the reservoir, away from wellbores, the Pc can still play a major role in the fluid flow through low-permeability porous media, leading to the question of the best way to capture the flow physics in this situation.
On the other hand, core flooding high-permeable core samples will exhibit a stronger capillary effect due to the low-pressure drop across the core. Relative permeability

obtained from this experiment will thus have within it the Pc effect. Therefore, it is important to know how to capture that in the numerical simulation, especially for reservoir-scale simulation.

Wettability of the rock surface is also important for the multiphase flow in porous media. The shape and endpoints of the kr curves, as well as the imbibition Pc, behave differently for water-wet, mixed-wet, and oil-wet rocks. In the water-wet system, the water-relative permeability endpoint (krw') should be low, whilst the oil-relative permeability endpoint (kro') should be higher compared to the mixed-wet system. Primary drainage Pc for both systems behaves similarly except that for the imbibition Pc, a water-wet system shows higher instantaneous imbibition, whilst the mixed-wet system demonstrates more forced imbibition [59].

Numerical simulation can be used to design a numerical core-flood experiment (NCFE) for the purpose of investigation. Various NCFEs can be generated to evaluate the effect of certain parameters and to conduct sensitivity studies and allocate more research resources towards the most influential parameters. Cumulative production and pressure data can be generated for different conditions and used, for example, to estimate the kr and Pc of a given system. In this section, the NCFE representing a water-wet system was modelled in Sendra (a software by Weatherford Petroleum Consultants) to obtain a set of kr and Pc and then tested at a reservoir-scale 2-D cross-section simulation (section 5.1). The fluid properties used in the NCFE to generate the input data are shown in Table 3-1:

Table 3-1: Fluid properties used in the NCFE - Sendra

Water Viscosity	Oil Viscosity	Injection Rate
μw = 0.6 cp	μo = 1.0 cp	10 cc/hr for 60 hours

The aim is to understand the role of Pc in multiphase flow simulations. NCFE was used to generate the required data for back calculating the flow functions for the following three cases:

1. Both Pc and kr are obtained simultaneously to match the numerical experimental data.
2. Pc is ignored (Pc is equal to zero), and kr is estimated to match the numerical experimental data.
3. Pc is given (assumed to be measured by different experiments), and kr is estimated to match the numerical experimental data.

Then the flow functions (kr and Pc) for each case are also used in a reservoir-scale 2D simulation model with similar properties to the NCFE to evaluate the difference in reservoir performance for each flow function (section 5.1).

The idea is that an NCFE with known oil-water kr and Pc curves can be used to generate numerical experimental data and then as a benchmark for the flow functions. Here, a realistic NCFE which does not represent any particular core was designed to examine the role of Pc in the core-scale simulation. The NCFE assumed a core saturated with oil at irreducible water saturation, and water is displacing oil to residual saturation (Sorw). The static properties for the NCFE are summarised in Table 3-2 below:

Table 3-2: Static properties of the core-flood simulation (water-wet)

Length/cm	Diameter/cm	Porosity/%	Swi/ %	Permeability/mD
60	5	20	20	100

Commercial software (Sendra 2015.2) was used to generate oil-water imbibition kr and Pc functions for a typical water-wet core using Corey and LET-imbibition models, respectively. The Corey relative permeability model has only one degree of freedom to estimate the shape of relative permeability. However, LET-imbibition model has more freedom to match the experimental data. Figure 3-4 shows the generated flow functions:

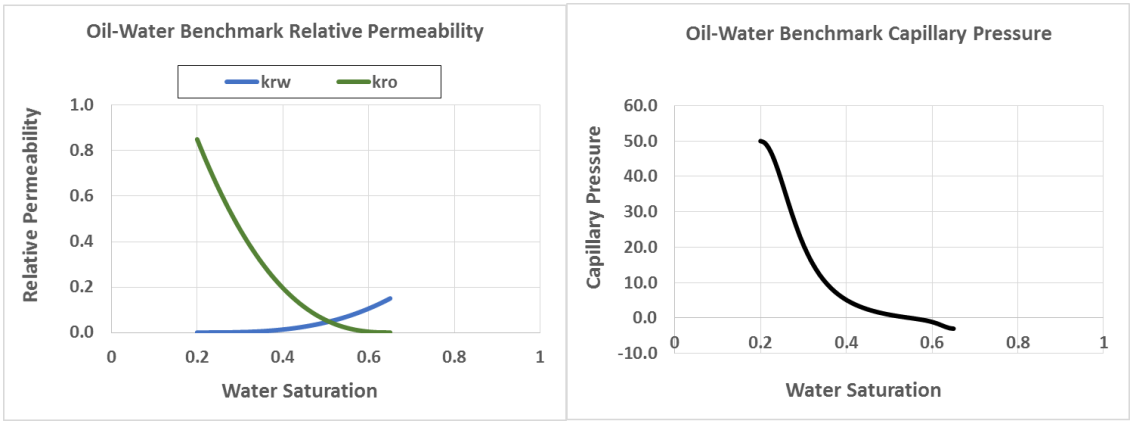

Figure 3-4: Oil-water imbibition kr and Pc (100mD)

The aim is to understand the role of Pc measurement and reduce uncertainty in obtaining kr through numerical simulation. First, the reliability of estimating both kr and Pc from given experimental data, which was generated numerically, is examined and compared to the benchmark flow functions; these are the input functions to the NCFE used to generate

the numerical experimental data. After that, the kr is estimated once by ignoring Pc and then by providing Pc before estimating oil-water kr that matches the experimental data.

3.2.1 Simultaneous Estimation of kr and Pc

Sometimes it is possible to simultaneously estimate kr and Pc for a given set of experimental data. However, this is not always recommended, especially if the *in situ* saturation measurement is not available [60]. Several researchers have suggested ways to improve the process of simultaneous calculation of kr and Pc from core-flood experiments even if the actual saturation profile is not measured [56, 60].

By using the reference oil-water relative permeability (krw, kro) and capillary pressure (Pcwo) from the NCFE shown in Figure 3-5, a core-flood process was simulated to get numerically calculated experimental data (cumulative oil production, cumulative water production, and pressure drop). Then the same commercial software was used to estimate oil-water imbibition kr and Pc that match the numerical experimental data by providing a range for Sor, krw (Sor), and kro (Swi). The match between simulated cumulative oil production (SIM_OPT) and the NCFE oil production total (EXP_OPT) was perfect, as it was with pressure drop (EXP_DP and SIM_DP), as shown in Figure 3-5:

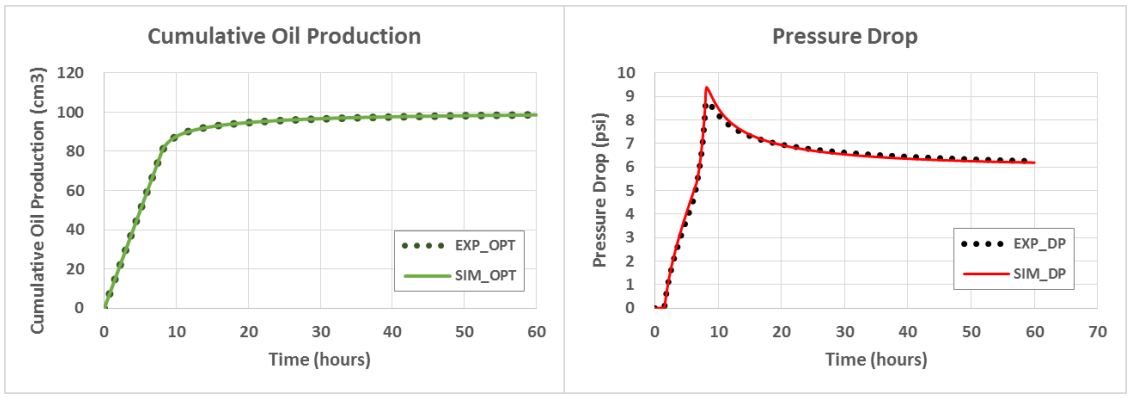

Figure 3-5: Experimental versus simulated oil production total (left) and the pressure drop (right) for the case where both kr and Pc were estimated simultaneously

The estimated kr and Pc for this scenario is labelled as (Pc_unknown) and shown in Figure 3-6:

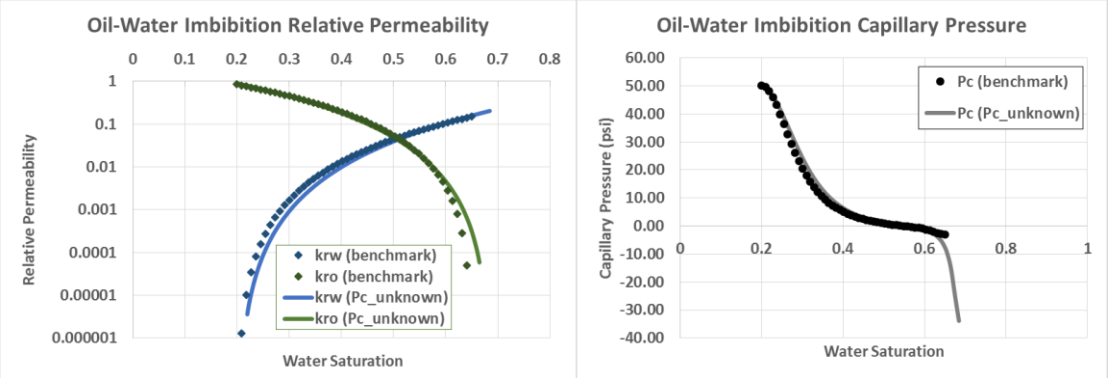

Figure 3-6: Estimated relative permeability and capillary pressure (Pc_unknown) (The dots are the benchmark flow functions used to generate the numerical experimental data.)

In Figure 3-6, the solid lines are the kr and Pc estimated by the commercial software which matched the numerical experimental data.

In real core-flood experiments, it is difficult to judge if the estimated kr and Pc are accurate or not. Here, since numerically generated experimental data is utilised, the benchmark flow functions can be used to judge the robustness of the estimation process. In this example, a reasonable range for Sor and kr endpoints was provided to guide the estimation process. The valid saturation interval starts from Sw=0.51 and goes to Sw=0.65. Even though the oil recovery and pressure drop were closely matched (almost identical), the resulting flow functions are different from the benchmark ones. Focussing on the valid saturation interval, the main difference is the residual oil saturation (Sor) due to the fact that the minimum Pc predicted by the software is lower than the benchmark Pc. Therefore, the estimated Sor becomes slightly lower than the benchmark Sor. To avoid this, the minimum Pc or the exact Sorw should be provided to guide the commercial software in the kr estimation.

3.2.2 Estimation of kr by Ignoring Pc (Pc=0)

Even though Pc plays an important role in multiphase flow behaviour, the imbibition Pc is often ignored in reservoir simulation studies [23, 61]. 'Ignoring Pc' here means that the imbibition capillary pressure is equal to zero. This assumption most likely would reflect any capillary force existing in the flow behaviour into the kr curve. To understand the effect of ignoring Pc, kr that matches the numerical experimental data by assuming that Pc is equal to zero was estimated. The match between the reference data and the simulated oil production total, as well as the pressure drop, is shown in Figure 3-7:

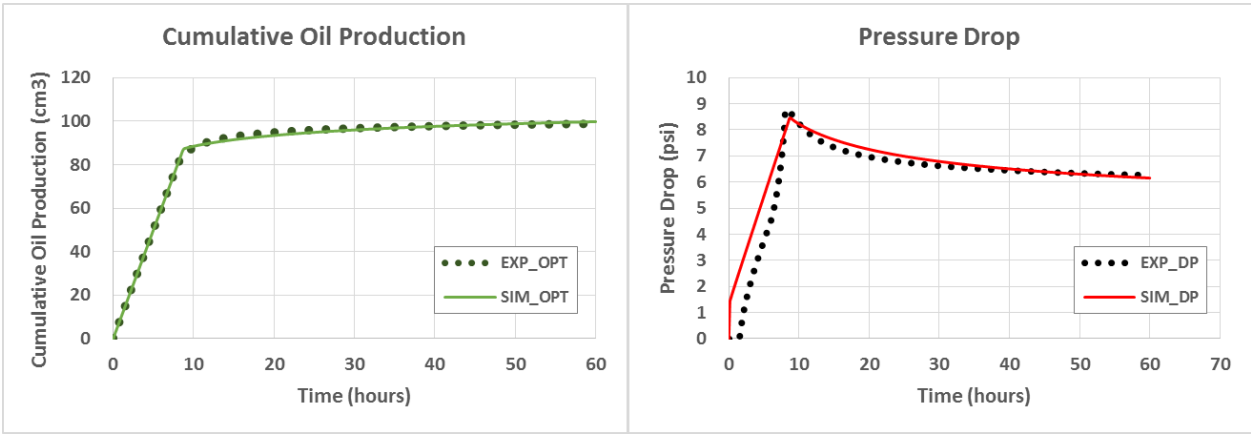

Figure 3-7: Experimental versus simulated oil production total and the pressure drop for the case where kr was estimated by assuming Pc is equal to zero

The estimated imbibition oil-water relative permeability when Pc is equal to zero is shown in Figure 3-8:

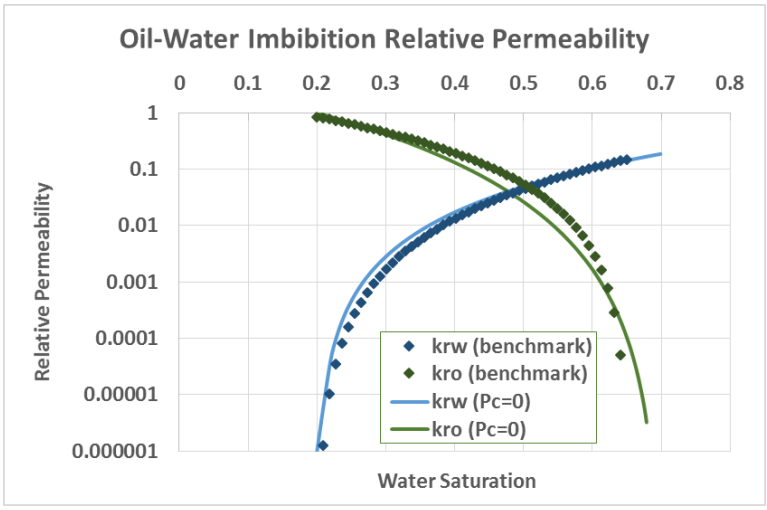

Figure 3-8: Best match relative permeability when Pc=0 (The dots are the benchmark flow functions used to generate the numerical experimental data.)

Figure 3-8 shows a clear difference between the benchmark and the estimated kr. The significance of such a difference is case dependent; therefore, further investigation is needed to understand how much the estimated kr when Pc is ignored can affect the reservoir-scale simulation. For that, a reservoir-scale cross-section mimicking similar core-flood properties is discussed in section 5.1. The estimated kr at the valid saturation range has lower oil-relative permeability (kro). When capillary pressure is ignored, water as the wetting phase will have higher mobility due to the absence of the force acting to disperse the wetting phase along the rock surface. Therefore, the oil will have lower mobility to mimic the same flow behaviour observed in the experiment. To avoid this difference, Pc should be properly accounted for.

3.2.3 Estimation of kr by Providing Pc

In this section, the Pc (assuming it could be obtained from different experiments) is provided for the kr estimation process. Here, the imbibition oil-water capillary pressure was used in addition to the same ranges for Sor, krw (Sor), and kro (Swi); then oil-water imbibition relative permeability was estimated to match the experimental data. The match with the reference experimental data was perfect, and the resulting kr, labelled as 'kr (Pc_known)', is shown in Figure 3-9:

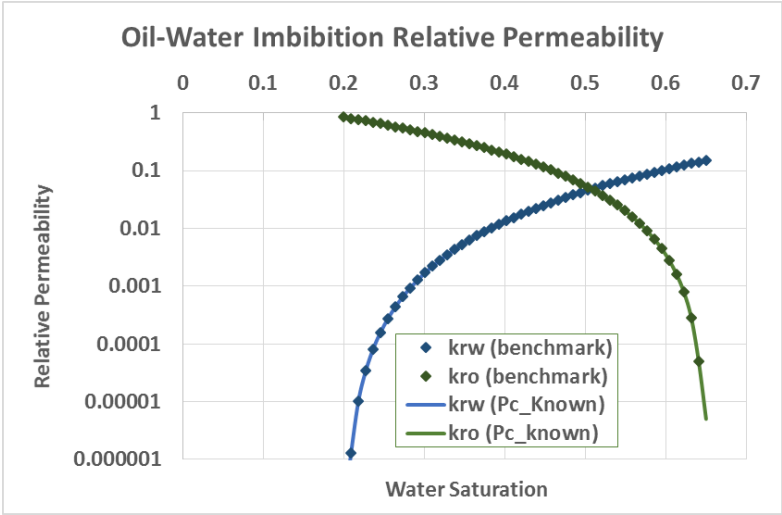

Figure 3-9: Relative permeability when Pc is given (The dots are the benchmark kr used to generate the numerical experimental data)

Figure 3-9 shows a better estimation of oil-water relative permeability when Pc is known. Here, the same software (solver) and mathematical formula to generate experimental data and flow functions (kr and Pc) and the same system complexity were used for simplicity. This scenario is equivalent to the case where Pc and kr are measured on the same core using the same core-flood experiment conditions. However, in real cases, actual experimental data will most likely be more complex, and the match will not be as easy and straightforward as in this study.

By comparing Figure 3-6, Figure 3-8, and Figure 3-9, it can be seen that providing Pc curve is an essential step before estimating kr from displacement experiments. Furthermore, the input two-phase kr and Pc are used by empirical models to estimate three-phase kr and Pc as discussed in the next section.

3.3 Three-Phase Relative Permeability Hysteresis Parameters

Because WAG injection is a three-phase process, an appropriate choice of a three-phase oil-relative permeability model, such as STONE I, STONE II, or saturation weighted

interpolation (SWI), must be included in the simulation model. (More details about these models can be found in sections 2.1.2 and 2.1.4 [32, 33, 39, 43, 45]).

In this thesis, the STONE I model is generally recommended for WAG injection simulation because it allows for residual oil modification based on trapped-gas saturation using a WAG-HYST model. However, this should be investigated thoroughly for any particular reservoir setting. Furthermore, in some cases, the STONE 1 Exponent model [40] should be used to improve the three-phase oil-relative permeability estimation (refer to section 2.1.5).

In addition, some specific input parameters for the numerical simulation model are required to define the cyclic-hysteresis behaviours based on the WAG-HYST model:

a. **Land's gas-trapping parameter [C]** controls the amount of trapped gas during the imbibition process (refer to section 2.1.1). If the WAG-HYST model is activated in the Eclipse simulator, then the simulator will use [C] and only the critical gas saturation [Sgc] from the input gas imbibition curve, and ignore the rest, to calculate the gas imbibition relative permeability.
b. **The gas secondary drainage reduction exponent [α]** is the exponent used to reduce gas-relative permeability during the gas secondary drainage (default is 0.1). More information can be found in section 2.1.7.1.
c. **The residual oil modification factor (a)** controls the minimum residual oil saturation (Sorm) when the STONE 1 model is used (refer to section 2.1.7.2). When (a) is equal to 1.0, then the same volume of trapped gas will be reduced from the minimum residual oil saturation. If (a) is less than 1, then only a fraction of the trapped gas will contribute to the reduction of the initial residual oil saturation.
d. **The three-phase water-relative permeability (krw^{3ph})** can be defined in the simulation model and is usually lower than two-phase water-relative permeability (refer to section 2.1.7.3).

To obtain the WAG-HYST parameters, several three-phase core-flood experiments are required (recommended). In the next section, these suggested three-phase displacement experiments are discussed.

3.4 Recommended Three-Phase Displacement Experiments

The WAG-HYST parameters can be estimated from carefully obtained experimental data. In addition, as established previously, the WAG injection can start with the water cycle (WAG) or the gas cycle (GAW). Therefore, it is recommended to perform the following experiments.

3.4.1 Three-Phase Water Imbibition [Sw = Swc] Experiment

Usually, the primary process means injecting a phase into a system for the first time. However, water naturally exists in the geological reservoirs before the oil has migrated to fill those reservoirs. Therefore, when the water phase is injected into the oil reservoirs, it should be a secondary process. Yet to keep the terminology similar to the gas injection cycles, the initial three-phase water imbibition process is called the 'water-oil-gas primary-imbibition' process. This means injecting water into a system containing movable oil and gas at initial connate water saturation (Swc) until the minimum possible residual oil saturation (Sorm) is reached. Figure 3-10 illustrates the water-oil-gas primary-imbibition process:

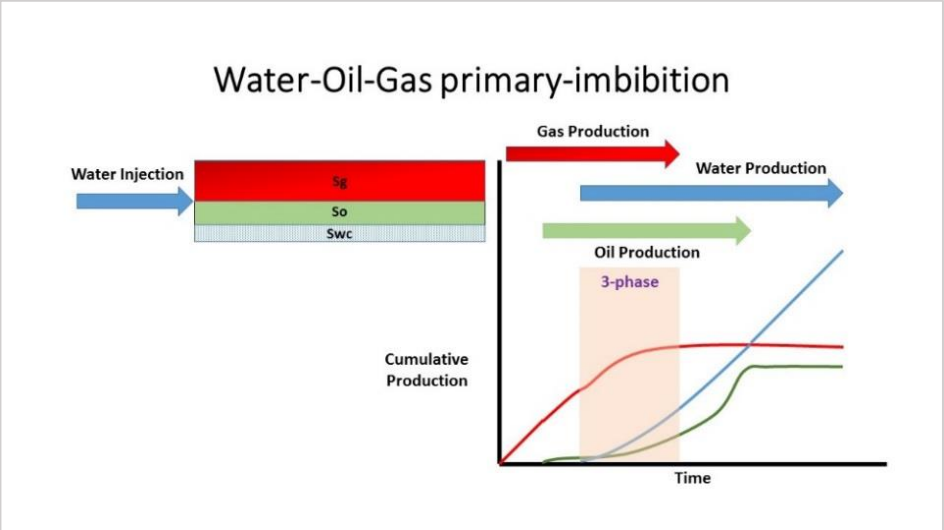

Figure 3-10: Water-oil-gas primary-imbibition process

When water is a wetting phase and is injected into a system containing movable oil and gas at initial connate water saturation (Swc), it should enter the smaller pores first. As a result, it can displace some oil (if any) from those small pores and then access the larger gas-filled pores. When the water enters the larger pores, it can displace some of the gas there. However, as a wetting phase, the water usually cannot displace all the gas, which will result in a trapped-gas saturation (at the middle of the pores). The valid three-phase

saturation range is when the three phases are simultaneously flowing out of the system (marked with three-phase shading in Figure 3-10).

3.4.2 Three-Phase Water Imbibition [Sw > Swc] Experiment

If water is injected into a three-phase system for the second time, the process is called a three-phase water secondary-imbibition process (Figure 3-11). This cycle means injecting water into a system containing movable oil, gas, and water saturation that is higher than the connate water saturation until the minimum possible residual oil saturation (Sorm) is reached. Figure 3-11 illustrates the three-phase water secondary-imbibition process:

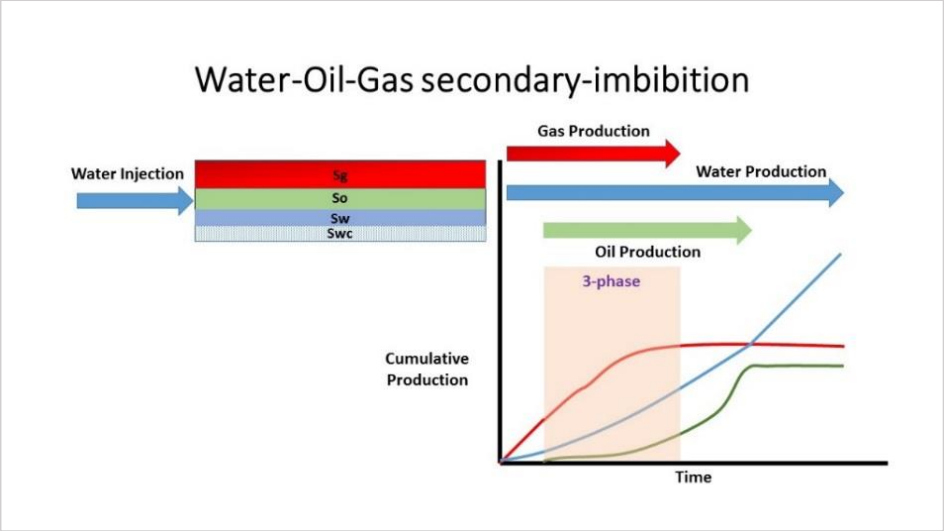

Figure 3-11: Water-oil-gas secondary-imbibition process

When gas is injected into a rock system, it will enter the larger pores first and poorly displace the existing water phase. Therefore, the water saturation that remains after the three-phase gas injection cycle is usually higher than the initial water saturation [Sw>Swc]. Thus, the three-phase water secondary-imbibition process is slightly different (in theory) than the three-phase water primary imbibition. For example, the [W3] cycle in the WAG process fits the definition of the three-phase water secondary imbibition where Sw is higher than Swc. However, the [W2] cycle in the GAW process fits the definition of the three-phase water primary-imbibition process [Sw=Swc]. This difference has not been previously discussed in the literature, but it is examined in more detail in chapter 4.

The valid three-phase saturation range is when the three phases are simultaneously flowing out of the system (marked with three-phase shading in Figure 3-11).

3.4.3 Three-Phase Gas Primary-Drainage [Sgi=0] Experiment

In this thesis, injecting gas for the first time into a system containing movable oil and water (Sw > Swc) until the minimum residual oil saturation (Sorm) is reached is called gas-oil-water primary drainage (Figure 3-12).

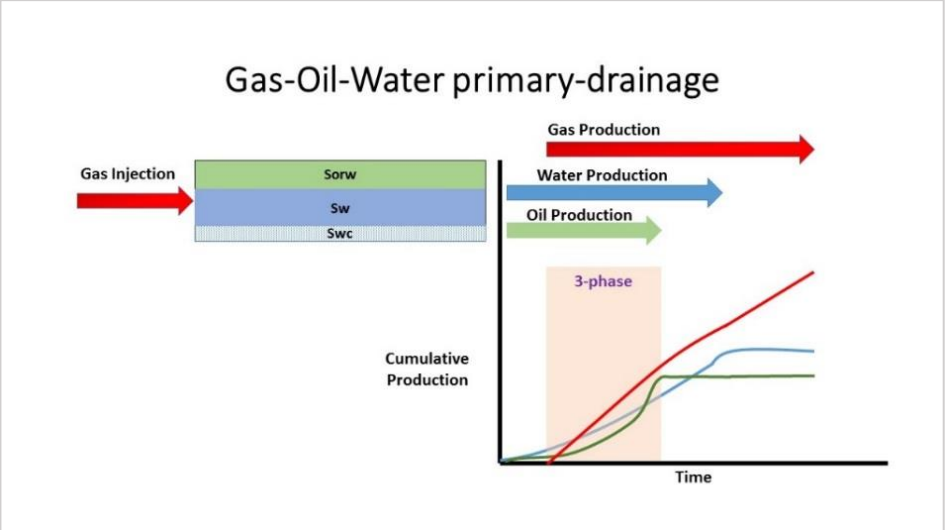

Figure 3-12: Gas-oil-water primary-drainage process

The gas injected into a three-phase system will displace the oil and water present in the larger pores first. However, the ability of the gas to displace water (if it is the wetting phase) is poor. Therefore, higher water saturation than Swc is expected to remain in the system after the gas cycle [Sw>Swc]. The WAG injection process [G2], which is the first gas injection cycle after the first water injection, is the best cycle to fit this drainage process. As mentioned, the valid three-phase saturation range is when the three phases are simultaneously flowing out of the system (marked with three-phase shading in Figure 3-12).

3.4.4 Three-Phase Gas Secondary-Drainage [Sgi>0] Experiment

The three-phase gas secondary-drainage process starts by injecting gas for the second time into a system containing movable oil, water, and gas, where the gas saturation is greater than zero (Sgi > 0), to reach Sorm (Figure 3-13).

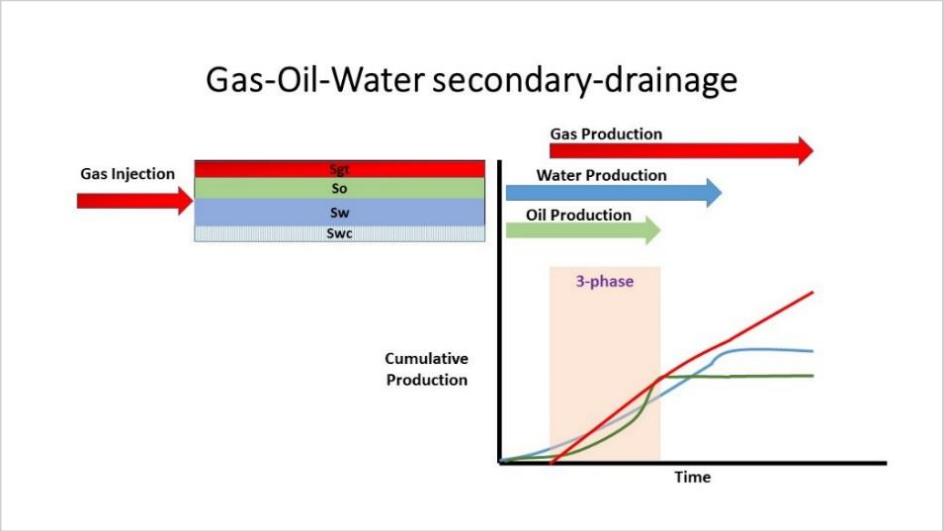

Figure 3-13: Gas-oil-water secondary-drainage process

There should be a difference between the gas injection cycle into a system for the first time, where Sg=0, and gas injection into a system for the second time, where Sg>0, especially if trapped-gas saturation [Sgt] is present. Therefore, in this thesis, a different definition is allocated for both cycles. The second gas injection cycle in the GAW injection process [G3] is an example of the three-phase gas secondary drainage. The valid three-phase saturation range is when the three phases are simultaneously flowing out of the system (marked with three-phase shading in Figure 3-13).

The three-phase core-flood experiments in this section should provide enough data to estimate the WAG-HYST parameters (section 3.3). The recommended estimation process is discussed in detail in the next section.

3.5 The Estimation Process of the WAG-Hysteresis Parameters

The WAG-HYST parameters introduced in section 3.3 are essential to properly account for three-phase cyclic hysteresis in simulating a WAG injection process. However, obtaining such parameters from a set of experimental data is not a straightforward exercise. Understanding the process to be modelled is critical in deciding which experimental condition is appropriate for estimating each parameter. Thus, the focus of this thesis is on the hysteresis behaviour affecting the relative permeability.

Furthermore, the Pc is also affected by the hysteresis process during cyclic injection of water and gas in that the two-phase Pc is somewhat easier to measure experimentally. However, for the three-phase flow system, measuring Pc is a challenge, and therefore it is often ignored. The current common ways to estimate three-phase Pc include network

modelling or an inverse approach of the modified Ensemble Kalman filter [62]. In the following sections, the estimation process for each hysteresis parameter is discussed.

3.5.1 Estimation of Land's Gas-Trapping Parameter [C]

The process of gas trapping is strongly influenced by the wettability condition as well as the pore structure. Theoretically, gas is trapped after water injection at the middle of the pores if the water is a wetting phase. However, if the water is not a strong wetting phase, it can displace the gas efficiently, and the Sgt will be very small. Similarly, gas will be trapped if the water could not enter the gas-filled pores due to pore distribution. Currently, the accepted relationship in the oil industry is Land's equation (Equation 2-1).

It has been observed by several researchers that the amount of trapped gas can vary in the same rock system if the WAG cycles are repeated several times. Based on the data analysed in this thesis, the same behaviour is observed [Figure 3-14]:

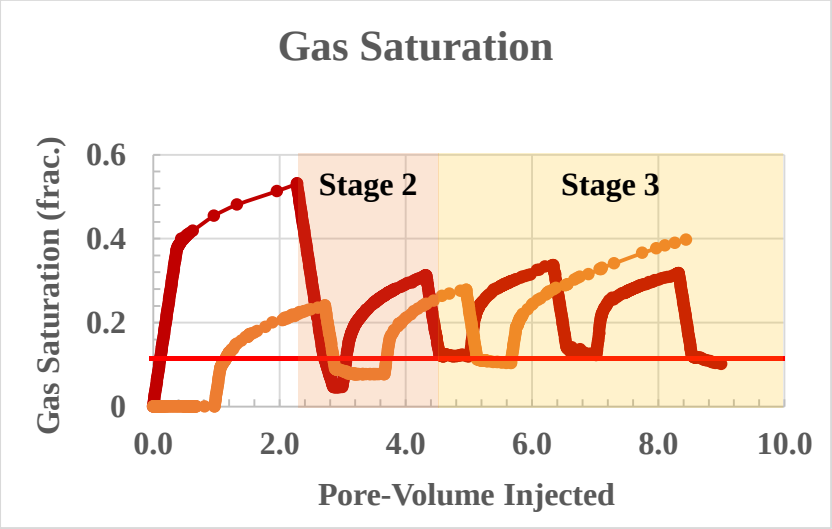

Figure 3-14: The gas saturation profile in the 65mD, mixed-wet core

Furthermore, this thesis suggests following the WAG injection process in three stages, as shown in Figure 3-14:

- **Stage 1:** the true two-phase flow system, where only two phases are flowing.
- **Stage 2:** the transition stage between two-phase to three-phase flow systems. This stage usually happens during the first three-phase water injection after the gas injection cycle. An example of such a process is the water injection cycle after gas injection in the GAW injection process [W2].

- **Stage 3:** the true three-phase flow system, where three phases have established their path in the system. This stage usually happens during the second three-phase water injection after the gas injection cycle. An example of such a process is the water injection cycle after the secondary-drainage gas cycle in the GAW injection process [W4].

Moreover, the trapped gas for stage 2 is different than in stage 3, as demonstrated in actual experimental data in Chapter 4.

Thus, this introduces the question of the best way to estimate gas-trapping behaviour in the WAG injection process. The suggested procedure to identify the gas-trapping parameter for any hysteresis cycle is introduced next. A hysteresis cycle here is any three-phase water injection cycle following a cycle of gas injection (water displacing gas in a three-phase system):

1) Identify the maximum gas saturation in the hysteresis cycle (usually the initial gas saturation).
2) Identify the minimum gas saturation [Sgt] in the hysteresis cycle.
3) Apply Equation 2-1 to calculate [C].

The calculated Land's parameter for stage 2 is sometimes lower than for stage 3. If the Land's gas-trapping parameter is different for the two stages, then the current WAG-HYST model cannot capture the true hysteresis behaviour. Therefore, different values of C should be used for each stage (section 6.2.5.1).

3.5.2 Estimation of Secondary Gas Drainage Reduction Exponent [α]

The gas secondary-drainage relative permeability is usually lower than the primary-drainage relative permeability. Such a reduction is related to the amount of free water present in the system. Therefore, the reduction exponent [α] will act to reduce the primary-drainage relative permeability curve based on Equation 2-2.

A commercial simulator would calculate the three-phase gas secondary-drainage relative permeability if the hysteresis option is activated. It would use the hysteresis parameters such as secondary drainage reduction exponent [α], Land's trapping parameter [C], and the input krg to estimate the gas secondary-drainage relative permeability.

By applying Equation 2-2, the secondary-drainage gas relative permeability [krg^{SD}] will be reduced based on the amount of free water available in the system. The higher the amount of movable water in the systems, the lower the gas relative permeability. Figure 3-15 shows the behaviour of the secondary-drainage gas relative permeability's endpoint [krg^{SD} (Sgmax)] as water saturation increases for various values of alpha:

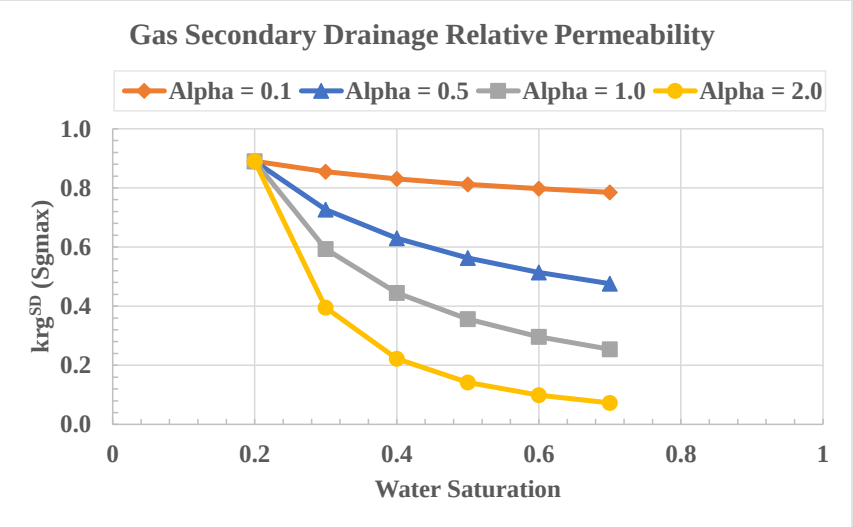

Figure 3-15: The behaviour of the secondary-drainage gas relative permeability's endpoint [krgSD (Sgmax)] as water saturation increases for various values of alpha

The drop in gas secondary-drainage relative permeability with increasing water saturation is significantly higher for higher values of alpha [α]. For example, as the water saturation increases from 0.20 to 0.70, the gas secondary-drainage relative permeability's endpoint is lowered from 0.89 to smaller values, as summarised in Table 3-3:

Table 3-3: The gas secondary-drainage relative permeability's endpoint for different values of [α] as the water saturation reaches 0.70 from the initial water saturation of 0.2

Alpha	krg^{SD} @ Sgmax
0.1	0.785
0.5	0.476
1.0	0.254
2.0	0.073

As the secondary-drainage gas relative permeability becomes lower, the pressure drop during secondary drainage becomes higher.

Alpha [α] is a very sensitive parameter that controls the pressure drop during three-phase gas injection cycles [DPg^{3ph}]. The best way to estimate [α] is to history-match the DPg^{3ph}

observed during the WAG injection experiments. However, before starting to tweak the values for the gas secondary-drainage reduction exponent [α], the input gas-trapping parameter [C] should be carefully obtained and inputted.

3.5.3 Estimation of Residual Oil Reduction Factor [a]

A WAG injection is an effective EOR method because it can reduce the residual oil saturation to a lower value. Therefore, more oil can be recovered by this process. However, the numerical simulation requests an input value [a] for each rock type to modify the two-phase residual oil saturation (Sori) when the WAG-HYST model is activated. By using the input residual oil reduction factor [a] in Equation 2-6, the minimum residual oil saturation (Sorm) can be calculated. As WAG injection is simulated, the simulator should reduce the residual oil saturation based on the amount of trapped-gas saturation calculated in each grid block.

The residual oil reduction factor [a] controls the ultimate additional oil recovery by WAG injection. The suggested process in this thesis is to use the following equation to assign an initial value for [a]:

$$a = \frac{Sori - Sorm}{Sgt} \qquad \textit{Equation 3-1}$$

where

a is the residual oil reduction factor;

$Sori$ is the initial residual oil saturation (two-phase);

$Sorm$ is the minimum residual oil saturation; and

Sgt is the trapped-gas saturation observed in the true three-phase process.

For example, if the initial residual oil saturation after the two-phase displacement experiment (Sori) is 30 per cent, after several WAG injection cycles, it is reduced to about 17 per cent. Then, by knowing the amount of trapped-gas saturation (15 per cent, for example), the initial guess for a-factor should be 0.87. In most cases, this would be a sufficient way to input the a-factor if the experimental data is analysed correctly. However, in some cases, the calculated value will be more than 1.0, especially for cases

where water blockage contributes to the additional oil recovery; then, a value of 1.0 should be used.

3.5.4 Estimation of Three-Phase Water Relative Permeability [krw^{3ph}]

The water relative permeability can significantly drop when free gas is present in the three-phase system. As a result, the pressure drops at the start of a three-phase water injection (DPw^{3ph}) usually increases until the saturation inside the system is reshuffled to allow the water to establish a flow path. After the water establishes a flow path, the DPw^{3ph} will start to decline but normally will be still higher than the maximum DP during two-phase flow [DPw^{3ph} > DPw^{2ph}].

The pressure drop (DP) data obtained from performing WAG injection experiments can provide valuable information about cyclic hysteresis. If DP during a three-phase water injection experiment (DP$_w^{3ph}$) is significantly higher than DP during a two-phase water injection experiment (DP$_w^{2ph}$), then the cyclic-hysteresis is important. Cyclic-hysteresis can reduce the three-phase water relative permeability (krw^{3ph}) based on the amount of free gas saturation to capture such increase in DP$_w^{3ph}$. An example of the difference in DP between two-phase and three-phase water injection is shown in Figure 3-16:

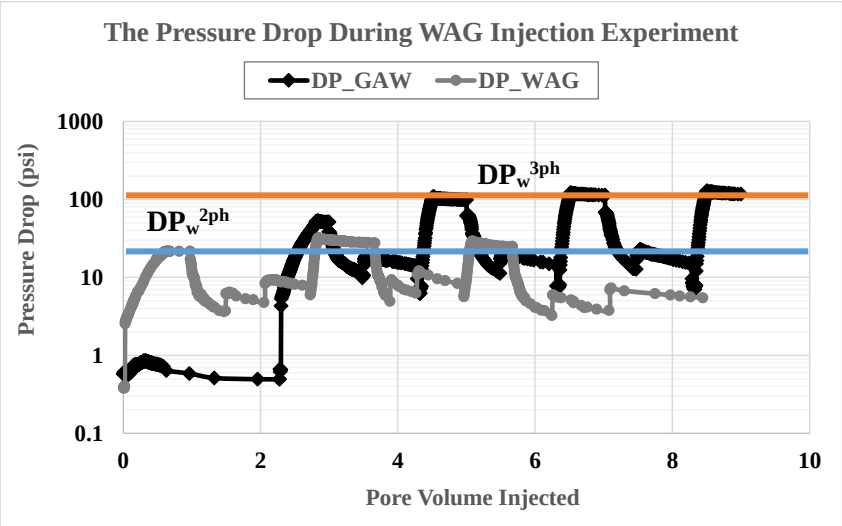

Figure 3-16: Pressure drop from three-phase core-flood experiments (WAG and GAW)

The blue line marks the DP during two-phase water injection [DP$_w^{2ph}$]. The DPw^{3ph} (the orange line) is significantly higher than the two-phase DP in a GAW injection process. To match the DPw^{3ph} in both processes, carefully estimated three-phase water relative

permeability (krw^{3ph}), which is lower than the krw^{2ph}, must be included in the simulation model.

The three-phase water relative permeability (krw^{3ph}) can be estimated from the data collected from a representative three-phase water injection process (section 3.4). From this cycle, the production and pressure data can be utilised to estimate the three-phase water-relative permeability by history-matching the data with a special emphasis on DPw^{3ph}. As currently there is no known commercial software to help in such an estimation process, this can be done using any automated history-matching tool or simply by using the following estimation process instead:

1) Calculate the difference in DP between two-phase water injection and true three-phase water injection processes.
2) Reduce the two-phase water relative permeability (krw^{2ph}) by multiplying the krw^{2ph} by the fraction [ω] calculated using the following equation:

$$\omega = \frac{DPw^{2ph}}{DPw^{3ph}} \qquad \textit{Equation 3-2}$$

The three-phase water relative permeability [krw^{3ph}] calculated by multiplying the krw^{2ph} by [ω] should be inputted into the simulation model as the three-phase water-relative permeability when the WAG-HYST model is activated. The value of ω can be used as a variable to match the DPw^{3ph}.

The efficiency of water displacement by gas is usually poor, and the minimum water saturation after gas injection is often much higher than connate water saturation. Therefore, the three-phase water-relative permeability must account for the minimum water saturation after the three-phase water drainage. Figure 3-17 shows the water saturation profile for both WAG and GAW in the 65mD mixed-wet core:

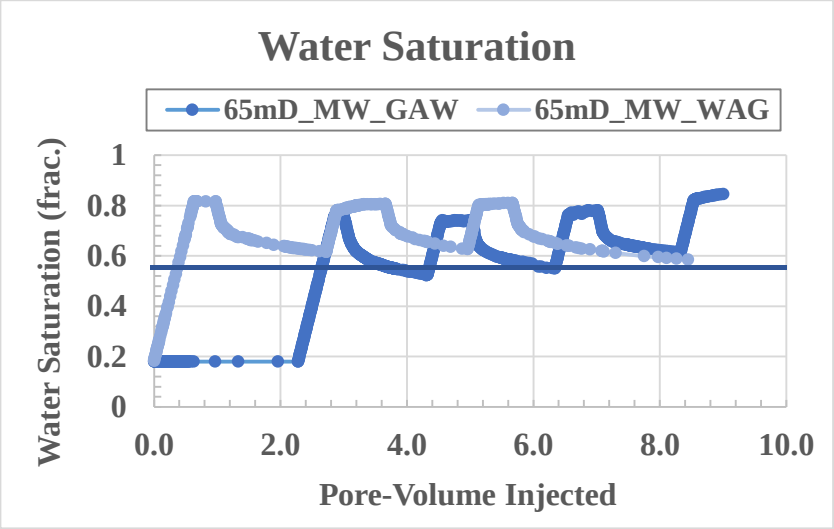

Figure 3-17: The water saturation profile for both WAG and GAW in the 65mD mixed-wet core

The connate water saturation (Swc) for the 65mD mixed-wet core is 0.20, and the average minimum water saturation in the three-phase system is about 0.58. To match the water saturation during three-phase flow, the minimum allowed water saturation must be kept around 0.58.

3.6 WAG Injection Experiments Utilised in This Thesis

A series of USS WAG injection experiments performed at water-wet and mixed-wet conditions were used in this study. These experiments were conducted by various researchers from Heriot-Watt University. To achieve near-miscible conditions with low gas/oil interfacial tension (IFT) of 0.04 mN/m, all experiments were conducted at 38°C (100°F) and 12.69 MPa (1840 psia). Furthermore, to eliminate the effect of gravity on the results of all experiments, the core was constantly rotated during the experiment [43, 53]. The reservoir cores leveraged in this study are either sandstone core samples (Sand) or limestone (Lime). The core properties and their most likely wettability conditions are listed in Table 3-4:

Table 3-4: Core properties for the experiments used to perform the core-scale simulation

#	Experiment	Core Length /cm	Core Diameter /cm	Permeability /mD	Porosity /%	Wettability
1	WAG_Sand	60.5	5	65	18	Water-Wet
2	GAW_Sand	60.5	5	65	18	Mixed-Wet
3	WAG_Sand	60.5	5	65	18	Mixed-Wet
4	GAW_Lime	60	5	45	15	Mixed-Wet
5	WAG_Lime	60	5	45	15	Mixed-Wet

Three fluids (water, gas, and oil) were used in these experiments. The water was prepared by dissolving 16 grams of NaCl and 4 grams of $CaCl_2$ in 2000 cubic centimeters distilled/degassed water [18]. The oil and gas phases were a binary mixture of 73.6 mole% of methane and 26.4 mole% n-butane. Furthermore, to ensure that no composition change (mass transfer) happened during the experiments, all the fluids were pre-equilibrated and kept at test pressure and temperature during the experiment [6].

The fluids properties used in the WAG injection experiments are listed in Table 3-5:

Table 3-5: Fluid properties for the experiments used to perform the core-scale simulation

Water (Brine)	Oil	Gas
10,000 ppm NaCl/$CaCl_2$	C1/nC4 mixture	C1/nC4 mixture
(μw) = 0.68 cp	(μo) = 0.0405 cp	(μg) = 0.0249 cp
(ρw) = 0.9929 g.cc	(ρo) = 0.3174 g.cc	(ρg) = 0.2114 g.cc

As stated in section 1.2, a different convention to refer to the injection cycles is used in this thesis: W to address water injection cycles and G for gas injection cycles. The first injection cycle is numbered as 1, the second cycle 2, and so forth, regardless of the phase type. This is to avoid having the same reference for a different process.

3.7 Conclusion

As petroleum reservoirs are located hundreds of metres underground, there are limitations to the information collected from these reservoirs. Some information can be obtained by logging multiple sections of the reservoir, flowing several wells, and recording pressure responses or collecting core samples to perform various laboratory experiments. However, most of the data collected by these methods must be processed and analysed to completely understand the results.

In this chapter, the process of obtaining, processing, and analysing rock-fluid properties such as kr, Pc, and cyclic hysteresis (WAG-HYST) parameters were discussed. These properties are usually estimated from core-scale data with the help of numerical simulation.

Since hydrocarbon's recovery is greatly controlled by both kr and Pc, their accuracy is crucial in any multiphase flow simulation. Two-phase kr and Pc are often numerically estimated from history-matching SS or USS core-flood experiments. As shown in this chapter, providing Pc (experimentally obtained) is essential in estimating kr for the same rock system. Failing to use the proper flow functions could lead to inaccurate results at two-phase and three-phase flow simulation.

Since WAG injection is a three-phase process, appropriate choices of the three-phase kr and cyclic hysteresis models are essential to accurately predict WAG injection performance at any scale. Currently, the oil and gas industry is accepting the use of core-scale experimental data to decide the proper three-phase model and hysteresis parameters. In this chapter, such experiments to collect enough data for WAG injection were suggested. Also, the procedure to obtain WAG hysteresis parameters was discussed. However, the demonstration of the process of obtaining such parameters from the experimental data is discussed in more detail in chapter 4.

The WAG injection experiments used in this thesis were introduced in this chapter as well (section 3.6), including a series of USS WAG injection experiments performed at water-wet and mixed-wet conditions. All experiments were conducted at near-miscible conditions with low gas/oil interfacial tension (IFT) of 0.04 mN/m. The analysis of and the WAG-HYST parameters for these experiments are discussed in the next chapter.

Chapter 4—Core-Scale WAG Injection Simulation

This chapter explains the numerical simulation process of a series of USS WAG experiments performed at Heriot-Watt University for the purpose of defining a methodology to obtain the WAG-HYST parameters and to identify the shortcomings of the commercially available cyclic-hysteresis models. The outcomes can provide a clear procedure to obtain WAG-HYST parameters from core-scale WAG injection experiments. This chapter also suggests a way to improve the accuracy of WAG injection simulation for future projects.

The ability to predict reservoir performance through numerical simulation is as good as the input parameters. If the latter do not represent the actual process, then the outcome of the simulation should be inaccurate. For example, inaccurate input of two-phase relative permeability should affect the ability of numerical simulation to correctly predict the water and oil production. It is similar for the three-phase relative permeability and hysteresis behaviour. Therefore, in this chapter, five actual WAG injection core-flood experiments are analysed and simulated using the methodology discussed in the following sections.

4.1 Core-Scale Simulation Model

Since all the experiments in this study were conducted in a way to eliminate the effect of gravity and mass transfer, a one-dimensional (1-D) black-oil simulation model should be sufficient. However, if the experimental procedure did not eliminate both gravity and miscibility effects during the experiments, a two-dimensional (2-D) compositional model will be more appropriate to model these experiments.

As widely published in the literature, there is usually a mismatch between experimental data and WAG injection core-scale simulation results. The reason for the mismatch, as explained in this thesis, is the misrepresentation of the real behaviour of cyclic hysteresis. Thus, in this section, the selection of the grid size and the process to model three-phase hysteresis in Eclipse-100 are discussed.

4.1.1 Selection of the Type, Size and Number of Grids

Simulation grids can be structured (regular shapes) or unstructured grids. The most common type of structured grids is the Cartesian grids. Structured grids can also be

defined in radial coordinates to construct cylindrical system. The radial system is usually used to model near-wellbore radial inflow dominated cases. The unstructured grids are irregular in shape which is constructed using several points. The unstructured grids are useful to define irregular reservoir geometry. Therefore, the selection of the type of grids depends on the objective of the simulation and the type of flow to be modelled. The flow in coreflood experiments are usually linear; therefore, a Cartesian grid should be sufficient to model the flow behaviour during coreflood WAG injection experiments.

The reservoir core samples used in the oil and gas industry are usually cylindrical in shape. However, the flow within the core is linear therefore the numerical simulation grids can be Cartesian (squared in shape). However, the bulk and pore volumes of the Cartesian grids must equal to the actual core volumes, as illustrated in Figure 4-1:

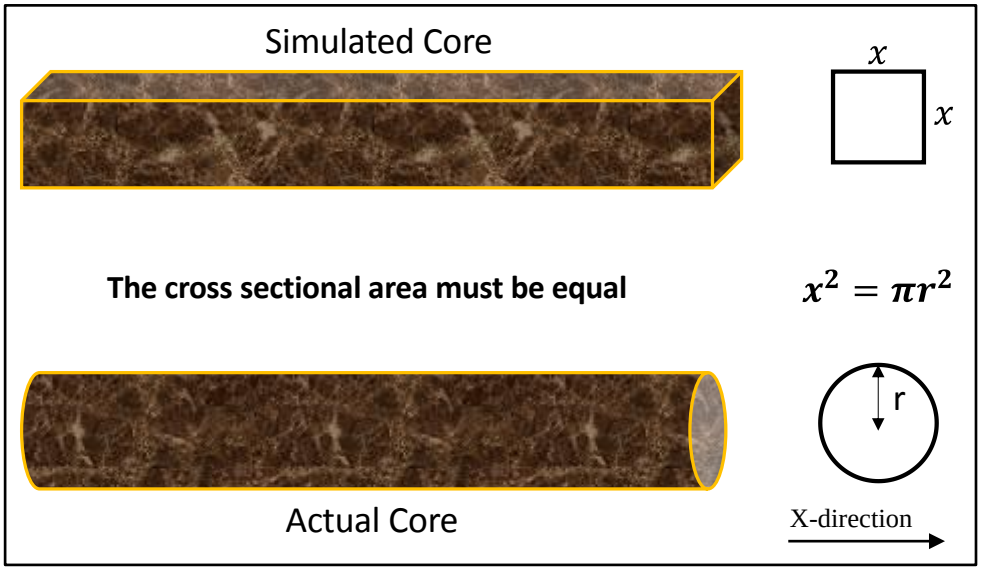

Figure 4-1: Converting the cross-sectional area for the actual core to a simulated core with Cartesian grids

For two-inch diameter cores, the DX (dimension in the x-direction) for the Cartesian grid should equal to 4.502cm [x = 4.502cm]. The accuracy of this calculation is essential to keep the core's pore volume (PV) the same. Therefore, it is recommended to have at least three decimal places for better accuracy.

In the core-scale simulation, especially for WAG injection, the recovery volume is normally small, and the numerical dispersion and convergence issues could significantly affect the simulation results. Thus, selecting the optimum number of grids to minimise

numerical dispersion is important. The most common and simplest way to do this is to run several scenarios, starting from the fewer number of grids and increasing it until the difference in the results is negligible. Then the number of grids where the results are preserved will be the optimum number. In this section, that came to one hundred grids for the five simulated core-flood experiments.

4.1.2 Selection of Time-Step Resolution

The numerical simulator solves the conservation of mass for each component (phase) in every grid block over time steps. If the change in saturation and pressure is rapid, then a smaller time step is needed. Each simulator is different; however, the user can decide a starting point where the simulator will use the input time step unless it needs shorter time intervals. In some cases, the simulator struggles to converge if the change in pressure (ΔP) and saturation (ΔS) is high during the time step requested. In this case, the solver might cut the time step and go for another one. However, there is a limit to the time-step cuts. Beyond this threshold, the simulation might take a very long time to complete. The user can reduce the threshold, allowing for more time-step cuts, but this should be done carefully to not affect the run time and the accuracy of the simulation results.

For the core-scale simulation, especially for WAG injection, the time-step selection is very important for stable simulation runs. Switching from one phase to another phase will cause a sharp shift in both pressure and saturation, which would mislead the simulator's guess of initial pressure and saturation in the next time step. Based on the Newton Raphson iteration process, the initial guess of each time step depends on the converged values of the previous time step [44, 63]. However, in WAG injection, the sharp change causes the simulator to cut numerous time steps in between cycles, which could lead to very long run times, and the simulator might stop running altogether. To limit further time step reductions, the solution is to have a very small time step between the cycles.

4.1.3 Model Validation Checklist

In the core-scale simulation, a small difference in pore volume or injected volumes could have a great impact on the simulation results. Therefore, the following checklist is recommended before starting the core-scale WAG injection simulation:

- ✓ Crosscheck the pore volume (PV) between the actual core and the simulation model (they must be equal).
- ✓ Double check the core dimensions and rock-fluid properties.
- ✓ Make sure the number of cycles and injected volumes are correctly modelled.
- ✓ Make sure the units used in the simulation match the units of input parameters.

It is a good practise to doublecheck the points above before any simulation project. The checklist for core-scale simulation is shown in Figure 4-2:

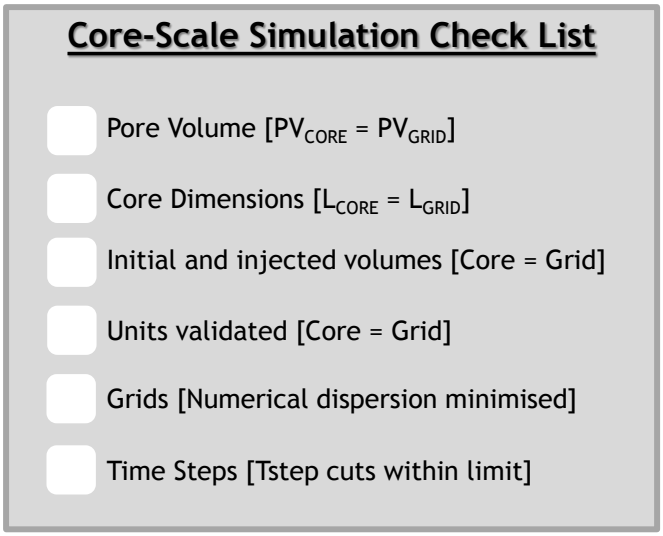

Figure 4-2: Core-scale simulation check-list

4.1.4 Simulation from Restart Files

A restart file is a simulation output file containing the required data to initiate the simulation from a specific time covered by the simulation run [44]. The advantage of this file is to allow the user to modify the input data (with some limitations) such as the number of wells, permeability, and relative permeability data. To write a restart file, the following steps are required:

- Run the base data file to the point of restart.
  - For example, run the base case until the gas secondary-drainage cycle [G1-W2-**G3**].
- Rename the base data file with a new file name.
  - For example, "RESTART_G3.DATA"
- Modify the input data in the new file as required (section 4.2).
- Edit "RESTART_G3.DATA":
  - Delete the equilibration data in the **Solution** section.

- Insert "RESTART" keyword in the **Solution** section to specify the restart file name and the report number.

- Delete the **Schedule** data included in the restart file.
  - For example, delete the schedule data from G1, W2, and G3 and keep the schedule data for the remaining cycles.
- Run the "RESTART_G3.DATA" file.

4.2 Suggested Methodology to Simulate WAG Injection Experiments

The hysteresis model for WAG injection (WAG-HYST), which was suggested by Larsen and Skauge [29], is based on limited cycles of WAG (G-W-G and W-G-W). Therefore, one could argue whether the WAG-HYST model can be used to match further cycles (W-G-W-***G-W-G*** or G-W-G-***W-G-W***). However, estimating the hysteresis parameters from the first hysteresis cycle and running a single-forward simulation might not correctly predict the WAG injection performance. Thus, some researchers suggested new three-phase models [31, 49]. Alternatively, the approach suggested in this thesis to update WAG-HYST parameters should improve the simulation match to the experimental data using the current simulator capabilities. Based on several tests, the following process produced better results:

1) Set up the simulation model in a way to allow flexible restart after each hysteresis cycle (section 4.1.4).
2) Ensure that the number of grids used in the model is sufficient to minimise numerical dispersion (one hundred grids were enough for this study, as mentioned in section 4.1.1).
3) Activate the hysteresis option (section 6.3), use the STONE 1 three-phase relative permeability model, and then run the first hysteresis cycle (W1-G2-W3 or G1-W2-G3) and stop the run to write a restart file. If needed, modify the following to improve the match:
   a. STONE 1 Exponent (η) to capture the oil recovery during three-phase gas injection if needed:
      i. For high oil saturation [S_o>0.30], use exponent values above 1.0.
      ii. For low oil saturation [S_o<0.15], use exponent values below 1.0.
   b. three-phase water-relative permeability (krw^{3ph}) to match the pressure drop during three-phase water injection (DPw^{3ph})
      i. Usually, krw^{3ph} is less than krw^{2ph} and could be ten times lower.

c. the gas secondary-drainage reduction factor (α) to capture the pressure drop during three-phase gas injection (DPg^{3ph})
d. the residual oil reduction factor (a) to capture the ultimate oil recovery or recovered oil volume after three-phase water

4) Calculate Land's trapping parameter (C) for G1-W2 or G2-W3 using the following equation:

$$C = \frac{1}{Sgt} - \frac{1}{Sgm}$$

5) When a match is achieved from the first run, use the restart file to run the second part of the experiment (G4-W5-G6 or W4-G5-W6) with a new calculated (C), and modify the following to improve the match.
   a. the gas secondary-drainage reduction factor (α) to capture DPg^{3ph}
   b. The STONE 1 Exponent may need to be reduced to capture oil recovery since oil saturation (S_o) is usually lower for the second run.
6) If the second run was not enough to match the rest of the experiment, then a run for each hysteresis cycle (G-W) might be needed.

In the next section, the analysis and the simulation results of the core-flood experiments are discussed.

4.3 Core-Scale WAG Injection Simulation Analysis and Results

In this section, the WAG injection experiments listed in Table 3-4 are analysed and simulated to match the experimental results. The methodology suggested in section 4.2 was used to achieve the best match in all the experiments, each of which is discussed in more detail in the following sections.

4.3.1 WAG Injection Experiment on 65mD Water-Wet Sandstone

The core-flood experiment discussed in this section was performed on a 65mD water-wet sandstone core sample at 38°C (100°F) and 12.69 MPa (1840 psia) (experiment 1 in Table 3-4). The imbibition two-phase oil-water relative permeability and drainage two-phase oil-gas relative permeability were estimated from history-matching of the USS core-flood experiments (refer to section 3.2):

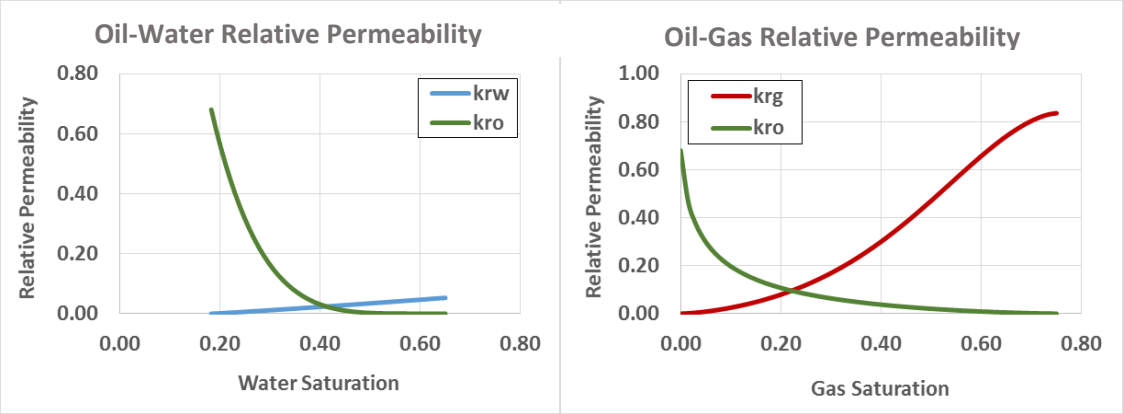

Figure 4-3: Imbibition two-phase oil-water and drainage oil-gas relative permeability for 65mD water-wet core

4.3.1.1 Analysis of the WAG Injection Experiment (65mD, Water-Wet)

The observed data from the near-miscible WAG injection experiment on a 65mD water-wet core revealed several key behaviours to be matched by simulation. The core was initially flooded by water to reach the residual oil saturation (Sorw), followed by gas and injection cycles. During each gas or water injection, additional oil was recovered to reach about 77 per cent of residual oil saturation after waterflood (about 32 per cent OOIP). Also, variable trapped-gas saturation (Sgt) was observed (Figure 4-4).

Since *in situ* saturation measurement was not available, saturation profiles were calculated from the injected and produced volumes of each phase. The average saturation profile of each phase can be calculated with the following equation:

$$Sn = Sni + (PVinj - PVprod) \qquad \textit{Equation 4-1}$$

where

Sn is the current phase's saturation;

Sni is the initial phase's saturation;

$PVinj$ is the cumulative pore volume injected of the particular phase; and

$PVprod$ is the cumulative pore volume produced of the particular phase.

Figure 4-4 shows the calculated average saturation profiles of each phase in this experiment:

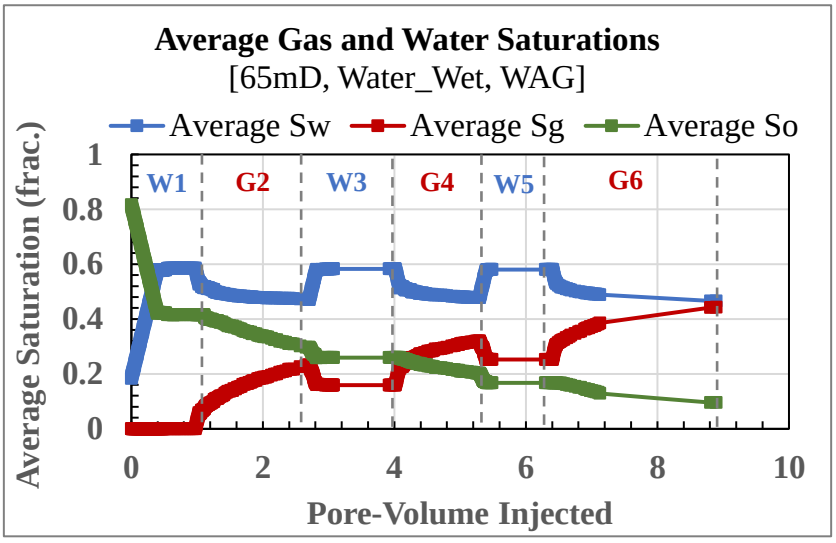

Figure 4-4: Water (blue), oil (green), and gas (red) saturation profiles for the 65mD water-wet core (WAG)

From the average saturation profiles of the near-miscible WAG injection experiment on a 65mD water-wet core, the following can be observed:

- During the second water injection cycle (W3), some oil recovery at the start of water injection was observed, but it stopped, and gas was trapped, with saturation around 0.156, and oil saturation ceased around 0.259.
- During the second gas injection cycle (G4), more oil was recovered after the gas injection.
- During the third water injection cycle (W5), some oil recovery at the start of water injection was observed, but it quickly stopped, and additional gas was trapped, with saturation around 0.252, which is higher than the first trapped gas saturation, and the new minimum oil saturation was about 0.169. The reduction in oil saturation is almost equal to the additional trapped gas saturation (0.09).
- During the third gas injection cycle (G6), more oil was recovered as the result of the gas injection.

Another important item of data to be matched is the DP across the core. The observed DP is illustrated in Figure 4-5:

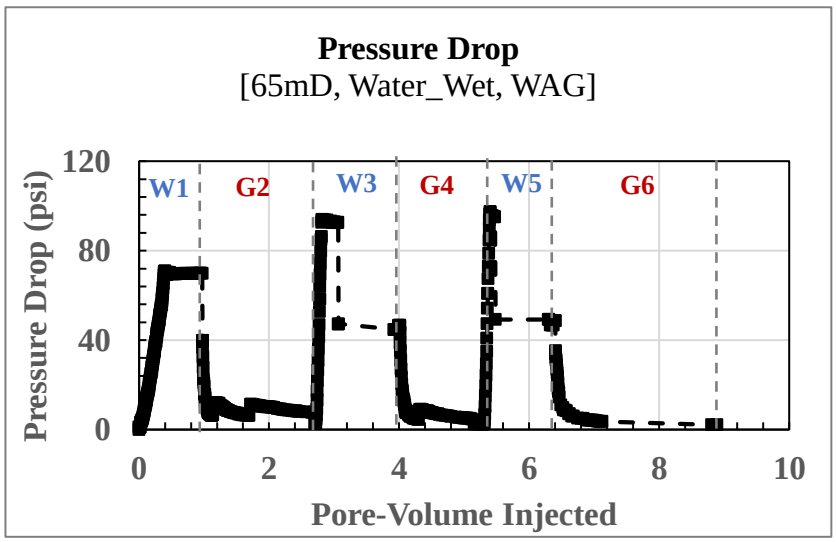

Figure 4-5: Pressure drop across the core during WAG injection performed on 65mD, water-wet (WAG)

The DP at the end of two-phase water injection (W1) was around 70 psi. As soon as the gas injection cycle (G2) started, the DP sharply dropped and fluctuated between 5 and 12 psi due to the bump floods with different gas injection rates. As soon as the injection phase changed from gas to water (W3), a significant DP was observed (93 psi). After approximately one pore volume injection, no more oil recovery was observed, and DP at the end of the cycle was around 45 psi. Similar behaviour was observed in further cycles. Therefore, matching these behaviours can be achieved by proper cyclic-hysteresis modelling.

4.3.1.2 Simulation Results and Discussions (65mD, Water-Wet, WAG)

As per the discussion in section 4.3.1.1, cyclic hysteresis is needed to capture such observed behaviours. Since the experimental trapped-gas saturation is variable, then a new methodology to update the hysteresis parameter is necessary. To illustrate the need for modifying the WAG-HYST parameters, two simulation runs were conducted. The first uses the parameters estimated from the first hysteresis loop (W1-G2-W3) for the entire experiment. However, by applying the procedure suggested in section 4.2, the modified simulation parameters were calculated and summarised in Table 4-1:

Table 4-1: Summary of the input parameters used in the simulation of 65mD water-wet core

Injection Cycles	STONE 1 Exponent (η)	Land's Parameter (C)	Reduction Exponent (α)
W1-G2-W3	6.5	2.00	0.45
G4-W5-G6	0.9	0.81	1.20

Both simulation results were compared, and the modified simulation showed a better match to the experimental data (Figure 4-6 and Figure 4-7).

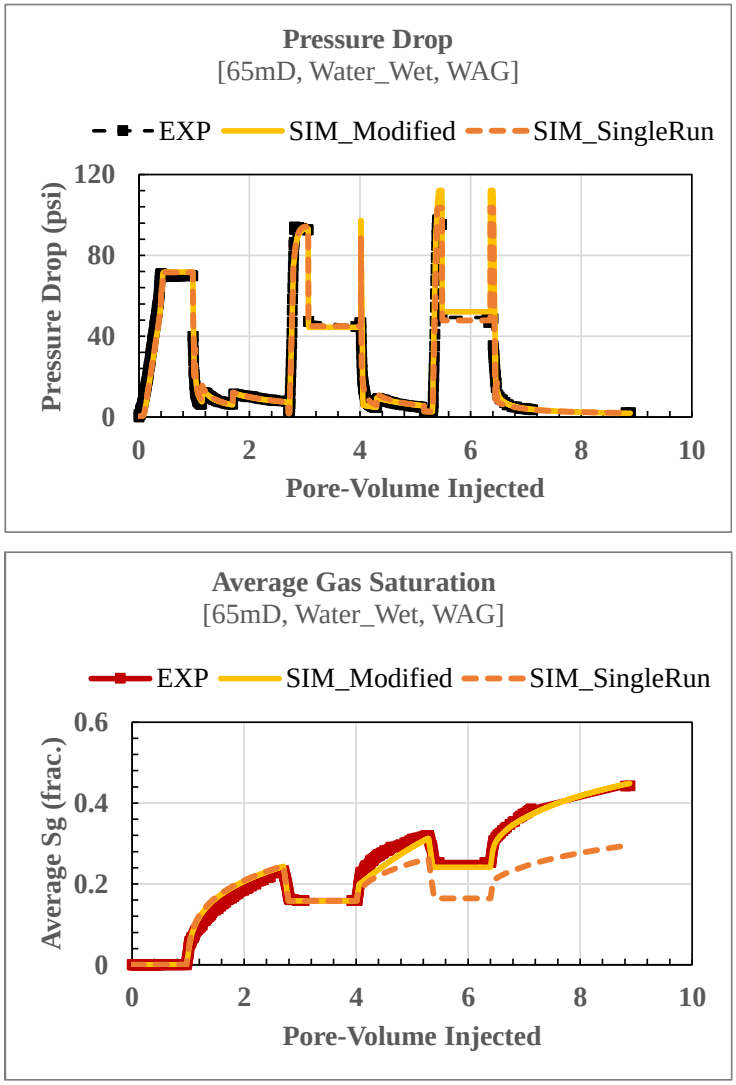

Figure 4-6: Simulation results for the 65mD water-wet WAG injection experiment (Top is the DP comparison of the experiment, single-run simulation, and modified simulation results. Bottom is the average gas saturation comparison of the experiment, single-run simulation, and modified simulation results.)

As shown in Figure 4-6, the modified simulation results matched the change in trapped-gas saturation and improved the DP match. Also, this modification improved the match for oil recovery, as shown in Figure 4-7:

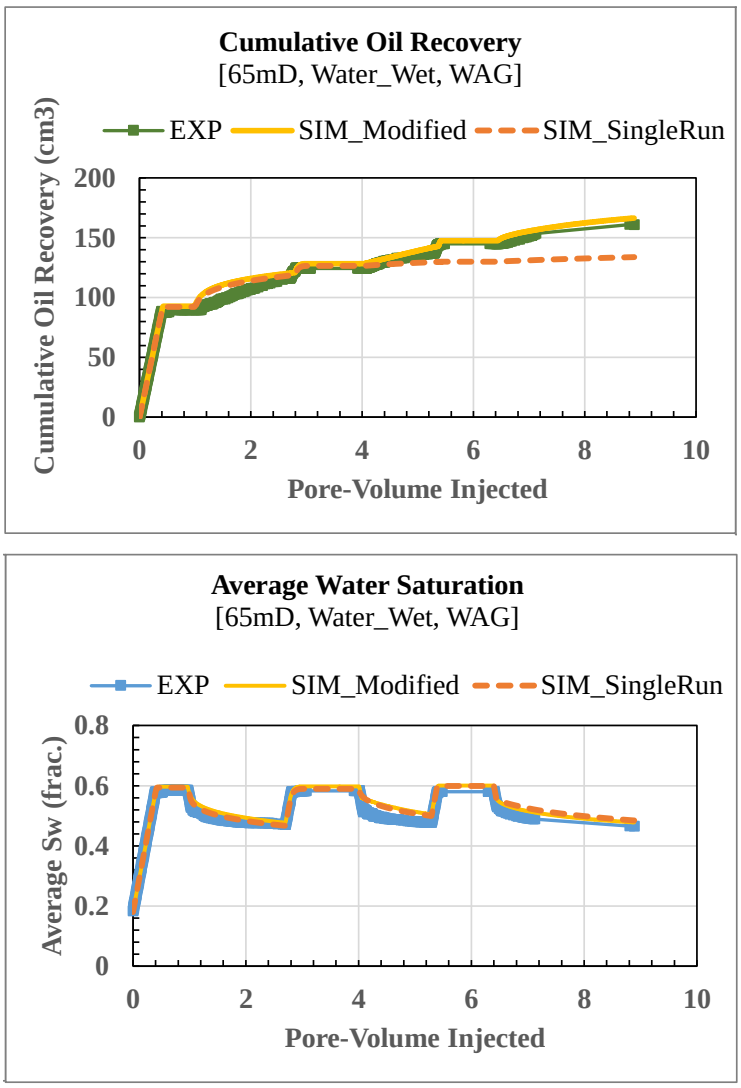

Figure 4-7: Simulation results for the 65mD water-wet WAG injection experiment. (Top is the cumulative oil recovery comparison of the experiment, single-run simulation, and modified simulation results. Bottom is the average water saturation comparison of the experiment, single-run simulation, and modified simulation results.)

As the DP during three-phase water injection cycles (DP_w^{3ph}) is significantly higher than during two-phase injection cycles (DP_w^{2ph}), the water-relative permeability must be reduced for the three-phase system, as shown in Figure 4-8:

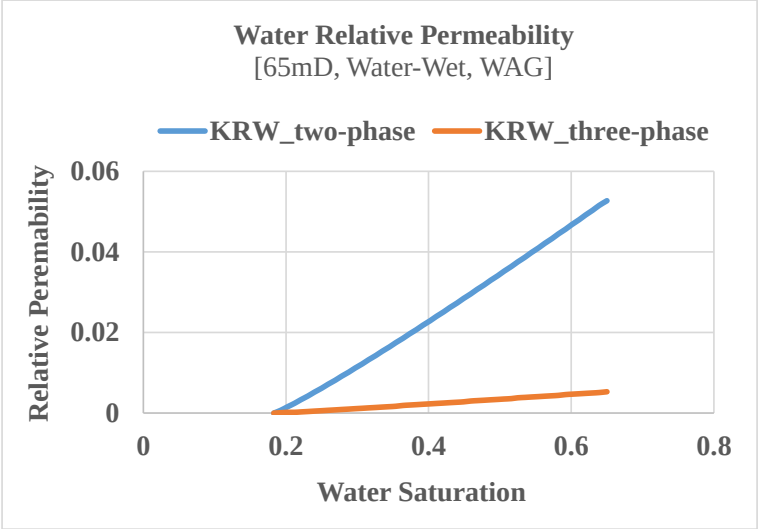

Figure 4-8: Two-phase and three-phase water-relative permeability for the 65mD water-wet core

Based on the input parameters mentioned in Table 4-1, and the DP matched by the three-phase water-relative permeability shown in Figure 4-8, the following observations could be drawn:

1) The STONE 1 Exponent must be higher than 1.0 initially when the oil saturation is relatively high (S_o=0.415), whilst the best match was achieved with an exponent less than 1.0 when the oil saturation decreased to lower values.
2) Land's parameter is kept as calculated from experimental data. For the first runs, Land's parameter was calculated to be 2.0, but for the second run, the calculation was 0.81.
3) For the first hysteresis cycle, the secondary gas reduction exponent was lower than in further gas injection cycles. This is probably due to the absence of trapped-gas saturation or the fact that this gas cycle (G2) fits the definition of neither a primary drainage-gas nor secondary drainage-gas injection cycle (refer to section 3.5.2 for more details).
4) Residual oil modification factor (a) was kept as 1.0 for the whole experiment.
5) The water-relative permeability was reduced ten times to match the DP during three-phase water injection (DP_w^{3ph}) (Figure 4-8).

4.3.2 WAG Injection Experiment on 65mD Mixed-Wet Sandstone

For this experiment, a complete set of core-flood experiments, performed on a 65mD mixed-wet sandstone core sample at 38°C (100°F) and 12.69 MPa (1840 psia), was used (the details of these experiments can be found in Fatemi et al., 2012 [6]). The calculated oil/gas interfacial tension (IFT) is 0.04 mN/m, which means the process is near miscible.

This mixed-wet sandstone core was used to perform several experiments to generate enough data for this study. One set of experiments started with a two-phase water imbibition process, followed by gas drainage, known as a WAG. Table 4-2 summarises the WAG experiments performed on the 65mD mixed-wet sandstone core:

Table 4-2: Summary of the WAG experiments performed on 65mD mixed-wet

Cycle	Description
W1-WAG	Two-phase water imbibition (water-oil)
G2-WAG	Three-phase gas drainage (gas-oil-water)
W3-WAG	Three-phase water secondary imbibition
G4-WAG	Three-phase gas secondary drainage
W5-WAG	Three-phase water secondary imbibition
G6-WAG	Three-phase gas secondary drainage

The imbibition two-phase oil-water relative permeability and drainage two-phase oil-gas relative permeability were estimated from history-matching of the USS core-flood experiments (G1 for gas-oil and W1 for water-oil) from experiments 2 and 3 from Table 3-4. The two-phase relative permeability curves are shown in Figure 4-9:

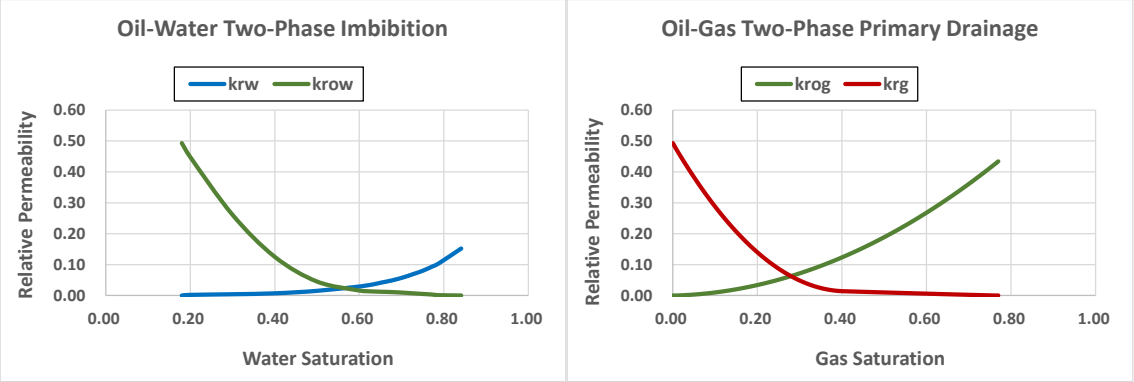

Figure 4-9: Imbibition two-phase oil-water and drainage oil-gas relative permeability for 65mD mixed-wet core

4.3.2.1 Analysis of WAG Injection Experiment (65mD, Mixed-Wet)

The average saturation profile for oil, water, and gas is shown in Figure 4-10:

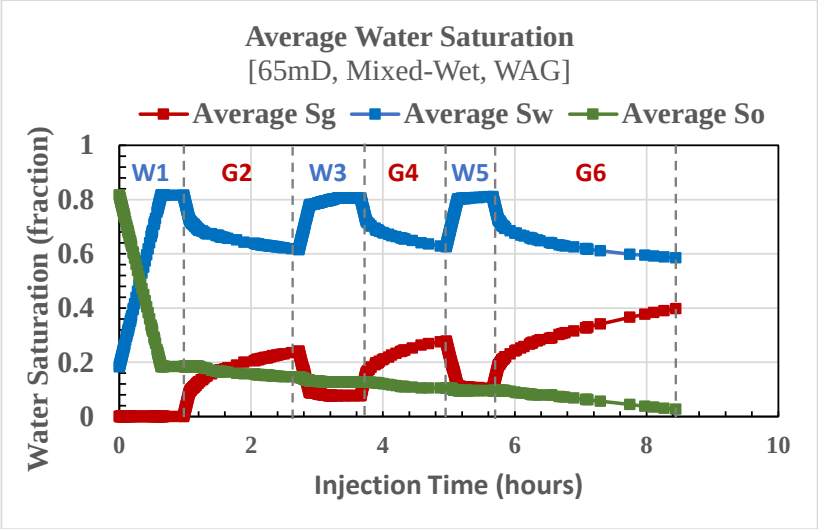

Figure 4-10: Water (blue), oil (green), and gas (red) saturation profiles for the 65mD mixed-wet core

From the average saturation profiles of the near-miscible WAG injection experiment on a 65mD mixed-wet core, the following can be observed:

- During the second water injection cycle (W3), some oil recovery at the start of water injection was observed, but it stopped, and gas was trapped, with saturation around 0.077, and oil saturation ceased around 0.127.
- During the second gas injection cycle (G4), more oil was recovered as the result of gas injection ($\Delta So = 0.022$).
- During the third water injection cycle (W5), some oil recovery at the start of water injection was observed, but it quickly stopped, and additional gas was trapped, with saturation around 0.103, which is higher than the first trapped gas saturation, and the new minimum oil saturation about 0.096. The reduction in oil saturation is almost equal to the additional trapped gas saturation (0.031).
- During the third gas injection cycle (G6), more oil was recovered as the result of gas injection ($\Delta So = 0.069$).

These six experiments (Table 4-2) are required to define the WAG injection recovery process. In addition, Figure 4-11 shows the DP for the WAG experiments performed on a 65mD mixed-wet core at low gas-oil interfacial tension (near miscible):

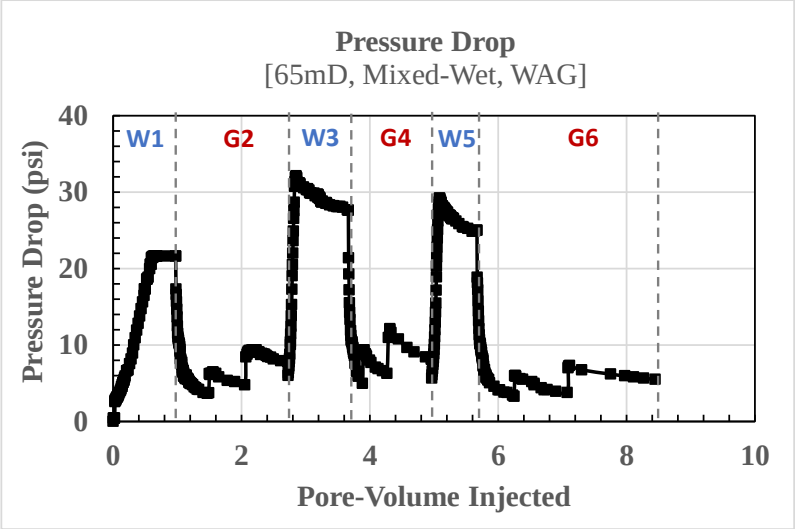

Figure 4-11: Pressure drop across the core during WAG injection performed on 65mD, mixed-wet

The DP at the end of the two-phase water injection (DPw^{2ph}) is equal to 21.6 psi. Then at the start of gas injection, it fluctuates between 4 and 10 psi due to the bump floods with different gas injection rates. As soon as the injection phase changed from gas to water (W3), the DP increased to around 30 psi. Similar behaviour was observed in further cycles. Therefore, matching such behaviours can again be achieved by cyclic-hysteresis mechanisms.

4.3.2.2 Simulation Results and Discussions (65mD, Mixed-Wet, WAG)

The WAG injection process was modelled and simulated using the methodology suggested in section 4.2. The hysteresis parameters used in both runs are summarised in Table 4-3:

Table 4-3: Summary of the input parameters used in the simulation of 65mD mixed-wet core (WAG)

Injection Modes	STONE 1 Exponent (η)	Land's Parameter (C)	Reduction Exponent (α)
W1-G2-W3	1.50	8.9	0.08
G4-W5-G6	0.90	5.9	0.08

The single-run, as well as the modified simulation, results are shown in Figure 4-12:

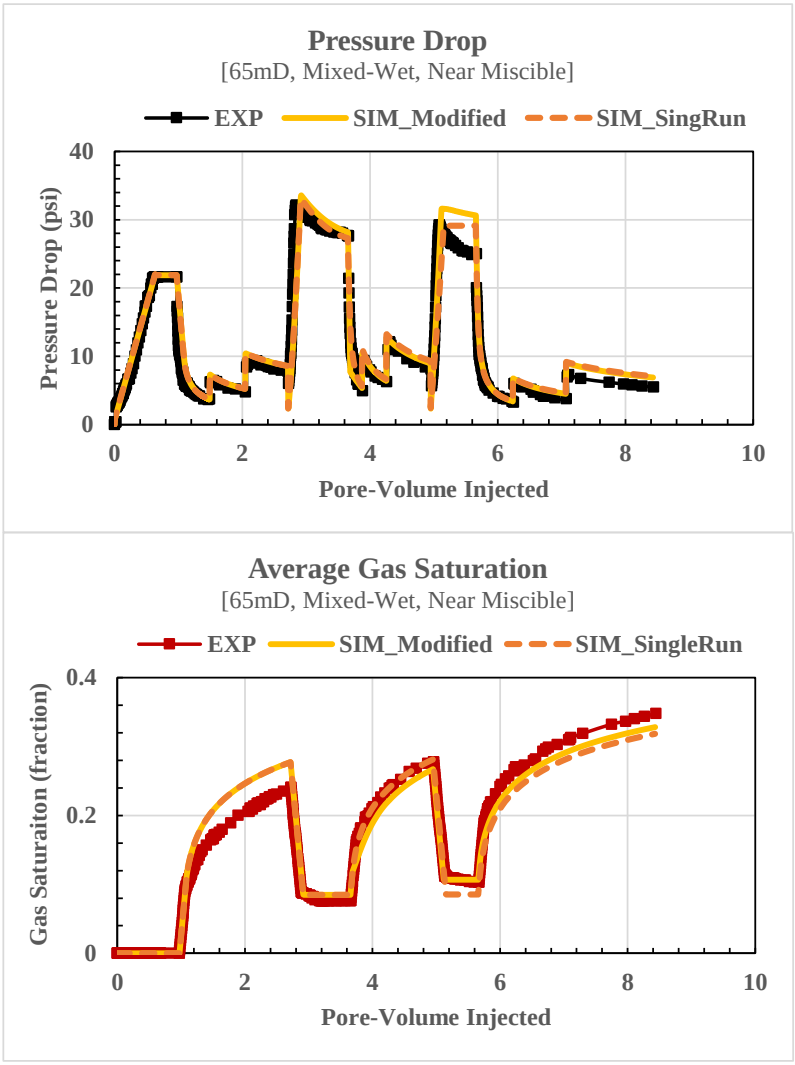

Figure 4-12: Simulation results for the 65mD mixed-wet WAG injection experiment. (Top is the DP comparison of the experiment, single-run simulation, and modified simulation results. Bottom is the average gas saturation comparison of the experiment, single-run simulation, and modified simulation results.)

The modified simulation results slightly improved the simulation prediction to the trapped-gas saturation in the W5 injection cycle. However, in general, both simulation runs reasonably predicted the experimental results as shown also in Figure 4-13:

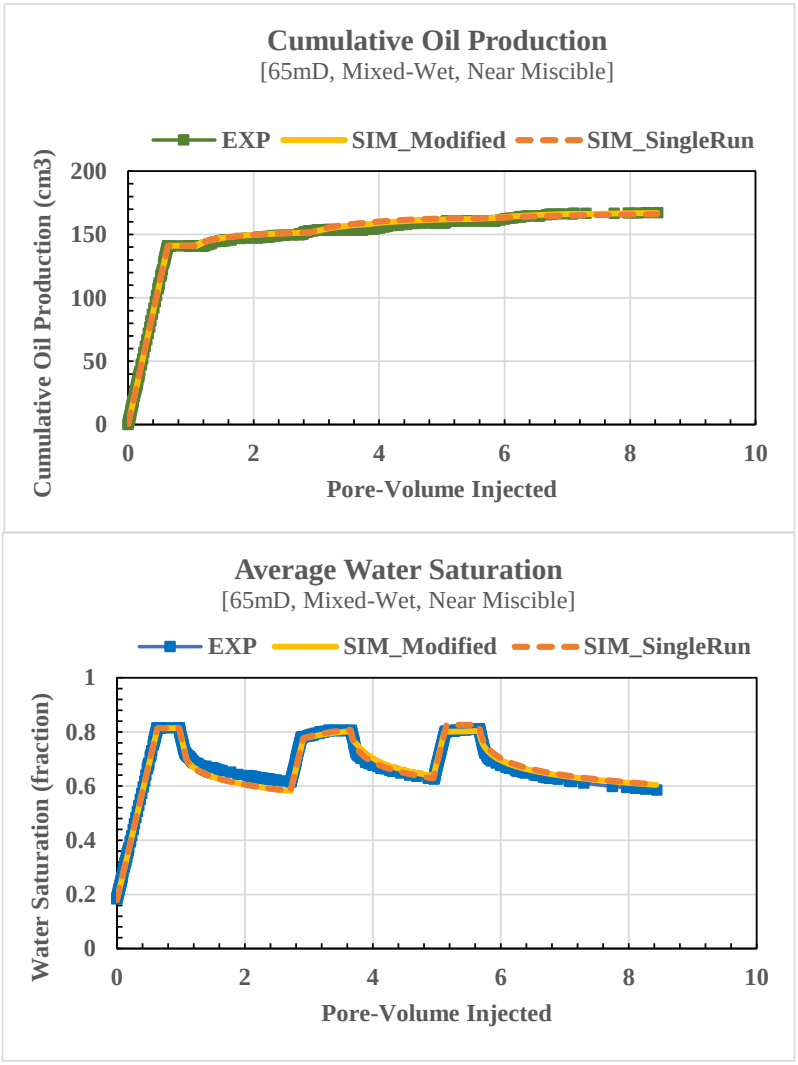

Figure 4-13: Simulation results for the 65mD mixed-wet WAG injection experiment. (Top is the cumulative oil recovery comparison of the experiment, single-run simulation, and modified simulation results. Bottom is the average water saturation comparison of the experiment, single-run simulation, and modified simulation results.)

The single-run and modified simulations are very similar. However, Land's trapping parameter must be modified slightly to better capture the Sgt, as shown in Figure 4-12 (bottom).

As the DP_w^{3ph} is higher than the DP during DP_w^{2ph}, the water-relative permeability must be reduced for the three-phase system, as shown in Figure 4-14:

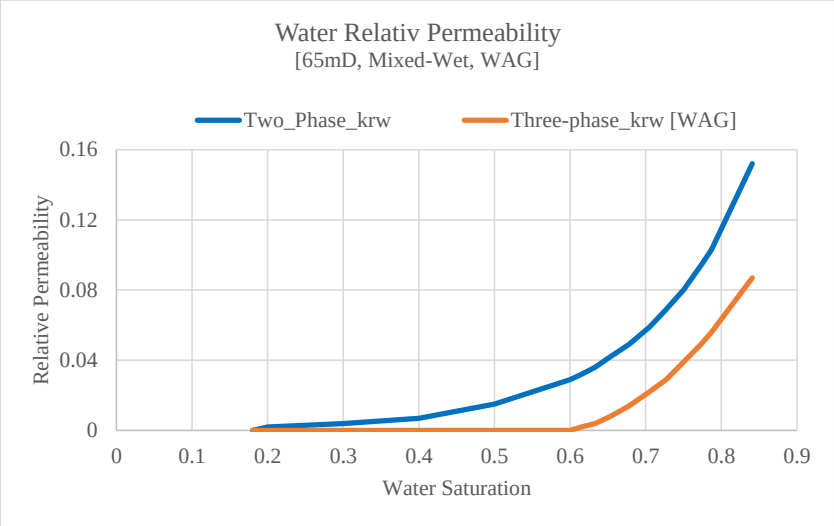

Figure 4-14: Two-phase and three-phase water-relative permeability for the 65mD mixed-wet core (WAG)

Based on the input parameters in Table 4-3, and the DP matched by the three-phase water-relative permeability shown in Figure 4-14, the following observations could be drawn:

1) The STONE 1 Exponent was modified to be slightly higher than 1.0 to improve the match of the oil saturation during three-phase gas cycles.
2) Land's parameter was kept as calculated from experimental data. For the first runs, the parameter was calculated to be 8.9, but for the second run, the calculation was 5.9.
3) The secondary gas reduction exponent was found to the same for both runs.
4) Residual oil modification factor (a) was estimated to be 0.32. However, for the last gas injection cycle (G6), residual oil modification factor [a] was assigned to be 1.0.
5) The water-relative permeability was reduced to match the DP during three-phase water injection (DP_w^{3ph}), as illustrated in Figure 4-14.

4.3.3 WAG Injection Experiment on 65mD Mixed-Wet Sandstone (GAW)

The second set of experiments performed on the 65mD mixed-wet core started with a two-phase gas drainage process followed by water imbibition, referred to as GAW. Table 4-4 summarises the experiments performed on the 65mD mixed-wet sandstone core:

Table 4-4: Summary of the GAW experiments performed on the 65mD mixed-wet sandstone core

Cycle	Description
G1-GAW	Two-phase gas first drainage (gas-oil)
W2-GAW	Three-phase water imbibition (water-oil-gas)
G3-GAW	Three-phase gas second drainage
W4-GAW	Three-phase water second imbibition
G5-GAW	Three-phase gas third drainage
W6-GAW	Three-phase water third imbibition
G7-GAW	Three-phase gas fourth drainage
W8-GAW	Three-phase water fourth imbibition

The imbibition two-phase oil-water relative permeability and drainage two-phase oil-gas relative permeability are the same as the ones shown in Figure 4-9.

4.3.3.1 Analysis of the WAG Injection Experiment (65mD, Mixed-Wet, GAW)

The average oil, water, and gas saturations are shown in Figure 4-15:

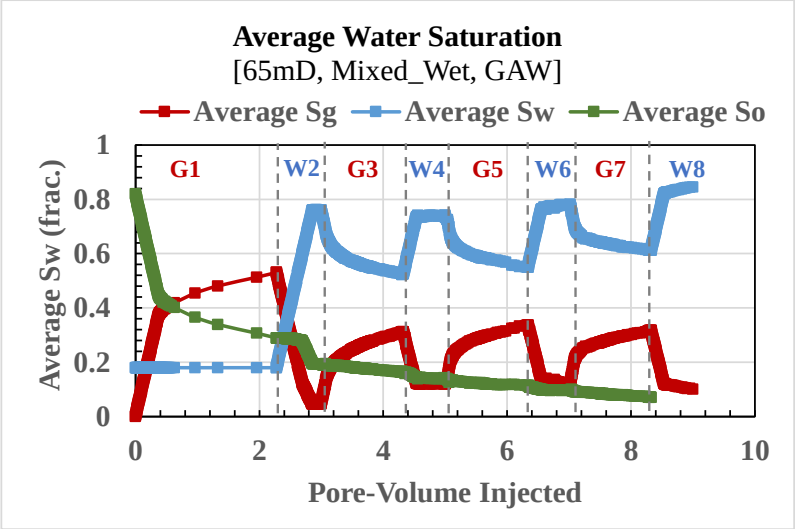

Figure 4-15: Water (blue), oil (green), and gas (red) saturation profiles for the 65mD mixed-wet core (GAW)

From the average saturation profiles of the near-miscible GAW injection experiment on a 65mD mixed-wet core, the following can be observed:

- During the three-phase water injection cycle (W2), there was significant oil recovery (11 per cent OOIP), which is around 21 cubic centimetres. The initial trapped-gas saturation in this cycle was around 0.046 and the minimum oil saturation around 0.193.

- During the second gas drainage cycle (G3), more oil was recovered (ΔSo = 0.03).
- During the second three-phase water imbibition cycle (W4), additional gas was trapped, with Sgt around 0.122, which is higher than the first trapped-gas saturation. The minimum oil saturation at the end of W4 was about 0.140. The reduction in oil saturation is equal to 0.053, which is approximately 70 per cent of the additional trapped-gas saturation (0.076). Therefore, the residual oil reduction factor (a) was inputted as 0.70.

Figure 4-16 shows the DP for the 65mD mixed-wet GAW experiments. There is a noticeable increase in DP between the first three-phase water injection (DP-W2 = 51 psi) and the second three-phase water injection cycles (DP-W4 ≈ 100 psi). This, of course, would affect the three-phase water-relative permeability input into the simulation model.

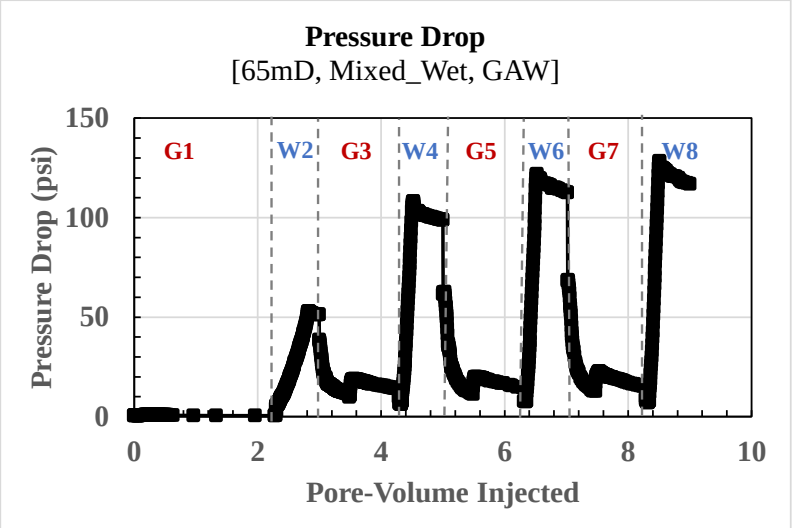

Figure 4-16 Pressure drop across the core during WAG injection performed on 65mD, mixed-wet (GAW)

The two-phase relative permeability here is the same as that shown in Figure 4-9. It should be noted that the input two-phase relative permeability will be used by the three-phase relative permeability model to calculate three-phase oil-relative permeability. Therefore, if the saturation range in the three-phase region is outside the valid saturation range in the two-phase experiment, then the three-phase model's ability to predict would be affected.

4.3.3.2 Simulation Results and Discussions (65mD, Water-Wet, GAW)

The GAW injection experiment was simulated using the methodology suggested in section 4.2. The parameters used in both runs are summarised in Table 4-5:

Table 4-5: Summary of the input parameters used in the simulation of 65mD mixed-wet core (GAW)

Injection Modes	STONE 1 Exponent (η)	Land's Parameter (C)	Reduction Exponent (α)
G1-W2-G3	8.5	18.1	0.85
W4-G5-W6-G7-W8	6.5	5.3	0.85

Both the single-run and the modified simulation results were compared to the experimental results, as shown in Figure 4-17:

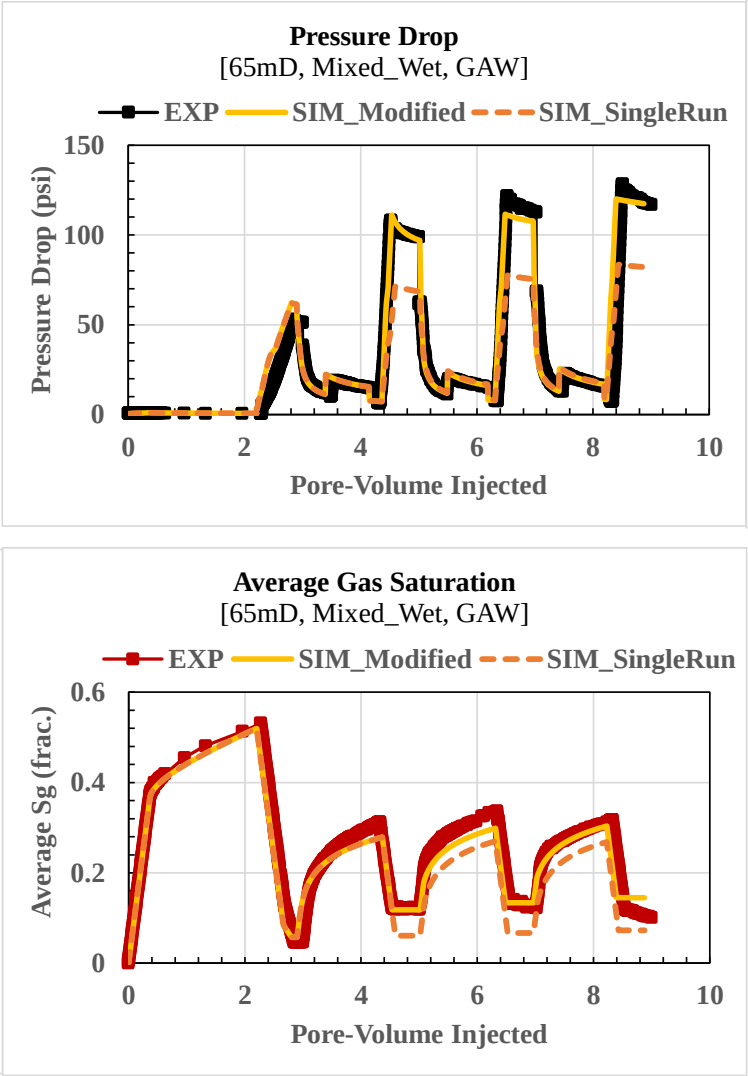

Figure 4-17: Simulation results for the 65mD mixed-wet GAW injection experiment (Top is the DP comparison of the experiment, single-run simulation, and modified simulation results. Bottom is the average gas saturation comparison of the experiment, single-run simulation, and modified simulation results.)

As illustrated in Figure 4-17, the modified simulation has considerably improved the simulation prediction of the trapped-gas saturation as well as the DP, which means that hysteresis behaviour has a major impact on the oil recovery process in this system. The

oil recovery, as well as the average water saturation simulation, results are shown in Figure 4-18:

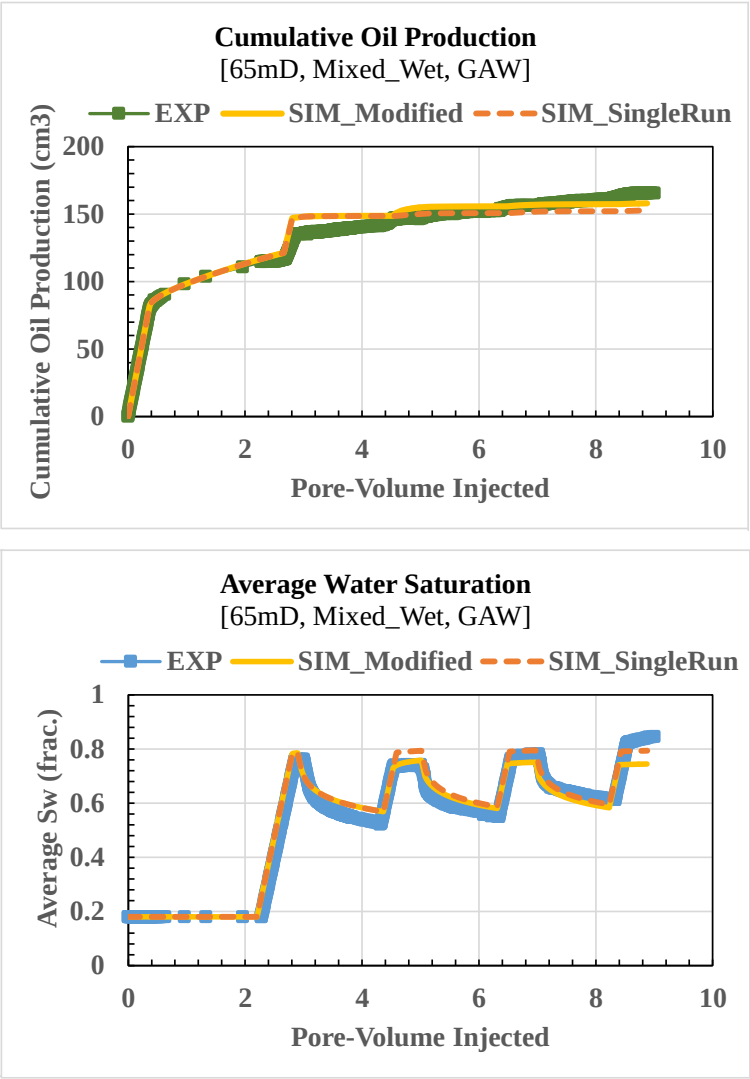

Figure 4-18: Simulation results for the 65mD mixed-wet GAW injection experiment. (Top is the cumulative oil recovery comparison of the experiment, single-run simulation, and modified simulation results. Bottom is the average water saturation comparison of the experiment, single-run simulation, and modified simulation results.)

The modified simulations have slightly improved oil recovery over the water saturation prediction. As discussed in section 4.2, the hysteresis parameters—namely, Land's gas trapping, secondary gas drainage reduction exponent, and the residual oil modification factor—can be altered along the hysteresis cycles to achieve better simulation results.

As the DP_w^{3ph} is almost double the DP during two-phase water injection (DP_w^{2ph}), the water-relative permeability must be further reduced for the three-phase system in this GAW experiment, as shown in Figure 4-19:

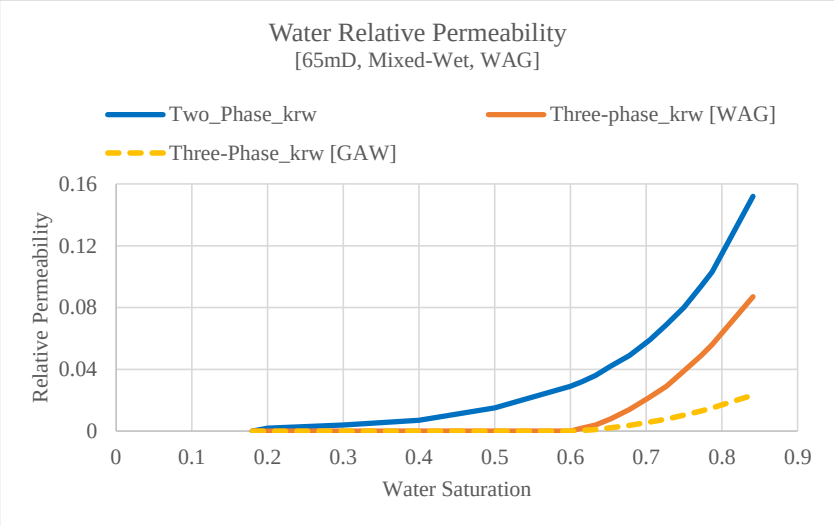

Figure 4-19: Two-phase and three-phase water relative permeability for the 65mD mixed-wet core (WAG and GAW)

Based on the input parameters in Table 4-5, and the DP matched by the three-phase water-relative permeability shown in Figure 4-19, the following observations could be drawn:

1) The STONE 1 exponent was modified to be higher than 1.0 to improve the match of the oil saturation during three-phase gas cycles.
2) Land's parameter was kept as calculated from experimental data. For the first runs, the parameter was calculated to be 18.10, but for the second run, the calculation was 5.30.
3) The secondary gas reduction exponent was found to be the same for both runs.
4) Residual oil modification factor (a) was calculated to be 0.70. However, this parameter was found to have a very limited effect on the simulation results.
5) The water-relative permeability was reduced to match the DP during three-phase water injection (DP_w^{3ph}), as illustrated in Figure 4-19.

4.3.4 WAG Injection Experiment on 40mD Mixed-Wet Limestone

In this section, the core-scale simulation results of WAG injection experiments on a carbonate core (Indiana limestone) are discussed. The results from this experiment would confirm if the hysteresis behaviour is different between carbonate and sandstone rocks. Thus, a WAG injection core-flood experiment was performed on a 40mD mixed-wet Indiana limestone core sample at 38°C (100°F) and 12.69 MPa (1840 psia). The details of these experiments can be found in Alkhazmi et al., 2018 [10].

The imbibition two-phase oil-water relative permeability and drainage two-phase oil-gas relative permeability were estimated from history-matching of the USS core-flood experiments (G1 for gas-oil and W1 for water-oil) [Figure 4-20]:

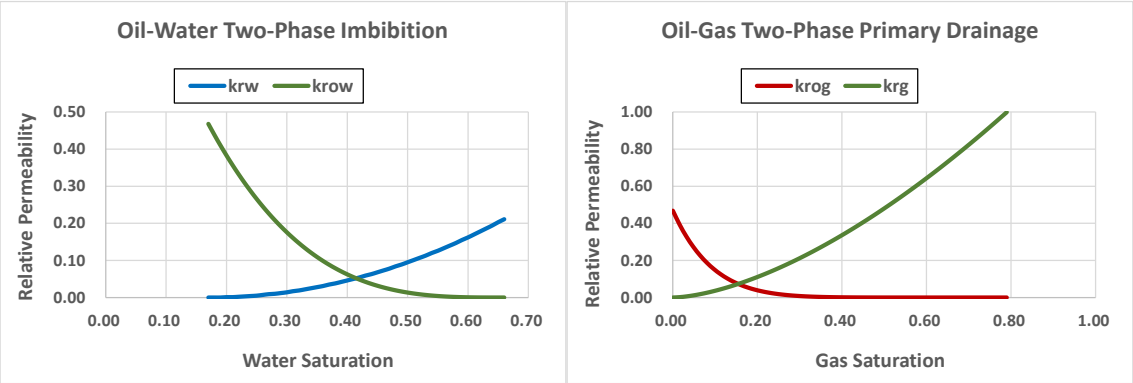

Figure 4-20: Imbibition two-phase oil-water and drainage oil-gas relative permeability for 40mD mixed-wet carbonate core

4.3.4.1 Analysis of WAG Injection Experiment (40mD, Mixed-Wet)

The average saturation for oil, water, and gas is shown in Figure 4-21:

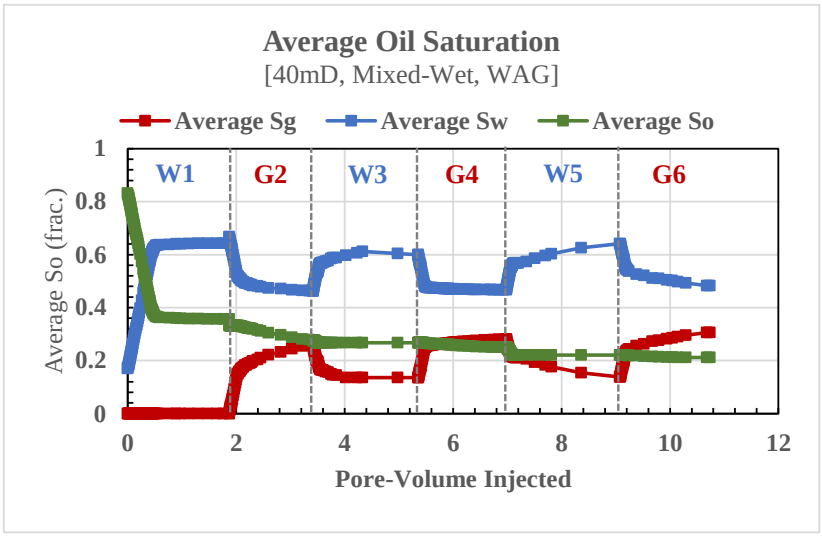

Figure 4-21: Water (blue), Oil (Green), And Gas (Red) saturation profiles for the 40mD mixed-wet carbonate core

From the average saturation profiles of the near-miscible WAG injection experiment on a 40mD mixed-wet core, the following can be observed:

- The first water injection cycle was a two-phase process, which reduced the initial oil saturation from 0.83 to 0.36 ($\Delta So = 0.47$). During the primary three-phase gas injection cycle (G2), additional oil recovery was observed, which reduced the oil saturation at the end of the cycle to 0.27.
- During the second water injection cycle (W3), there was very little oil (less than 1cc) observed at the start of water injection, and gas was trapped, with saturation around 0.137, and oil saturation ceased around 0.267.

- During the second gas injection cycle (G4), more oil was recovered as the result of gas injection (ΔSo = 0.017).
- During the third water injection cycle (W5), there was some oil recovery at the start of the water injection, but it quickly stopped. The reduction in oil saturation was approximately equal to 0.03.
- During the third gas injection cycle (G6), some more oil was recovered as the result of gas injection (ΔSo = 0.01).

Figure 4-22 shows the DP for the WAG experiments performed on the 40mD mixed-wet core at low gas-oil interfacial tension (near miscible):

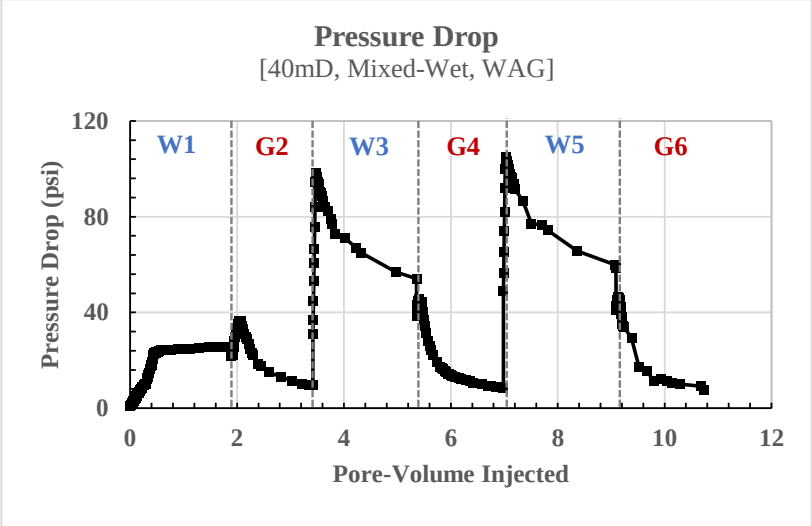

Figure 4-22: Pressure drop across the core during WAG injection performed on 40mD, mixed-wet carbonate core

The DP at the end of the two-phase water injection (DP_w^{2ph}) is equal to 25.7 psi. At the start of gas injection (G2), the DP increased to around 36 psi and then dropped to 10 psi. As soon as the injection phase changed from gas to water (W3), the DP sharply increased to almost 100 psi (four times higher than DP_w^{2ph}). Similar behaviour was observed in further cycles. Therefore, matching such behaviours can again be achieved by cyclic-hysteresis mechanisms.

It seems that the DP behaviour in this carbonate rock is a combination of kr hysteresis (reduction in phase-relative permeability) and the heterogeneity of the rock itself. In previous experiments, the DP during gas injection cycles would drop as soon as the injection phase changed from water to gas. The gas phase would usually prefer to fill to the larger pores first (less resistance); therefore, its DP is usually less than the water, whose preferential path is to smaller pores first due to the higher Pc. However, in this experiment, the DP initially increased, which indicates that the gas has limited access to

the water-filled pores, and then dropped when the DP exceeded the resistance of the water to access the large pores or vugs (cavities in the rock caused by physical or chemical processes). The internal pore structure of the rock sample used in this experiment is illustrated in Figure 4-23 (performed in the Centre for Environmental Scanning Electron Microscopy of Heriot-Watt University):

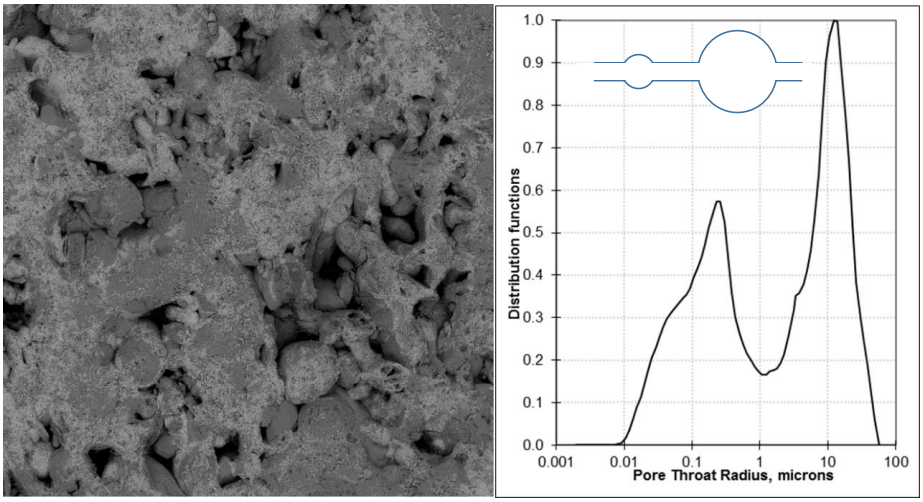

Figure 4-23: ESEM scan of Indiana Limestone (This ESEM scan was performed in the Centre for Environmental Scanning Electron Microscopy of Heriot-Watt University.)

As usually observed in most carbonate rocks, vugs are surrounded by smaller pores with fine pore throats. By the WAG injection process, water will fill the smaller pores with higher Pc first and then proceed to the connected vugs. Then as the gas is injected, it must displace the water in the small pores to access the vugs, which are characterised by the initial increase in DP. As the gas establishes its path, the DP will drop, as observed in Figure 4-22.

4.3.4.2 Simulation Results and Discussions (40mD, Mixed-Wet, WAG)

The WAG injection experiment was modelled in a similar way as the previous experiments using the methodology suggested in section 4.2. The parameters used in both runs are summarised below:

Table 4-6: Summary of the input parameters used in the simulation of 40mD carbonate mixed-wet core (WAG)

Injection Modes	STONE 1 Exponent (η)	Land's Parameter (C)	Reduction Exponent (α)
W1-G2-W3	3.0	3.5	2.0
G4-W5-G6	3.0	3.1	1.8

The single-run, as well as the modified simulation, results are shown in Figure 4-24:

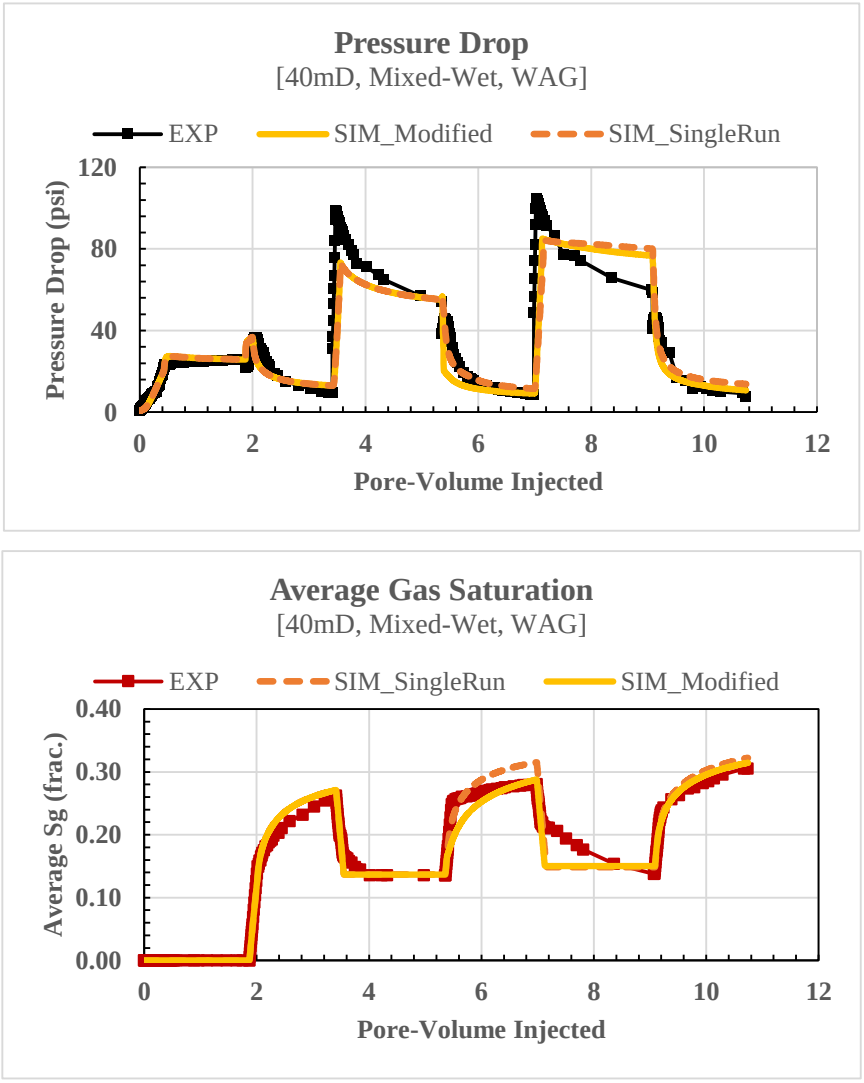

Figure 4-24: Simulation results for the 40mD carbonate mixed-wet WAG injection experiment (Top is the DP comparison of the experiment, single-run simulation, and modified simulation results. Bottom is the average gas saturation comparison of the experiment, single-run simulation, and modified simulation results.)

The modified simulation results slightly improved the simulation prediction of the trapped-gas saturation, especially in the G4 injection cycle. However, in general, both simulation runs reasonably predicted the experimental results, as shown in Figure 4-25:

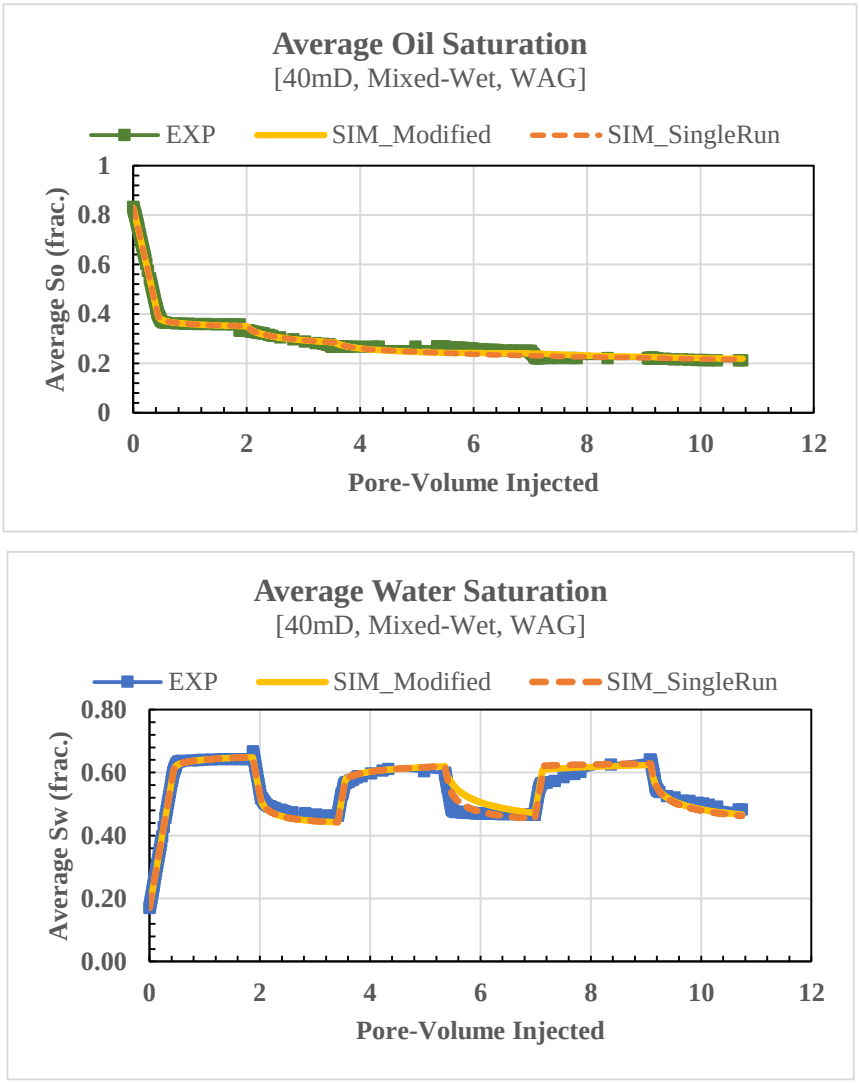

Figure 4-25: Simulation results for the 40mD carbonate mixed-wet WAG injection experiment (Top is the cumulative oil recovery comparison of the experiment, single-run simulation, and modified simulation results. Bottom is the average water saturation comparison of the experiment, single-run simulation, and modified simulation results.)

The single-run and modified simulations produce very similar results. The DP_w^{3ph} is higher than the DP_w^{2ph}; therefore, the water-relative permeability must be reduced for the three-phase system, as shown in Figure 4-14:

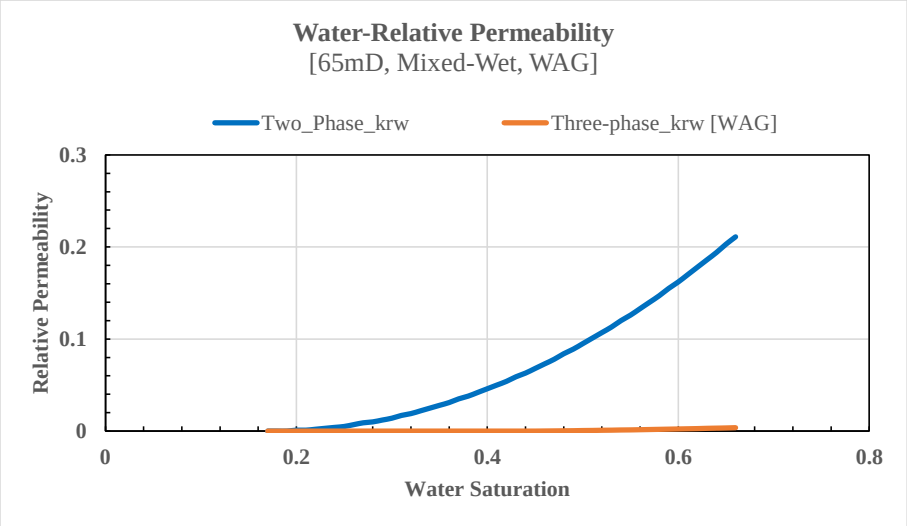

Figure 4-26: Two-phase and three-phase water-relative permeability for the 40mD carbonate mixed-wet core (WAG)

Based on the input parameters in Table 4-6, and the DP matched by the three-phase water-relative permeability shown in Figure 4-26, the following observations could be drawn:

1) The STONE 1 Exponent was modified to be higher than 1.0 to improve the match of the oil saturation during three-phase gas cycles.
2) Land's parameter was kept as calculated from experimental data. For the first runs, the parameter was calculated to be 3.5, but for the second run, the calculation was 3.1, which is essentially the same.
3) The secondary gas reduction exponent was found to be almost the same for both runs. However, the (α) was reduced slightly to try to match the Sg profile during the G4 cycle.
4) Residual oil modification factor (a) was kept as 0.5 for the whole experiment.
5) The water-relative permeability was significantly reduced to match the DP during three-phase water injection (DP_w^{3ph}), as illustrated in Figure 4-26.

4.3.5 WAG Injection Experiment on 40mD Mixed-Wet Limestone (GAW)

In this section, the GAW injection experiment on a carbonate core sample of Indiana limestone is discussed. The two-phase relative permeability is the same as in Figure 4-20.

4.3.5.1 Analysis of WAG Injection Experiment (65mD, Mixed-Wet, GAW)

The average saturation calculated for oil, water, and gas is shown in Figure 4-27 :

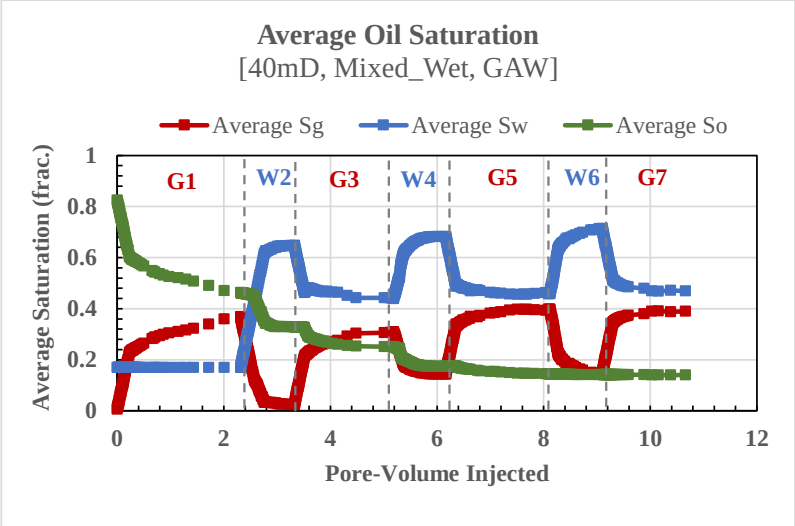

Figure 4-27: Water (blue), Oil (Green), And Gas (red) saturation profiles for the 40mD mixed-wet carbonate core (GAW)

The behaviours observed from the saturation profiles are discussed below:

- The first gas injection cycle (G1) is a two-phase process, which reduced the initial oil saturation from 0.83 to 0.46 ($\Delta So = 0.37$).
- During the first three-phase water injection cycle (W2), significant oil recovery was observed, which reduced the oil saturation at the end of the cycle to 0.33. The trapped-gas saturation (Sgt) was observed to be only 0.024.
- During the second gas drainage cycle (G3), more oil was produced to reduce the oil saturation to 0.25.
- During the second water injection cycle (W4), the trapped-gas saturation was approximately 0.144. Additional oil was recovered to reduce the average oil saturation in the core to about 0.17.
- Only a small amount of oil recovery was observed after this cycle ($\Delta So \approx 0.03$).

Figure 4-28 shows the DP for the WAG experiments performed on the 40mD mixed-wet core at low gas-oil interfacial tension (near miscible):

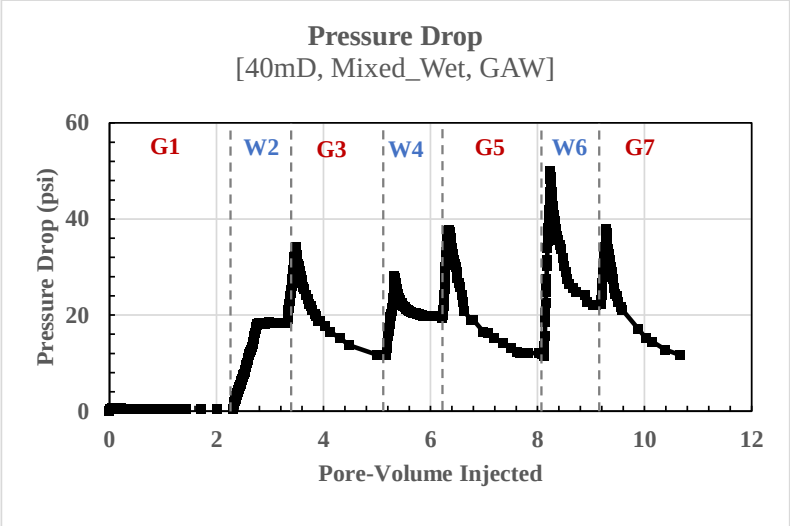

Figure 4-28: Pressure drop across the core during GAW injection performed on 40mD, mixed-wet carbonate core

The DP at the end of three-phase water injection W2 was less than DP_w^{2ph} of 25.7 psi, as shown in Figure 4-28. However, at the start of gas injection (G3), the DP increased to around 36 psi and then dropped to just above 10 psi. As soon as the injection phase changed from gas to water (W4), the DP increased to almost 40 psi. Again, the DP behaviour in this experiment seems to be a combination of relative-permeability hysteresis and the heterogeneity of the rock.

4.3.5.2 Simulation Results and Discussions (40mD, Mixed-Wet, GAW)

This experiment was modelled using the methodology suggested in section 4.2. The parameters used in both runs are summarised in Table 4-7:

Table 4-7: Summary of the input parameters used in the simulation of 40mD carbonate mixed-wet core (GAW)

Injection Modes	STONE 1 Exponent (η)	Land's Parameter (C)	Reduction Exponent (α)
G1-W2-G3	0.7	38.8	2.10
W4-G5-W6-G7	0.1	4.4	2.25

Both the single-run and the modified simulation results are shown in Figure 4-29:

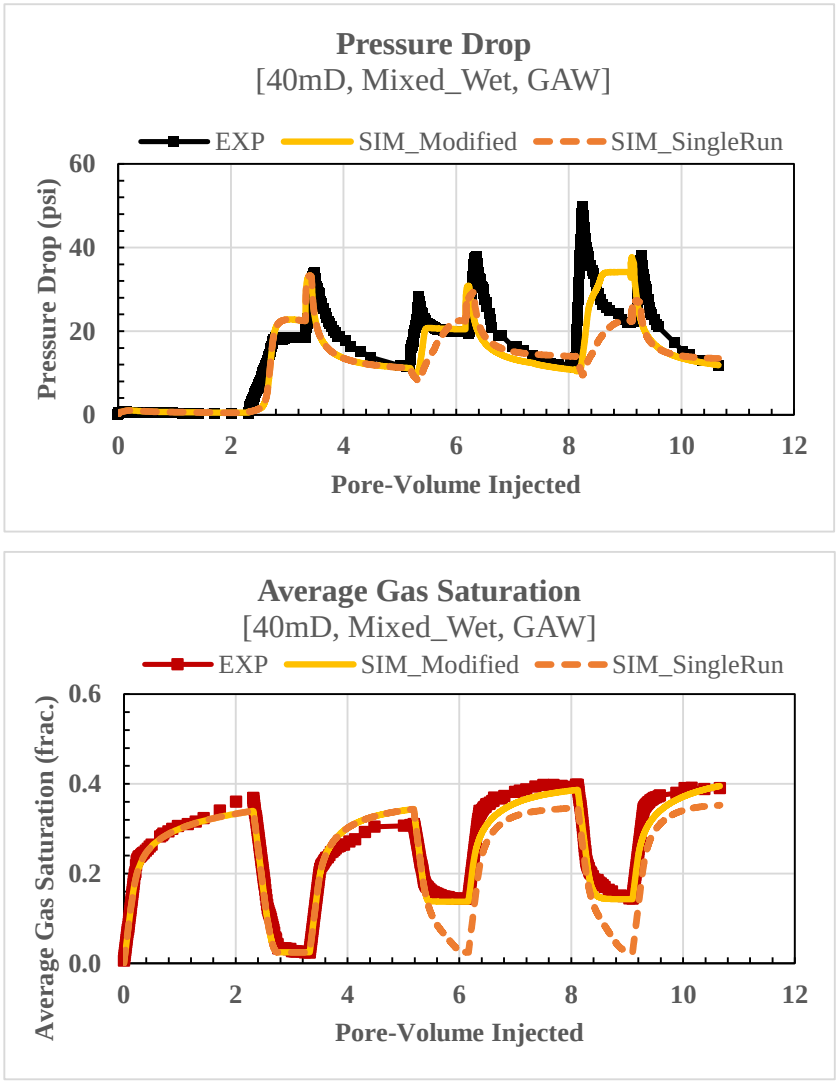

Figure 4-29: Simulation results for the 40mD carbonate mixed-wet GAW injection experiment (Top is the DP comparison of the experiment, single-run simulation, and modified simulation results. Bottom is the average gas saturation comparison of the experiment, single-run simulation, and modified simulation results.)

The modifications to the WAG-HYST parameters and the STONE1EX have improved the simulation prediction of the trapped-gas saturation, especially in the W4 water injection cycle. Also, the DP predictions are somewhat better in the modified simulation. However, the complex pore structure in this core sample makes the DP increase at the start of each injection cycle to reshuffle the phases within the pores. The simulation results for the average oil and water saturations are shown in Figure 4-30:

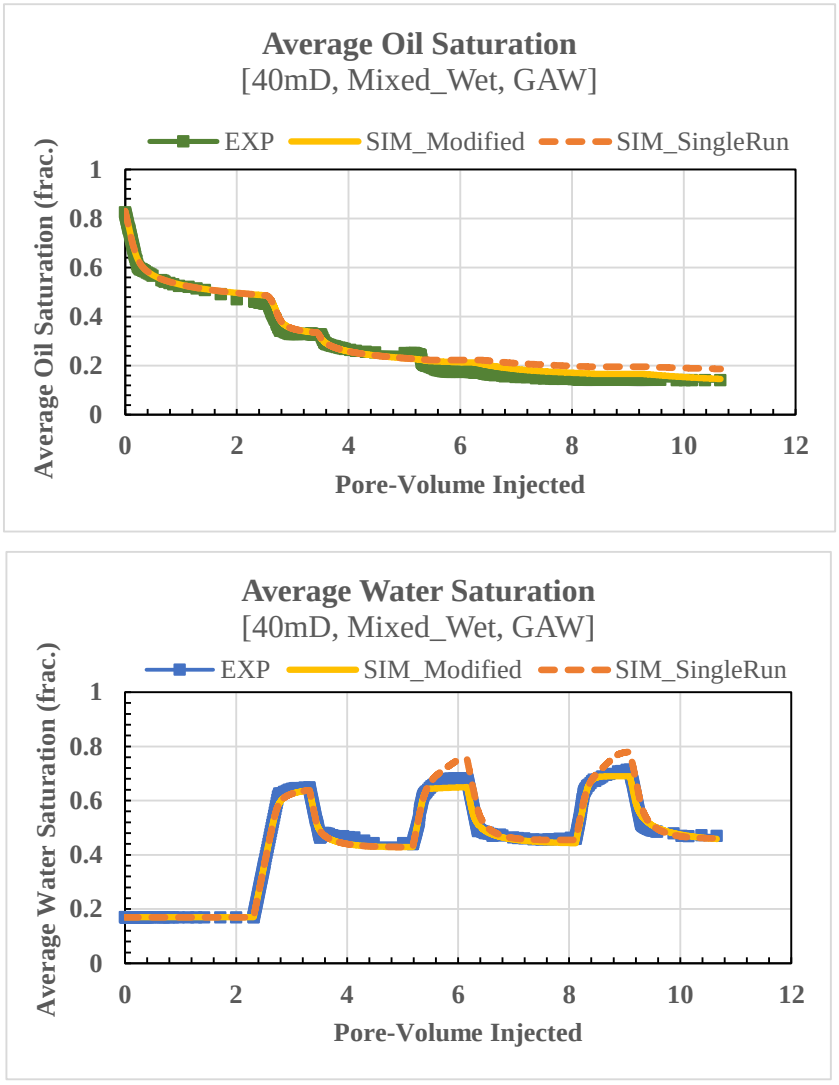

Figure 4-30: Simulation results for the 40mD carbonate mixed-wet GAW injection experiment (Top is the cumulative oil recovery comparison of the experiment, single-run simulation, and modified simulation results. Bottom is the average water saturation comparison of the experiment, single-run simulation, and modified simulation results.)

The modified simulations, in general, better predict the experimental results than the single-run simulation. The DP_w^{3ph} is higher than the DP_w^{2ph}; therefore, the water-relative permeability must be reduced for the three-phase system, as shown in Figure 4-31:

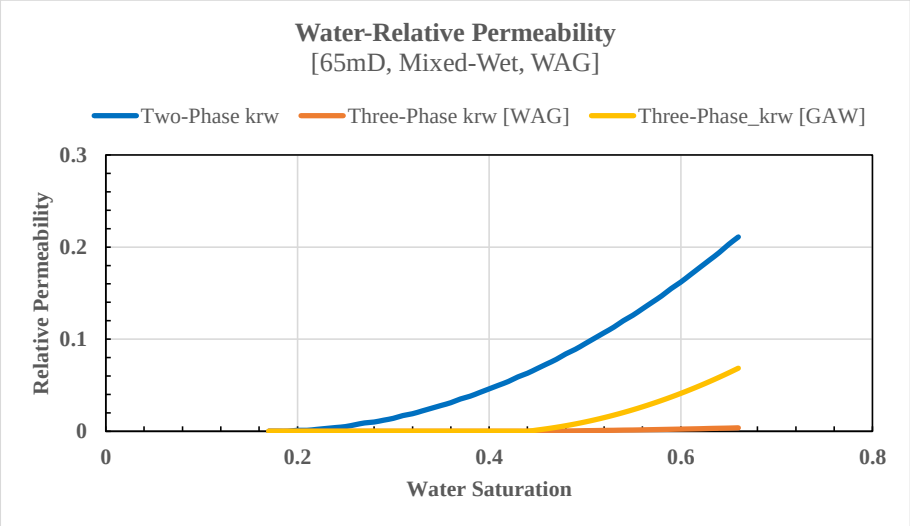

Figure 4-31: Two-phase and three-phase water-relative permeability for the 40mD carbonate mixed-wet core (WAG and GAW)

Based on the input parameters in Table 4-7, and the DP matched by the three-phase water-relative permeability shown in Figure 4-31, the following observations could be drawn:

6) The STONE 1 exponent was modified to be less than 1.0 to improve the match of the oil saturation during three-phase gas cycles.
7) Land's parameter was kept as calculated from experimental data. For the first runs, the parameter was calculated to be 38.8, but for the second run, the calculation was 4.4.
8) The secondary gas reduction exponent was modified from 2.10 in the first run to 2.25 reduction exponent in the second run.
9) Residual oil modification factor (a) was kept as 1.0 for the whole experiment.
10) The water-relative permeability was significantly reduced to match the DP during three-phase water injection (DP_w^{3ph}), as illustrated in Figure 4-31.

4.4 Discussion of the Core-Scale WAG Injection Simulation Results:

After matching the observed production and pressure data from the five WAG injection experiments, in-situ saturation status can be plotted from the simulation results. The in-situ saturation can provide valuable information about each injection cycle. Therefore, an example of the saturation distribution during each injection cycle for the 65mD water-wet GAW experiment is discussed below. The oil, water, and gas saturation in the simulation grids after 10 per cent of pore volume injection is plotted versus core length. Each line represents situation in situ after 10% pore volume has been injected during each cycle:

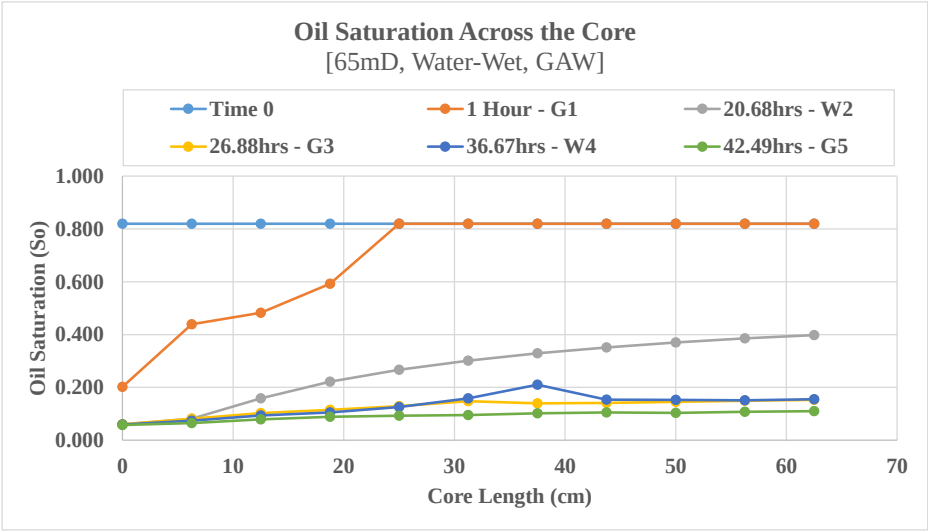

Figure 4-32: In-situ oil saturation along the 65mD, water-wet, GAW coreflood experiment after 10 per cent pore volume has been injected during each stage

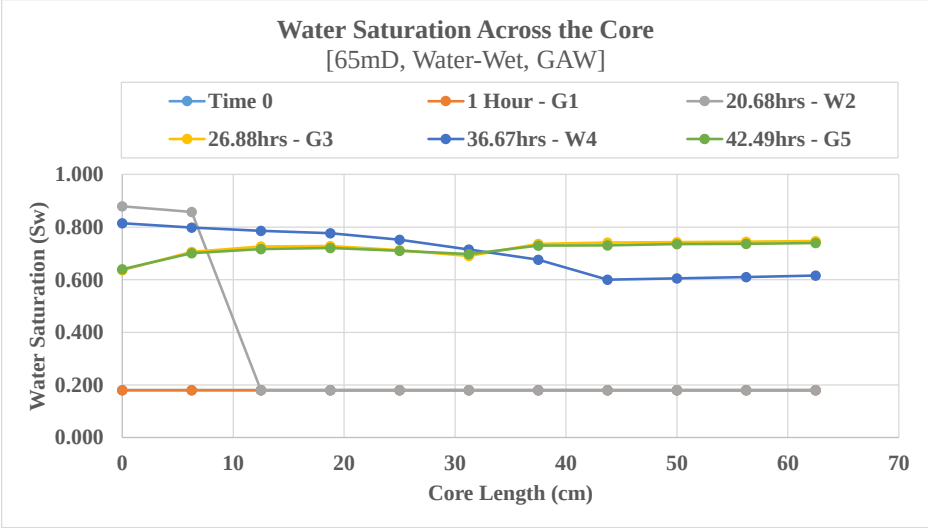

Figure 4-33: In-situ water saturation along the 65mD, water-wet, GAW coreflood experiment after 10 per cent pore volume has been injected during each stage

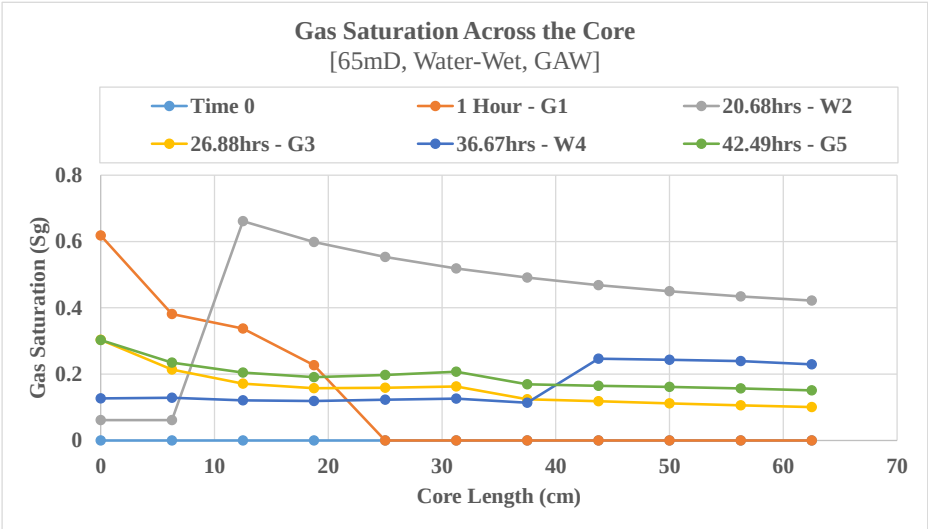

Figure 4-34: In-situ gas saturation along the 65mD, water-wet, GAW coreflood experiment after 10 per cent pore volume has been injected during each stage

It is apparent from the in-situ saturation plots (Figure 4-32, Figure 4-33, and Figure 4-34) that the status during G1 and W2 is very different than during subsequent gas and water cycles. The in-situ saturation distribution during G1 is different than the status during G3, and G5 which are similar. Also, the status during W2 is very different than the saturation during W4. This observation supports the methodology suggested in this thesis to update the WAG hysteresis parameters in the later injection cycles.

There is an oil bank 35 centimetre into the core during W4 (Figure 4-32). This oil volume during W4 is greater than the oil during G3. However, this clearly cannot be the case as this is immiscible displacement. Therefore, at 35 centimetre must be where new gas injected during a gas cycle has reached after 0.1PV of that cycle.

In almost all experiments, except the 40mD, Water-Wet, WAG experiment, η had to be adjusted to match the oil recovery (Figure 4-35). Further investigation is still needed to understand the relationship between oil saturation and the need to adjust η; however, these results highlighted the role of η in WAG injection simulation.

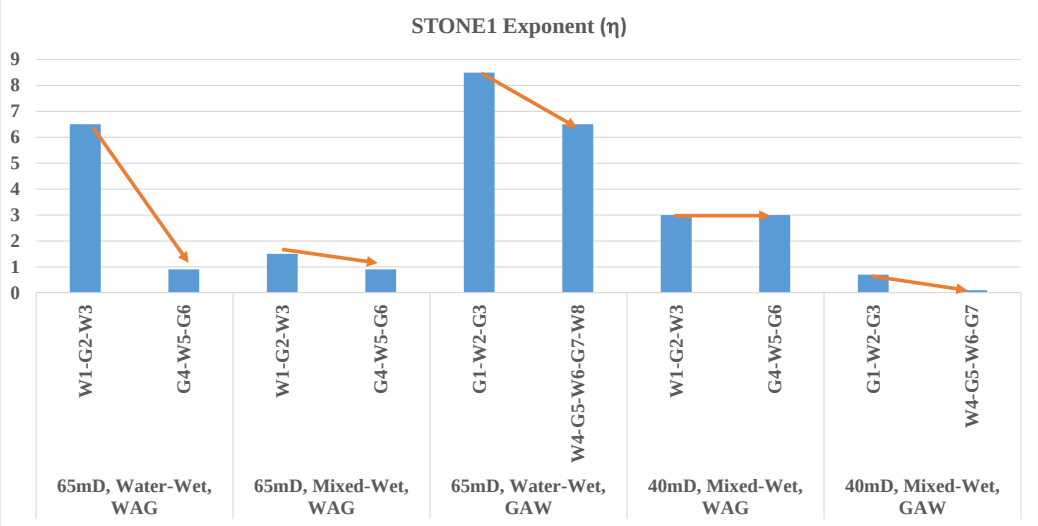

Figure 4-35: The STONE1 Exponent for the different WAG injection coreflood simulated experiments

The calculated Land's parameter C for the first run had to be reduced for the second run in all simulated experiments. However, the amount of reduction in the GAW experiments is more significant than the WAG experiments (See Figure 4-36). The reason for such difference is due to the different trapping behaviour between W2 and W3 (section 3.5.1).

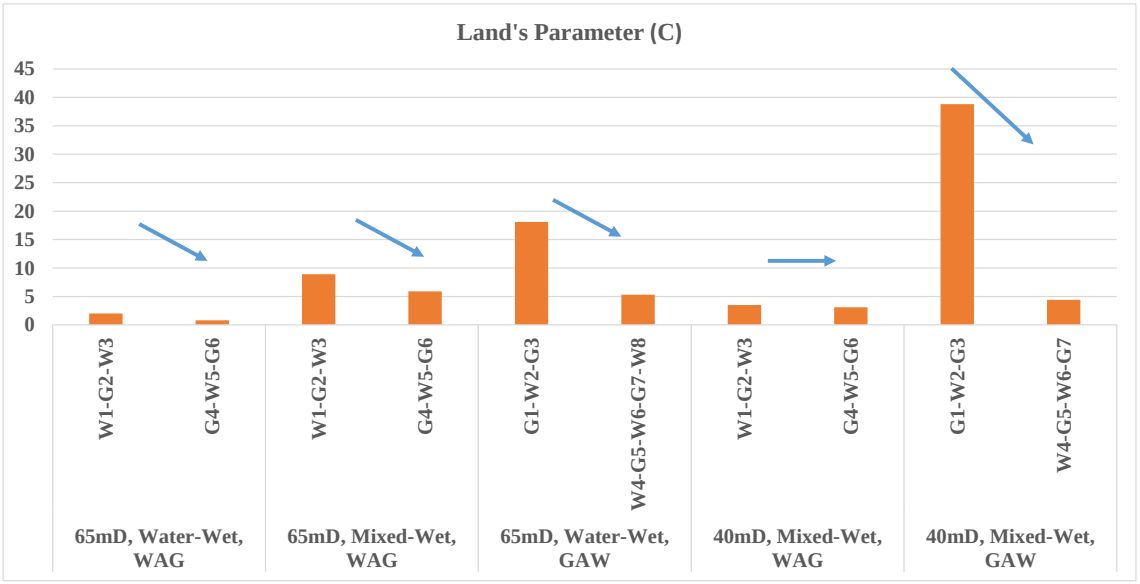

Figure 4-36: Land's gas-trapping parameter for the different WAG injection coreflood simulated experiments.

The estimated α for the first run and the second run is almost the same for most cases except the 65mD, Water-Wet, WAG experiment as shown in Figure 4-37:

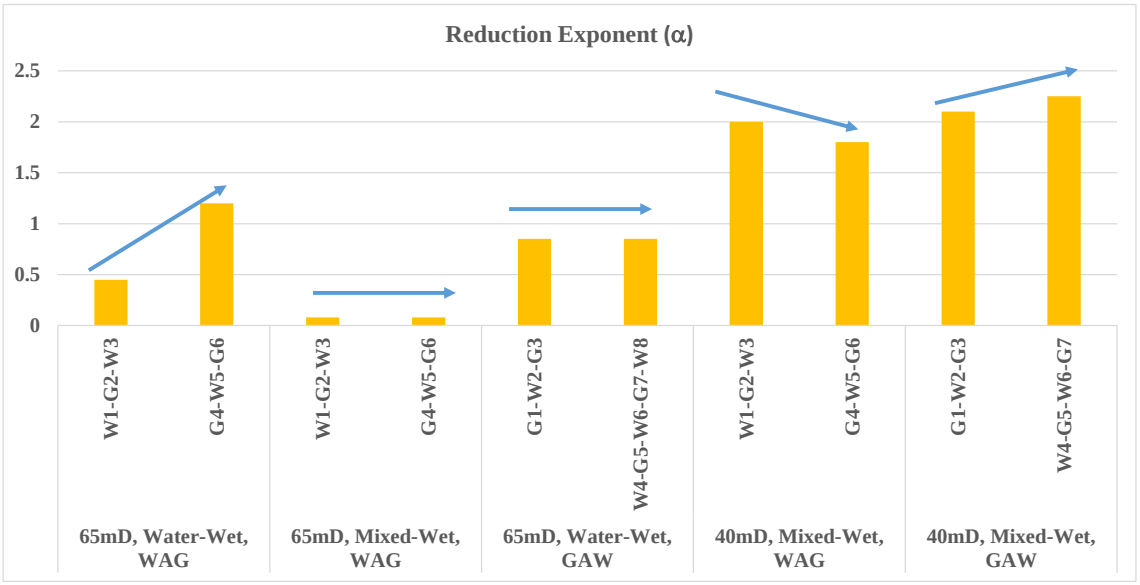

Figure 4-37: Gas secondary-drainage relative permeability reduction parameter [α] for the different WAG injection coreflood simulated experiments.

Further investigation is still needed to understand the behaviour of this exponent during cyclic hysteresis. However, the exponent α can be used to improve the match of DP_g^{3ph}.

4.5 Conclusion

The process of obtaining the WAG hysteresis parameters from the various WAG injection experiments (chapter 3) was discussed in this chapter. As widely published in the literature, there is usually a mismatch between WAG injection experimental data and simulation predictions. The reason for the mismatch suggested in this chapter is that the hysteresis model (WAG-HYST) by Larsen and Skauge is based on limited cycles of WAG (G-W-G and W-G-W). Therefore, it could be argued whether the WAG-HYST model can be used to match further cycles (G-W-G-***W-G-W*** and W-G-W-***G-W-G***). As shown by this thesis and other publications, the current WAG-HYST model needs to be extended to match the further WAG cycles.

As discussed in section 3.5.1, Land's gas-trapping parameter [C] could be different for each hysteresis cycle. This observation became obvious as more WAG cycles were implemented beyond a single hysteresis loop. Furthermore, the variable gas-trapping behaviour has been confirmed by several authors since 2003 [47]. Therefore, a new approach to manipulate the simulation and update WAG-HYST parameters was suggested.

The results obtained from the simulation of the five different WAG injection experiments discussed in this chapter confirmed that updating the gas-trapping parameter significantly improves the ability of the simulation to match WAG experimental results. As the Land's gas-trapping parameter changes, the other parameters might need to be adjusted as well. For example, in some cases, the STONE1EX parameter must be adjusted as oil saturation goes from higher to lower values, and as a result, the gas secondary drainage reduction exponent [α] must be modified. Table 4-8 summarises the obtained hysteresis parameters for all five experiments:

Table 4-8: summary of the obtained WAG-HYST parameters from the five experiments

Experiment	Injection Modes	STONE1 Exponent (η)	Land's Parameter (C)	Reduction Exponent (α)
65mD, Water-Wet, WAG	W1-G2-W3	6.5	2.00	0.45
	G4-W5-G6	0.9	0.81	1.20
65mD, Mixed-Wet, WAG	W1-G2-W3	1.50	8.9	0.08
	G4-W5-G6	0.90	5.9	0.08
65mD, Water-Wet, GAW	G1-W2-G3	8.5	18.1	0.85
	W4-G5-W6-G7-W8	6.5	5.3	0.85
40mD, Mixed-Wet, WAG	W1-G2-W3	3.0	3.5	2.0
	G4-W5-G6	3.0	3.1	1.8
40mD, Mixed-Wet, GAW	G1-W2-G3	0.7	38.8	2.10
	W4-G5-W6-G7	0.1	4.4	2.25

The values shown in Table 4-8 is illustrated in Figure 4-35, Figure 4-36, and Figure 4-37.

In the next chapter (chapter 5) the significance of WAG hysteresis and the best practices for WAG injection simulation at reservoir scale are discussed.

Chapter 5—Reservoir-Scale WAG Injection Simulation

For oil reservoirs previously flooded with water as a secondary recovery method, the oil production would start to decline due to increasing water cuts in the production wells. At this stage, operators would investigate various action plans to improve oil recovery. If WAG injection is proven beneficial based on general knowledge of the reservoir, then further evaluation is needed to investigate and quantify the additional oil recovery expected from it. However, to perform such an investigation, major laboratory studies are required in addition to some simulation work.

In the laboratory, WAG injection core-flood experiments are required (see chapter 3) to estimate the following:

- How much additional oil recovery is likely to be realised by WAG injection?
- What is the dominant process in such a method?
- What are the key simulation input parameters?

After finishing the laboratory study, numerical simulations of the core-flood experiments (see chapter 4) play a major role in understanding the oil recovery process and optimising the flood design. The end goal, of course, is to implement the WAG injection at the reservoir scale in a real field. However, there are several challenges expected at the reservoir scale:

- **Reservoir heterogeneity:** vugs, fractures, super-k layers, discontinuous sands, variation in wettability and rock types, and barriers/baffles
- **Gravity segregation:** The gas phase tends to rise to the top of the reservoir, whilst the water phase sinks to the bottom. Because of such natural behaviour, the three-phase zone becomes very small, and hence the additional oil recovery becomes low.
- **Secondary oil recovery due to gas injection**: At the reservoir scale, some layers, especially at the top of the reservoir, were not flooded by water during the waterflood; therefore, the oil recovery from WAG injection can be confused with the oil recovery from those zones, making quantification of actual oil recovery by WAG injection quite a challenge.
- **Modelling hysteresis at reservoir scale**: The first question is whether or not hysteresis is significant when WAG injection is applied. Also, it should be

determined which parameters to input into the numerical simulation to model the WAG hysteresis process. The challenge is how to quantify the following:

- nonwetting phase trapping
- mobility or relative permeability reduction of injected fluids
- miscibility of the injected gas into the reservoir fluids

In addition to the abovementioned challenges, numerical convergence issues, as well as a longer run time, are often encountered in the numerical simulation when simulating WAG injection. Such issues make the simulation process less efficient and sometimes unfeasible. The commercial viability of WAG injection can be weakened by the fact that oil recovery through this process is affected by the following:

- delayed response (late oil bank arrival) due to the process of nonwetting phase trapping and mobility reduction of injected fluids
- low oil rate in addition to the expensive operations
- the high cost of gas compression and gas handling
- the cost of modifying some surface lines to prevent corrosion
- the additional cost of monitoring and surveillance

Accounting for the issues above, WAG injection can be more efficient if the following measures are applied:

- accelerating oil bank arrival to minimise the period of negative cash flow
- maximising the oil rate due to WAG injection (three-phase oil)
- optimising the gas requirement scf (gas)/bbl (oil)
- delaying the gas breakthrough time and gas production
- minimising the required volume of injection gas

Numerical simulation can be used to improve the efficiency of oil recovery by WAG injection. However, the question remains of how complex the simulation model should be to reasonably predict WAG injection performance at the reservoir scale. To answer this, the objectives from the simulation model must be clearly defined at the early stages. Those objectives are likely to be:

- Identify the additional oil recovery from WAG injection.
- Estimate the expected oil rate from WAG injection.

- Quantify the fluid-handling capacity for surface facilities.
- Predict the gas breakthrough time.

Each objective can be linked to several effective simulation parameters, which could be static or dynamic, in addition to hysteresis and miscibility dependencies. Also, the simulation modelling process itself can affect the ability to accurately predict the outcome of these objectives. In the following sections, several sensitivity studies are highlighted to investigate the effect of flow functions, heterogeneity, anisotropy, and cyclic hysteresis.

5.1 Effect of Flow Functions on Reservoir-Scale Simulation

As discussed in section 3.2, different relative permeability curves can be obtained by matching the same experimental data. That leads to the question if different relative permeability used in a reservoir-scale simulation will cause a significant difference in oil recovery prediction.

5.1.1 Effect of Relative Permeability on Reservoir-Scale Simulation

To evaluate the effect of flow functions on a reservoir-scale simulation, a two-dimensional cross-section with homogenous properties, similar to the core-flood properties, was constructed. The three scenarios were tested at a larger scale with fine grids (DX=5 feet). The results are summarised in Table 5-1:

Table 5-1: The plateau length and the oil recovery factor at 5,400 days for three different scenarios

	Ignored Pc (Pc = 0)	**Estimated Pc**	**Given Pc**
Plateau length, days	2950	3400	3360
RF @ 5400days, %	48.2	51.4	51.0

Table 5-1 illustrates the plateau length and the oil recovery factor at 5,400 days for three different scenarios. The first column shows the results when Pc is equal to zero, the second column when Pc is simultaneously estimated with kr, and the last column is when the benchmark Pc is given whilst estimating the kr. Both plateau length and recovery factor are very close when Pc is considered (within 40 days). However, when Pc is ignored, the plateau length is shorter by more than 400 days, and the recovery factor is less. Figure 5-1 shows the difference in flood front shape for the three cases:

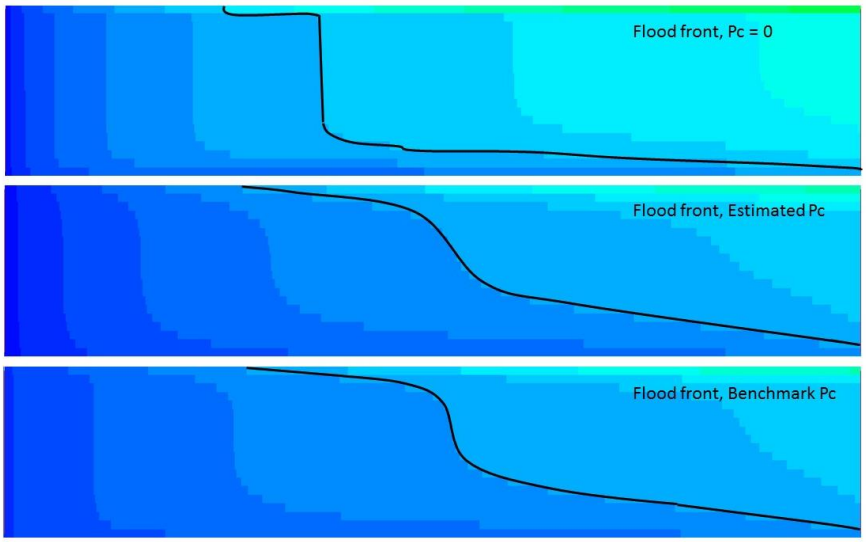

Figure 5-1: Waterflood front shape after breakthrough for the three cases (The top cross-section shows the flood front when Pc=0, the middle cross-section shows the flood front when Pc is estimated, and the bottom cross-section is when benchmark Pc is given.)

When Pc is ignored (top cross-section) the simulated water front is sharper compared the cases where Pc is considered. Therefore, proper consideration of Pc during the estimation process of relative permeability is critical to ensure that reservoir-scale simulation can reliably predict multiphase flow behaviour.

5.1.2 Effect of Capillary Pressure and Grid Size on Reservoir-Scale Simulation

As highlighted in the previous section, the estimation of kr should properly consider Pc. The Pc used during the estimation of kr should always be utilised in the simulation model as well. However, if the Pc is changed at any stage during the simulation model, the kr should be re-estimated to ensure that the multiphase flow is correctly represented. The situation evaluated here is when kr is estimated by providing a measure of Pc; then at another stage, the Pc is ignored without modifying kr.

In this section, the properties of the reservoir-scale model are different from those in the previous section. The aim here is to have an order-of-magnitude higher permeability (1000mD) and investigate the effect on Pc in such a case. Of course, the flow functions in higher permeability will be different. Therefore, a NCFE was performed with typical parameters of 1000mD water-wet rock to generate appropriate flow functions. The generated flow functions for the high permeability case are shown in Figure 5-2:

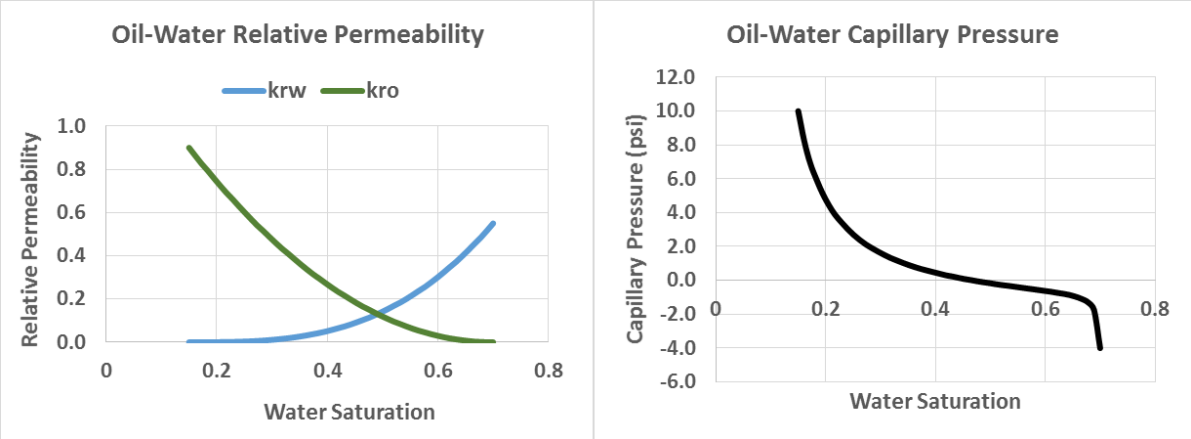

Figure 5-2: Oil-water imbibition kr and Pc (1000mD)

The maximum Pc and Corey exponents for relative permeability here are different from those in the 100mD NCFE to represent a typical high-permeability (1000mD) water-wet rock. These flow functions are used in a two-dimensional model to demonstrate the role of Pc in reservoir-scale waterflood simulation. The model has two active wells, one injector on one side of the model and a producer well on the other side 3,000 feet away. The thickness of the model is 120 feet with homogenous permeability of 1000 mD and 20 per cent porosity. There are 20 layers in the z-direction and only one layer in the y-direction. The permeability in the x and y directions are the same, and the vertical permeability is assumed to be 10 per cent of the horizontal permeability. The model was initialised with a pressure of 1840 psi and 15 per cent initial water saturation (Swi).

At the core-scale, it is often possible to use a fine enough grid size to eliminate numerical dispersion. However, in reservoir scale, the size of grids is usually coarser, which introduces numerical dispersion and also mitigates the effect of Pc. The DP across a coarse grid is sometimes higher than the Pc, and that suppresses the role of Pc in the flow behaviour. Therefore, in this section, various grid sizes were generated, starting from five feet in x-direction (DX) up to a DX of 200 feet.

The objective of this section is to evaluate the effect of including imbibition Pc in fine- and coarse-grid reservoir-scale simulation. Two scenarios were evaluated, the first one accounting for Pc and the second with zero Pc for a range of grids sizes. The results of the two runs are summarised in Figure 5-3:

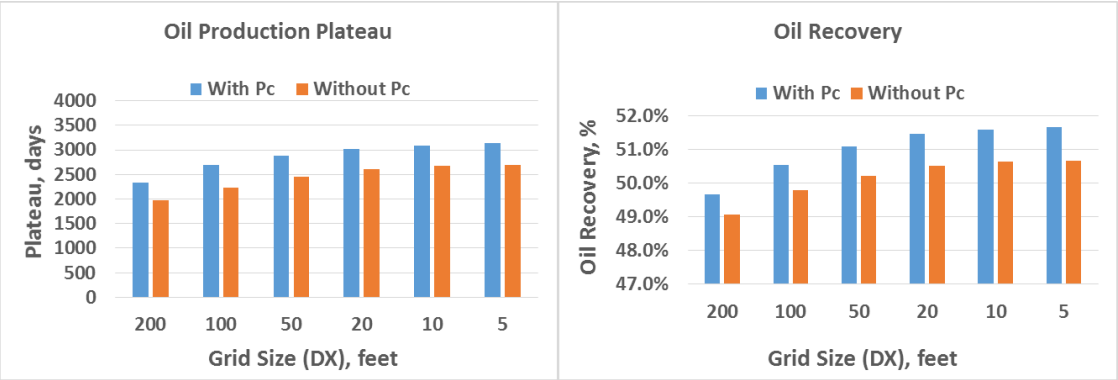

Figure 5-3: Oil production plateau length in days (left) and cumulative oil production (right) comparison plot

From the results in Figure 5-3, ignoring Pc could lead to a noticeable difference in oil production plateau and oil recovery. The difference is sustained for the various grid sizes with almost the same magnitude and is mainly due to the inaccurate representation of the flood front shape and speed when Pc is ignored. Therefore, for grid analysis in similar conditions, Pc does not significantly change the conclusion of the optimum grid size. However, Pc is important to accurately predict water breakthrough, plateau time, and cumulative oil production.

The Pc in the water wet system disperses the water from regions of high-water saturation to regions of low-water saturation. Therefore, as shown in Figure 5-1, water is dispersed laterally at the waterflood front, which slows down the waterflood advancement, allowing better sweep efficiency. However, if the viscous or gravity forces are higher than the Pc, the effect of capillary force will not be as significant.

Figure 5-4 illustrates the oil and water saturation in a cross-section during waterflood, highlighting the role of Pc in the shape of a waterflood front:

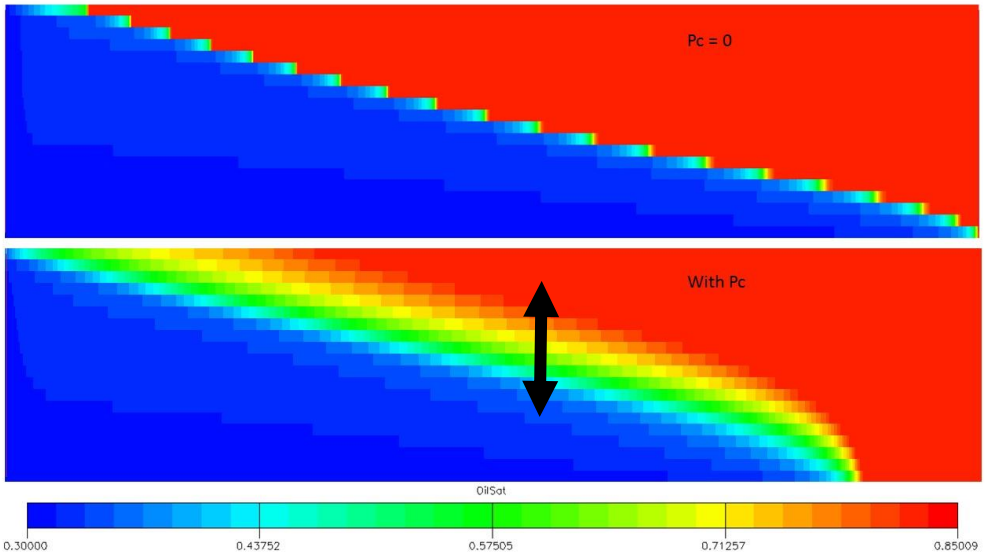

Figure 5-4: Cross-sections illustrating the waterflood front shape (The top plot shows the oil [red] and water [blue] saturation when Pc=0. The bottom plot shows the shape of the waterflood when Pc is considered.)

The cross-sections in Figure 5-4 are both taken at the same time step, but the top one shows the waterflood front when Pc is ignored (Pc=0). The bottom cross-section, where Pc was accounted for, demonstrates how Pc, in this case, spreads out the water to occupy a larger space, which results in a slower flood front advancement. This effect can be different for lower permeability, more heterogeneous rock, or different wettability conditions.

5.2 Effect of Vertical Permeability on WAG Injection Performance

The vertical permeability is usually lower than the horizontal permeability. A common practice in the industry is to represent this as vertical to horizontal permeability ratio (kv/kh), which could be very different for different rock types, especially when using coarse simulation grids. However, simulation engineers often use the same kv/kh ratio even after grid refinement.

To understand the role of kv/kh ratio in capturing the fluid flow during WAG injection, a quarter five-spot model was used to illustrate the importance of vertical permeability in the WAG injection process. The distance between two producers is assumed to be 1,000 feet; therefore, the quarter five-spot pattern is 500' x 500', and the model thickness is assumed to be 100 feet. To have a reasonable grid size, each grid cell is 20' x 20' x 5', and this will make a total of 20 layers in the vertical section (Figure 5-5):

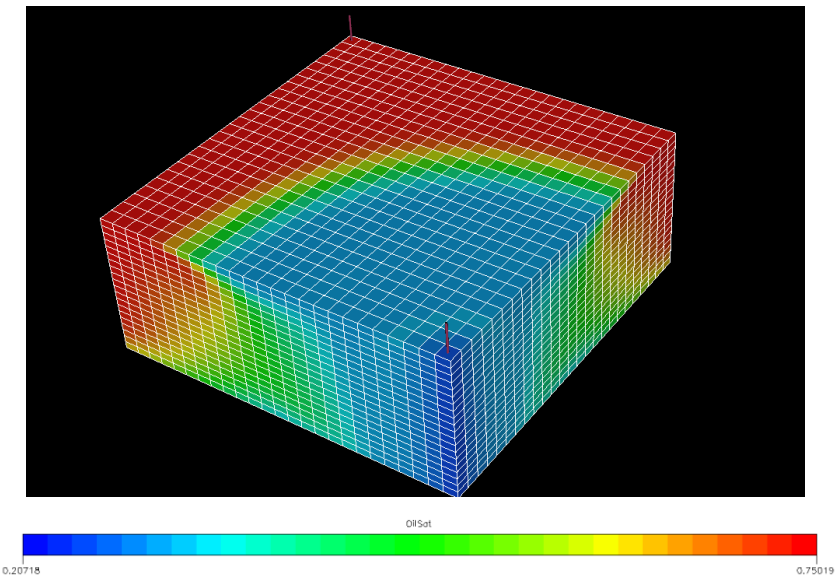

Figure 5-5: The quarter five-spot model

By using the quarter five-spot model, the effect of vertical permeability on oil recovery after ten years was compared for waterflooding and WAG/GAW injection. The results are shown in Figure 5-6:

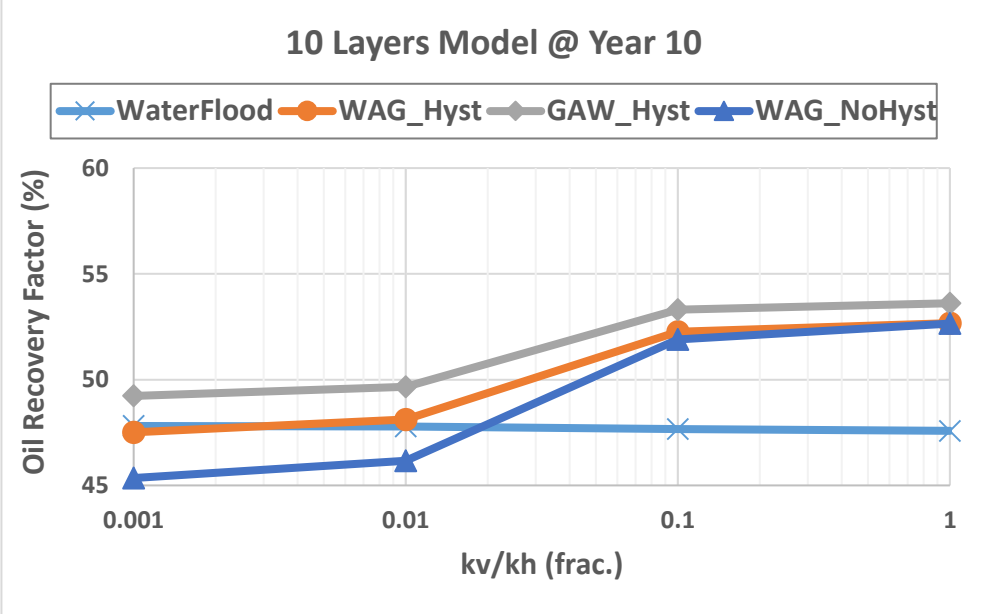

Figure 5-6: The results of the quarter five-spot model comparing waterflooding to WAG injection at different kv/kh ratios

In Figure 5-6, the x-axis shows the kv/kh ratio starting from 0.001 up to 1.0 on a logarithmic scale. The y-axis shows the oil recovery after ten years in percentage. Based on this simulation study, the difference in oil recovery by water flooding after ten years for these different kv/kh ratios is negligible. However, for all cases of WAG, there is a considerable difference in oil recovery based on the value of the kv/kh ratio. Also, based on this simulation study, it can be concluded that at lower vertical permeability (0.001-

0.100), WAG hysteresis is more significant if compared to the higher vertical permeability (0.1-1.0). A possible explanation for why vertical permeability significantly affects the oil recovery in waterflooding is that water tends to flow in the same direction of gravity, which minimises the effect of vertical permeability in waterflooding. Since the tendency is for the gas phase to rise to the top of the reservoir against the direction of gravity, then vertical permeability plays a major role in the gas flow in the reservoir. Furthermore, when vertical permeability is high, WAG hysteresis becomes less important because gas can flow quickly to the top of the reservoir, making the three-phase zone very small, and therefore the hysteresis effect is negligible.

Based on the results discussed above, vertical permeability can be misrepresented in the simulation grids, especially after refining the grid cells for WAG injection simulation, and can affect the simulation prediction of oil recovery during WAG injection. This is particularly important in carbonate reservoirs where vertical permeability can vary between rock types.

In conclusion, when refining the grid cells for simulating the WAG injection process, the vertical permeability assigned for them was often kept the same as the coarser model. It was demonstrated in this study that for WAG injection, the kv/kh ratio plays a more significant role in the prediction of oil recovery compared to the waterflood. Therefore, when refining the simulation girds, kv/kh ration should be adjusted accordingly.

5.3 Effects of Heterogeneity, Anisotropy, and Cyclic Hysteresis on WAG Injection Performance

Significant oil volume can be recovered from reservoirs if the oil recovery is improved even by a few percentages. However, to enhance oil recovery by WAG injection, accurate modelling of the key processes at reservoir scale is essential. Numerical simulation is normally utilised to give ideas about the following objectives:

- identifying the additional oil recovery from WAG injection
- estimating the expected oil rate from WAG injection
- quantifying the fluid-handling capacity for surface facilities design
- predicting the oil bank arrival and gas breakthrough time

To assess the sensitivity of heterogeneity, anisotropy, and cyclic hysteresis on WAG injection performance, a reservoir-scale simulation model with three different rock types is utilised to conduct a sensitivity study. The sensitivity study usually varies some key parameters within their reasonable ranges and assess their impact on key performance indicators and allocate more resources to finetune the most sensitive parameters (results are discussed in the follow sections).

5.3.1 Model Description

The numerical model used in this study is a modified corner-point geometry model refined in between the wells to reduce numerical dispersion. The original model was taken from a reservoir simulation tutorial by Heriot-Watt University. The modified model has five layers with the following properties (Table 5-2):

Table 5-2: The static properties for the simulation model

Layer	Permeability	Porosity	Rock Type	kv/kh
1	10	26%	A	0.70
2	100	23%	C	0.10
3	1000	20%	B	0.02
4	10	17%	A	0.70
5	100	14%	C	0.10

The original oil in place is around 5.9 MMstb. Oil and water viscosities at a pressure of 5111psi are 0.489 cp and 0.8 cp, respectively. Rock compressibility is 4.0E-06 1/psi. This model has only one producer and one injector. Figure 5-7 shows the simulation grids coloured by the initial oil saturation and the location of the wells:

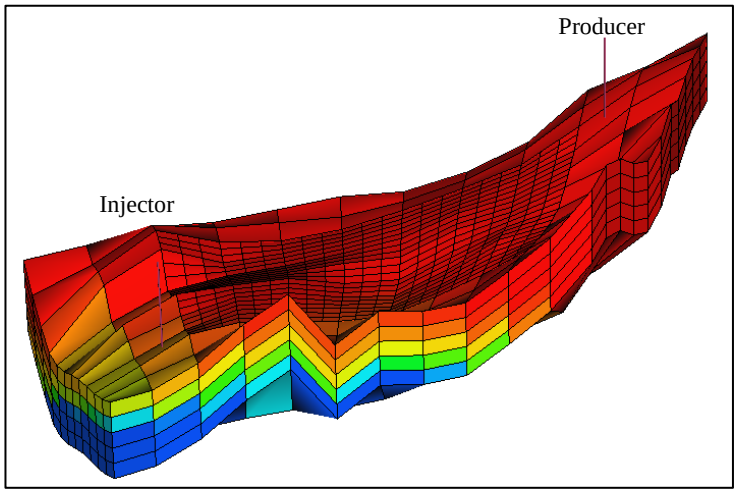

Figure 5-7: Reservoir-scale simulation model coloured by initial oil saturation

The simulated oil reservoir is connected to a small aquifer and started on production from a single well for almost a year. After that, water injection was introduced to maintain reservoir pressure, and waterflooding continued for approximately fifteen years. A WAG injection scheme was added to this model to improve the oil recovery after waterflooding and to increase the oil production rate.

To reflect a reasonable heterogeneity in the reservoir model, three main rock types were assumed to be present in the studied reservoir: high-permeability, medium-permeability, and low-permeability rock. The high-permeability rock type is modelled at the middle of the vertical section, whilst the low quality is at the top. This distribution should avoid the artificial exaggeration of early breakthrough of gas if the high-permeability rock is modelled at the top or early water breakthrough if the high-permeability layer is modelled at the bottom. Having an early breakthrough could hinder the ability to understand the real effect of properly modelling the effects of various rock types on WAG injection performance.

5.3.1.1 Rock Type A (Low Permeability)

Based on past experiences, many reservoirs in the Middle East would have a low permeability layer at the top. Therefore, the assumption here is that low-permeability rock type A will be modelled at the top. Figure 5-8 shows the assumed relative permeability for oil-water (left) and oil-gas (right):

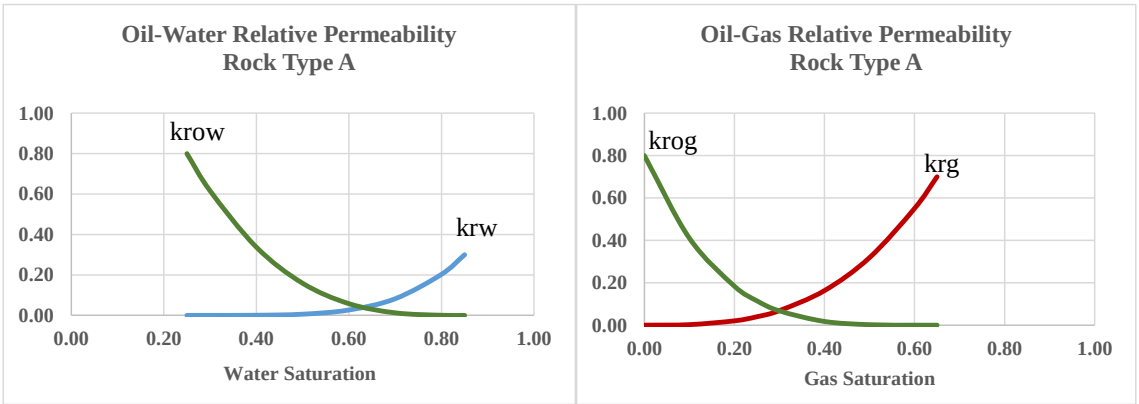

Figure 5-8: The relative permeability for oil-water (left) and oil-gas (right) for rock type A (low permeability)

The three-phase water-relative permeability for each rock type was reduced to capture proper three-phase hysteresis for the water; the one for rock type A is shown in Figure 5-9 below:

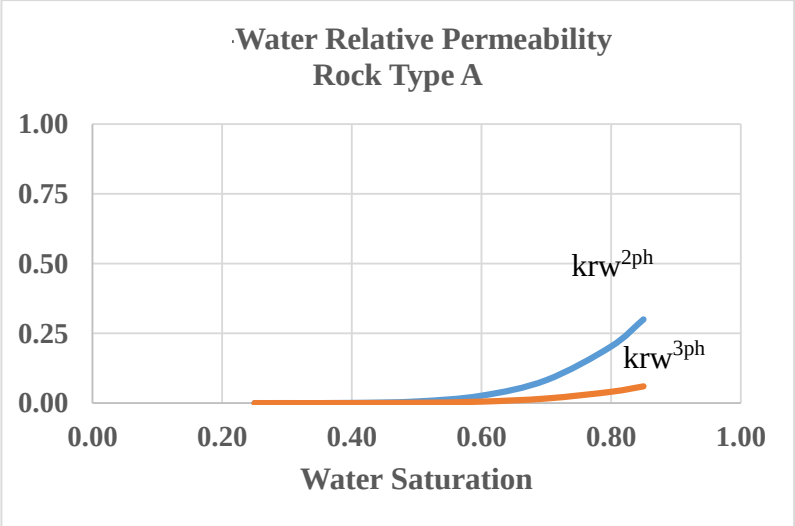

Figure 5-9: The three-phase water-relative permeability for rock type A

5.3.1.2 Rock Type B (High Permeability)

The high-permeability rock type B is assumed to be at the middle of the vertical section. Figure 5-10 shows the input-relative permeability in the simulation model for oil-water (left) and oil-gas (right):

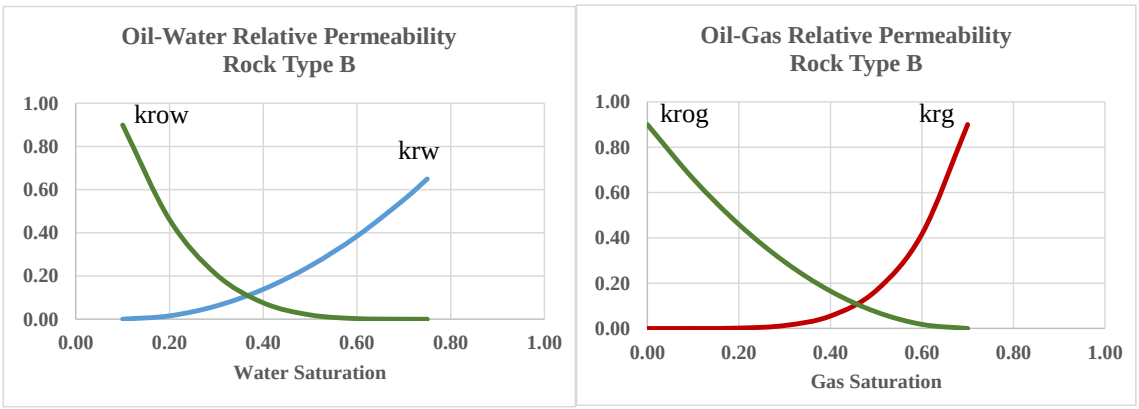

Figure 5-10: The relative permeability for oil-water (left) and oil-gas (right) for rock type B (high permeability)

The three-phase water-relative permeability for each rock type was reduced to capture proper three-phase hysteresis for the water. The three-phase water-relative permeability for rock type B is shown in Figure 5-11 below:

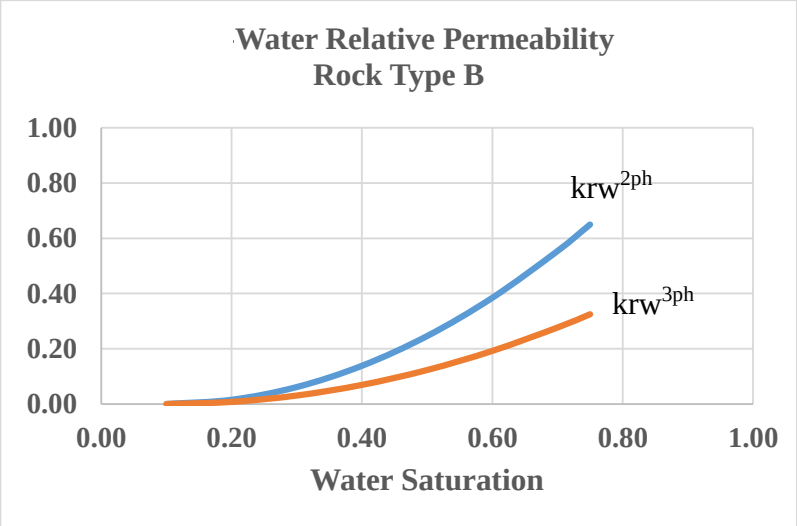

Figure 5-11: The three-phase water-relative permeability for rock type B

5.3.1.3 Rock Type C (Medium Permeability)

The bottom layers of the model used in this study were assumed to have 100mD average permeability at the bottom of the reservoir. Rock type C has the following relative permeability for oil-water (left) and oil-gas (right) [Figure 5-12]:

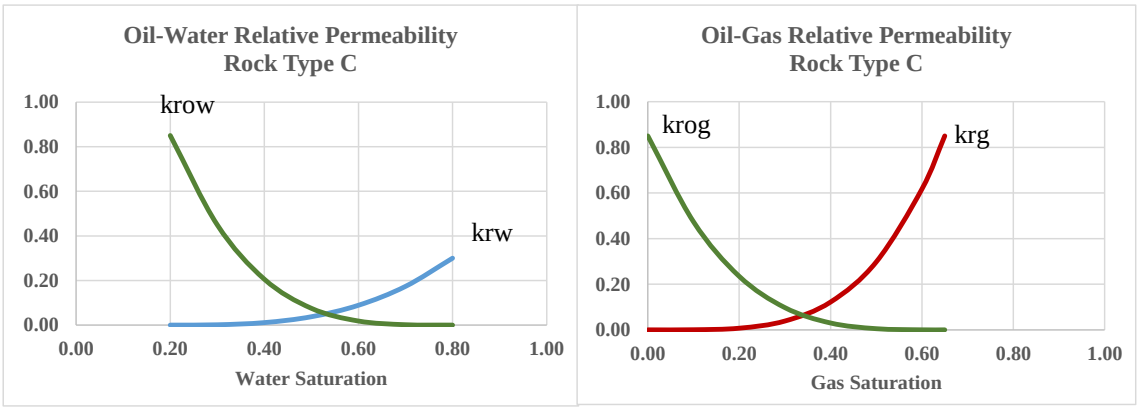

Figure 5-12: The relative permeability for oil-water (left) and oil-gas (right) for rock type C (medium permeability)

As mentioned, the three-phase water-relative permeability for each rock type was reduced to capture proper three-phase hysteresis for the water. The three-phase water-relative permeability for rock type C is shown in Figure 5-13 below:

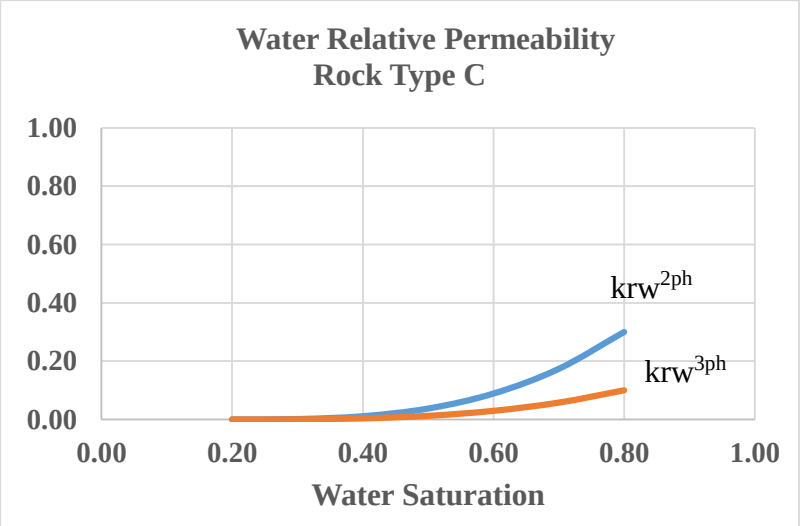

Figure 5-13: The three-phase water-relative permeability for rock type C

5.3.1.4 The Average Rock Type

Scaling up from a detailed geological model to a coarser dynamic simulation model is a common practise in the industry [64]. Therefore, averaging static and dynamic properties to model the average rock type (composite rock type) is necessary here. There are several methods to average flow functions:

- **Dynamic pseudos** is a method to come up with pseudo flow functions from the results of a fine-grid simulation to be used in a coarse-grid simulation and reproduce the same flow accuracy ([64-68].
- **Effective properties** is a method of calculating the effective properties of an isolated block at the viscous or capillary limit to represent the flow in an upscaled cell ([64].

The average two-phase relative permeability for the average rock type used in the simulation model is shown in the bold black curve in Figure 5-14, which also shows the average relative permeability compared to the other rock types:

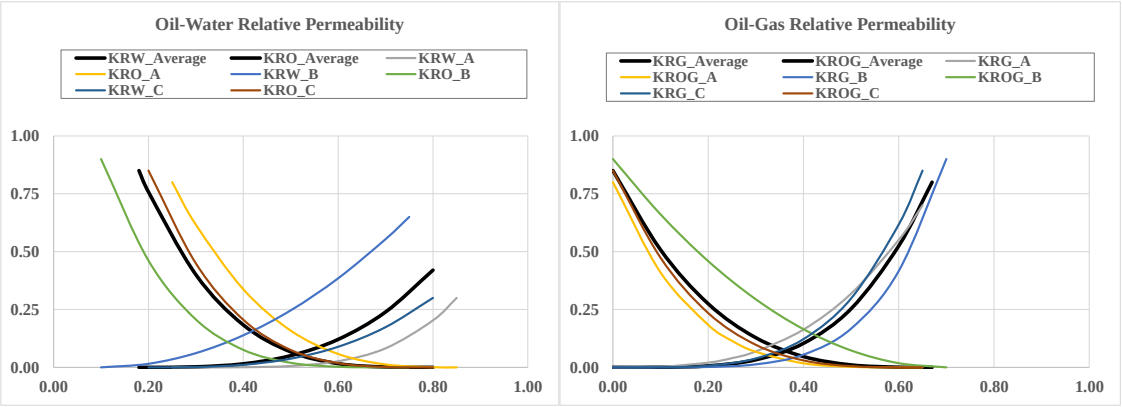

Figure 5-14: Oil-water relative permeability for each rock type along with the average kr (left); oil-gas relative permeability for each rock type along with the average kr (right)

5.3.2 The Effect of Gridding on WAG Injection Performance

As the number of grids in the simulation model increases, the simulation time, as well as the resources needed to complete the simulation study, will be higher. Therefore, to decide the optimum size and number of the simulation grids used in the WAG simulation model, the objective of the study must be clearly defined. The optimum resolution of the simulation model depends on the availability of the relevant data from the project area, the time required to make a decision, and the available resources. Thus, the balance amongst the required accuracy, decision time, and available resources is critical to overcoming challenges facing WAG simulation.

The size of the simulation grid plays an important role in the accuracy of estimating fluid flow in porous media. The coarser the grid size, the more numerical dispersion is expected in the simulation results. Numerical dispersion means that any small saturation of fluids has to instantly occupy the whole grid block so that as soon as a fluid flows from one grid the size of 200 metres, for example, it would reach the end of the neighbouring grid (200+ metres), which is not true in reality. The solution is to refine the grid blocks to a point that the error is negligible. In most cases, the numerical dispersion cannot be eliminated but instead minimised to a level where it will not change the conclusion.

The vertical grid resolution in simulating WAG injection is of great importance due to the flow characteristics of the gas. The injected gas into oil reservoirs often get segregated by the effect of gravity and flow towards the top of the reservoir creating a thin gas tongue flowing at a high velocity towards the production well. Having at least a few layers (2 or

3 layers) within the gas tongue is recommended to correctly capture the gas flow behaviour in the numerical simulation.

Therefore, in WAG injection, the size of the grid is of great importance. To understand the role of the number of layers as well, the following cases were evaluated [Table 5-3]:

Table 5-3: Grid dimensions for the three tested scenarios

Case	Grid DX [feet]	Grid DY [feet]	Grid DZ [feet]
Ref	**40**	**40**	**5**
Fine	**17.5**	**17.5**	**5**
Layers	**40**	**40**	**1**

The reference case had a reasonably fine grid (40'X40'X5'), but it was refined to 17.5'X17.5', and the thickness was kept the same as five feet (fine case). Next was another case where the reference grid size was kept the same for X and Y directions, but the thickness of the grid blocks were reduced to one foot instead of five feet. The effect of the three different grid sizes on WAG injection performance is shown in Figure 5-15 below:

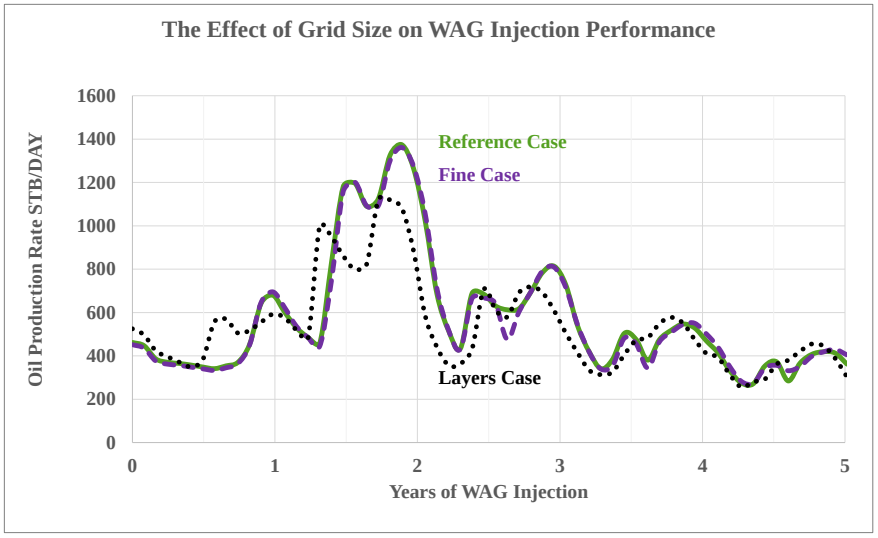

Figure 5-15: The effect of the three different grid sizes on WAG injection performance

The fine and reference cases have very negligible effects on the WAG injection oil recovery within the first five years, based on this model. However, the case with more layers showed a noticeable difference in oil recovery behaviour within the first five years of WAG injection, based on this model. Therefore, higher vertical resolution (more layers) is more important than high horizontal resolution (finer grids) in WAG injection performance. If the grid size would have been coarser than the reference case, some difference might have been noticed; however, this would not be recommended in any case.

5.3.3 The Effect of Cyclic Hysteresis on WAG injection performance

Many studies in the literature ignore hysteresis when simulating the WAG injection process. However, cyclic hysteresis is important to capture the correct process of oil recovery during WAG injection. In most cases, additional oil recovery during WAG injection was mobilised due to one or more of the following processes:

- nonwetting phase trapping
- mobility reduction of injectants (gas and water)
- change in composition (miscibility)

The first two processes above are directly linked to relative permeability hysteresis. Therefore, each rock type in the reservoir should be modelled using relevant WAG-HYST parameters. Table 5-4 summarises the assumed rock types and their properties:

Table 5-4: The WAG-HYST parameters for the three different rock types

Rock Type	Permeability [mD]	kv/kh	Land [C]	Alpha [a]	a-factor
Low Perm [A]	10	0.7	10.0	0.50	1.0
High Perm [B]	1000	0.02	1.0	1.00	1.0
Medium Perm [C]	100	0.1	2.0	1.50	1.0
Average Rock Type	n/a	0.07*	3.31**	0.89**	1.0

*harmonic average

**geometrical average

To understand the role of cyclic hysteresis in WAG injection simulation, two simulation cases were conducted. The reference simulation model, which includes the three-phase

hysteresis model (noted as ‘Reference Case—with Hysteresis’) was compared to the ‘No Hysteresis Case’. The oil production rates for the first five years of WAG injection are shown in Figure 5-16:

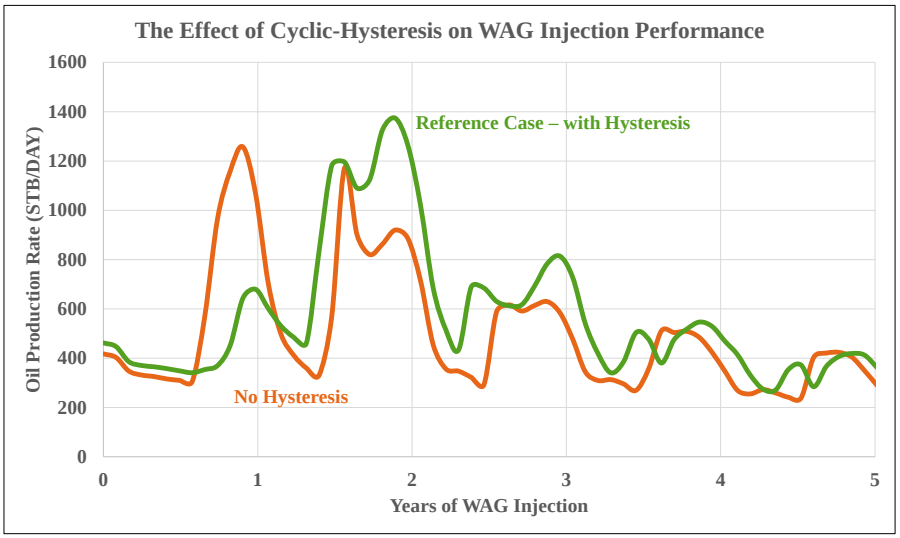

Figure 5-16: Oil production rates after WAG injection for the two cases (The orange curve is oil production rate for the case where no hysteresis model was used. The green curve shows the oil production rate for the case of a WAG hysteresis model.)

In Figure 5-16, the green curve shows the oil rate for the WAG hysteresis model, whilst the orange curve is the oil rate for the ‘no hysteresis’ case (only STONE 1 three-phase oil-relative permeability is included). As illustrated by the orange curve (no hysteresis), the oil production rate started to increase after only six months of WAG injection when hysteresis was ignored. The early oil bank production predicted by the ‘no hysteresis’ case seems to be mainly produced from the top layers, as shown in the grid sections in Figure 5-17:

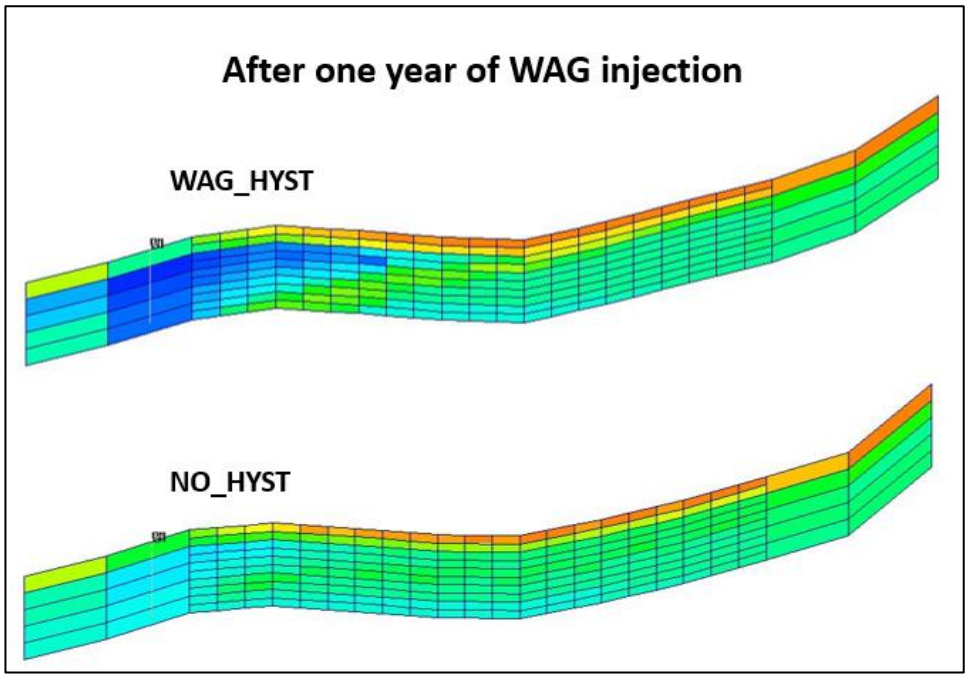

Figure 5-17: Cross sections show oil saturation distribution along the model layers for (top cross-section) the WAG hysteresis case and (bottom cross-section) the 'no hysteresis' case.

In the 'no hysteresis' case, the three-phase gas-relative permeability is not reduced by cyclic hysteresis, which allowed the gas to move more quickly and form an early oil production kick. The cyclic-hysteresis process reduces the three-phase gas-relative permeability and makes an oil bank form and move at a much slower pace, as noted in the WAG hysteresis case. It is important to remember, though, that this exercise is looking for the differences in both cases, not the exact timing.

Furthermore, the breakthrough time and the volume of gas production will be significantly different if hysteresis is dominant in the reservoir. To understand the difference, cumulative gas production for the two cases is shown in Figure 5-18:

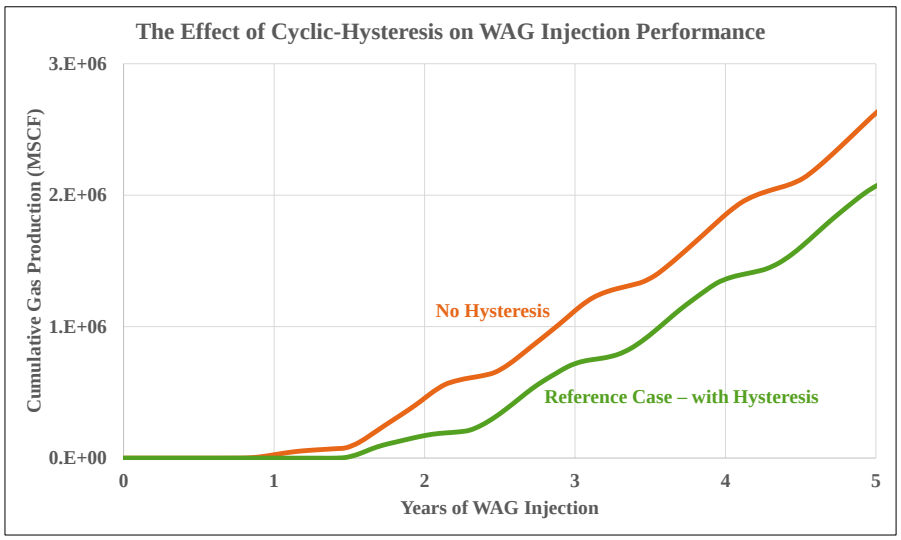

Figure 5-18: Cumulative gas production (The orange curve is for the 'no hysteresis' and the green curve is for the WAG hysteresis model.)

As expected, the 'no hysteresis' model would estimate an earlier gas breakthrough and higher gas production volume. If such a model is used in a reservoir where hysteresis is essential, the capacity of surface gas-handling facilities and injection gas requirements will be overestimated.

5.3.4 The Effect of Heterogeneity on WAG Injection Performance

The majority of oil reserves are remaining in carbonate reservoirs. However, the geology of carbonate rocks is more complex than that of sandstone reservoirs, and adding to its complexity is hysteresis when alternating water and gas injection in carbonate reservoirs. The main focus of most researchers is highlighting the role of three-phase cyclic hysteresis in oil recovery by WAG injection. In this section, more specifically, the focus is on understanding the challenges in simulating WAG injection scenarios in carbonate reservoirs.

Carbonate reservoirs are known to be heterogeneous and anisotropic, which makes the simulation of WAG injection behaviour in carbonate rocks more challenging. Figure 5-19 shows four cartoonish rock cross-sections to illustrate the heterogeneity and anisotropy where the cross-section (b) shows a heterogeneous and anisotropic type of rock, and the cross-section (a) is a homogeneous and isotropic rock type.

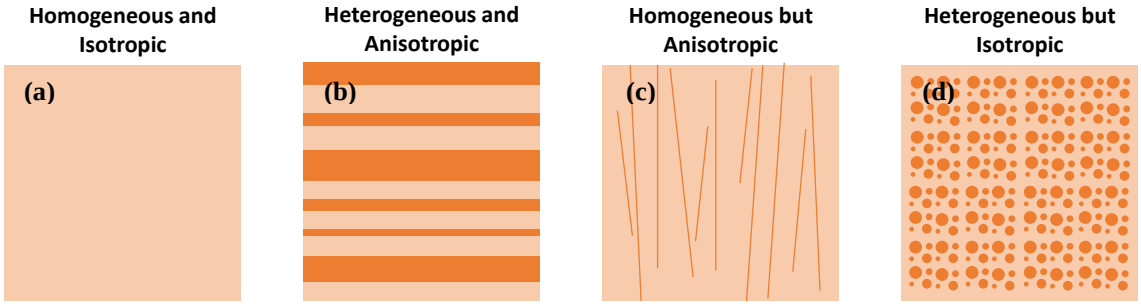

Figure 5-19: An illustration of the heterogeneity and anisotropy on a cross-section

Carbonate reservoirs often have all of these rock types in different parts of them, which adds more complexity to the hysteresis behaviour in WAG injection, making the numerical simulation of the WAG injection process in carbonate reservoirs a challenge. Moreover, the gridding of each rock type should be done in a way to preserve the heterogeneity and anisotropy of the rock:

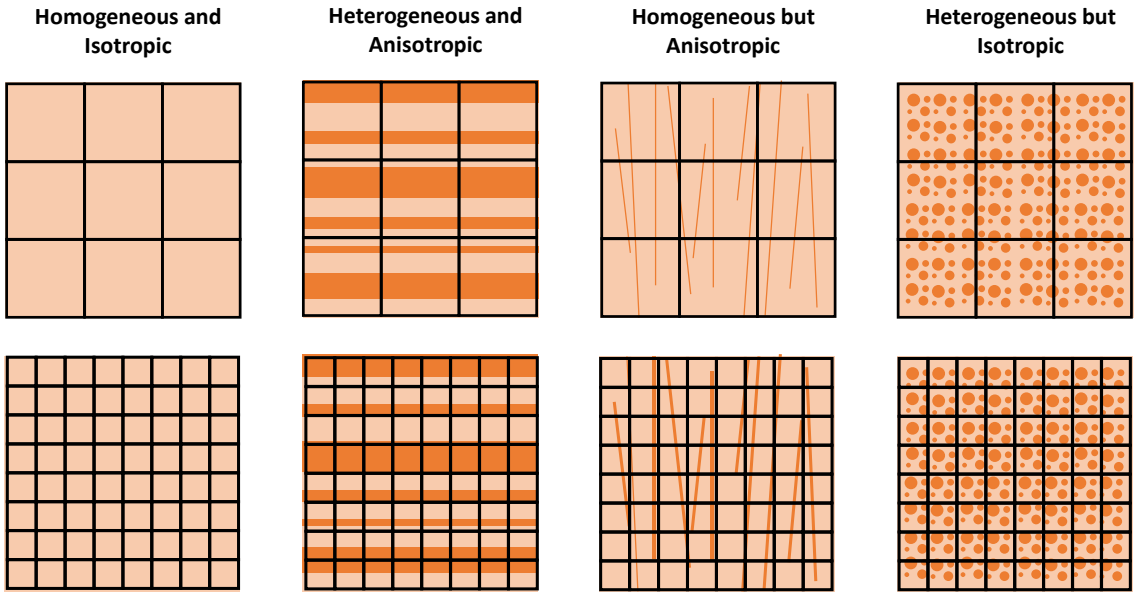

Figure 5-20: Coarse versus fine grids on each rock type

The coarser grids are usually used in waterflooding, whilst the finer grids are used with the WAG injection scenarios. For the isotropic rock types, the refining process would not significantly affect the vertical flow direction. However, for the anisotropic rock types, the coarser grids should have different pseudo functions to represent the same flow behaviour (section 5.3.1.4).

The reference case has three rock types distributed into the various layers of the reservoir. In some cases, only one average set of relative permeability is used in the simulation models due to the lack of such data in most reservoirs. However, this could have a severe effect on WAG injection performance. To test the effect of such dynamic heterogeneity on WAG injection performance, a simulation case with the average relative permeability

(section 5.3.1.4) was compared to the reference case. Figure 5-21 illustrates the difference in oil production rate in the first five years of WAG injection based on this scenario:

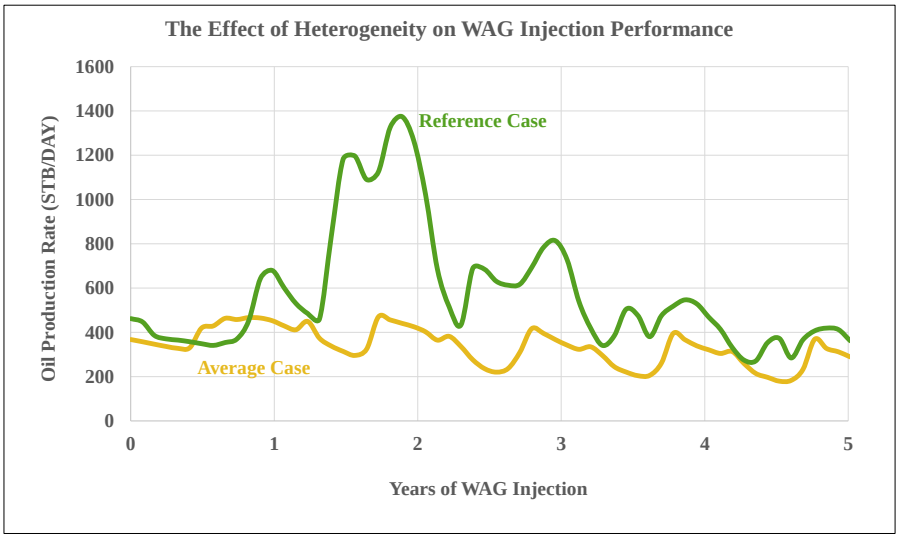

Figure 5-21: A comparison between oil production rate for the reference case (green) and the average flow functions case (yellow)

The difference is significant, which means that correctly representing the two-phase relative permeability for each rock type is essential in predicting the performance of WAG injection.

5.3.5 Discussion of the Sensitivity Results:

In this section, various parameters were evaluated to understand their effect on the simulation results. Section 5.3.2 evaluated the effect of gridding in WAG injection simulation by varying the grid size. If the grid size is refined from 40 to 17.5 feet in the x and y directions, the ultimate oil recovery was not significantly affected as shown in Figure 5-22. However, if the number of layers is increased from 20 to 100 layers, the oil recovery factor slightly dropped by 0.5% (Figure 5-22). The most significant drop in oil recovery was related to the averaging of relative permeability and hysteresis parameters. The reference case predicted the oil recovery after 5 years of WAG injection to be 71.2% while the averaged relative permeability case predicted only 61% oil recovery after the same period of WAG injection. Finally, Section 5.3.3 evaluated the effect of cyclic-hysteresis on WAG injection. When the cyclic-hysteresis was ignored, the oil recovery after five years of WAG injection predicted by the simulation was only 68% (Figure 5-22).

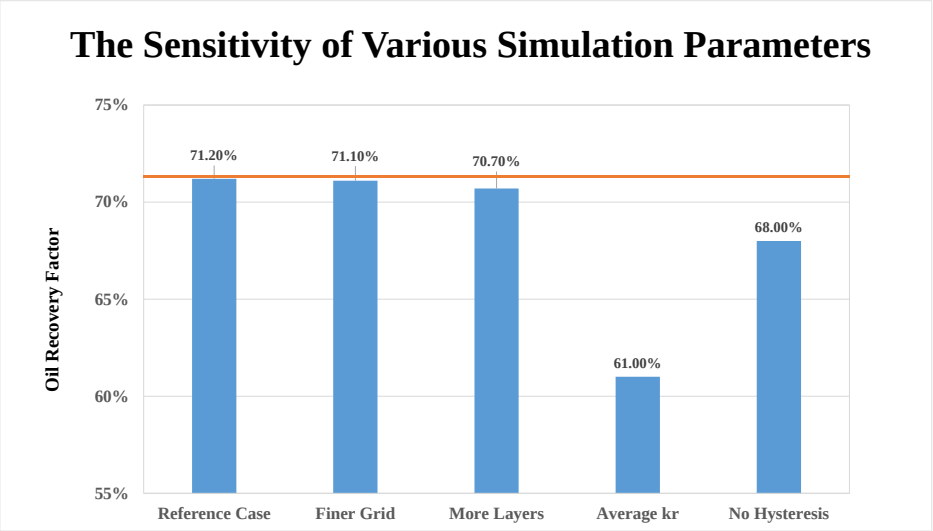

Figure 5-22: a bar chart summarising the sensitivity results

5.4 Effect of Non-Linear Convergence in WAG injection

Each simulator has an internal default process to decide how many time steps will be used to move from one reporting time to the next reporting time. Such default values might sufficiently work for the usual simulation cases i.e. reservoir depletion above the bubble point pressure, waterflooding, gas flooding... etc. However, for the WAG injection, these values often do not work properly.

To understand the process in which the simulator solves the non-linear equation, the following diagram illustrate the process [44]:

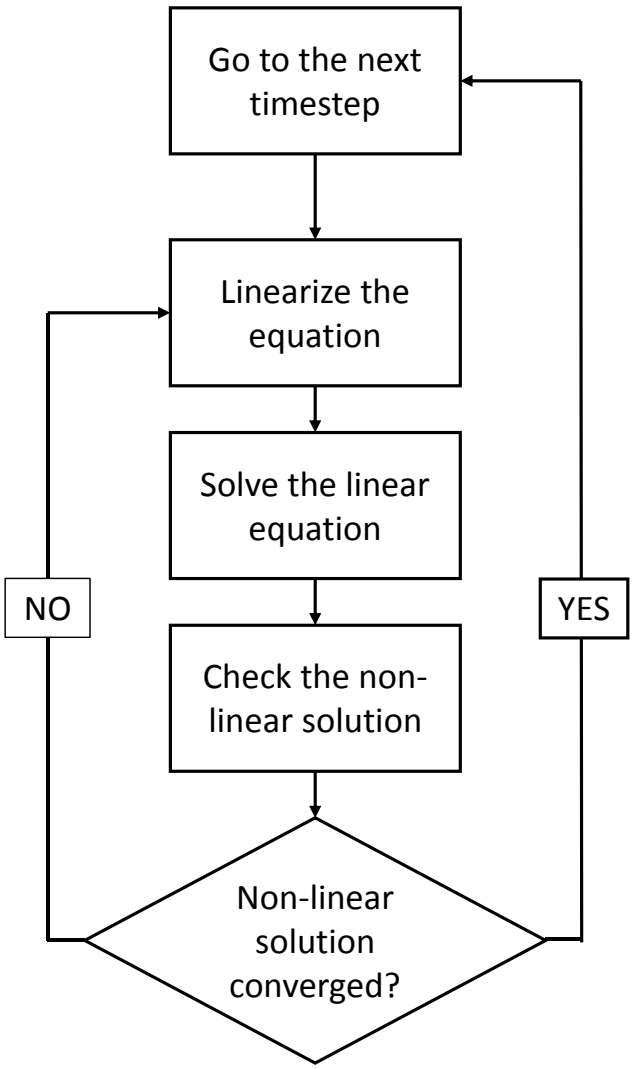

Figure 5-23: the process in which ECLIPSE simulator solves the non-linear equation [44]

There are many variables to be solved in each simulation grid cell at each reporting time. These variables are usually solved using the iteration process shown in Figure 5-23. However, cyclic-hysteresis in WAG injection scenarios often causes the non-linear solution convergence to fail between injection cycles. This results in an unstable numerical solution which usually hinders the ability to perform a reservoir-scale simulation of WAG injection process. To avoid such a problem, two approaches can be suggested:

1) Adjusting to the convergence criteria; or
2) Shortening the requested time-step between injection cycles.

5.4.1 Adjusting the Convergence Criteria:

Numerical simulators have internal protocols to converge non-linear solutions by Newton iterations. These protocols were set for normal oil and gas simulation procedures.

However, for the WAG injection process, these protocols can be altered carefully to fit with the process. For example, the default maximum number of iterations in ECLIPSE simulator is 12 Newton iterations and the default convergence criteria for the pressure is 0.1 atm. By using the TUNING keywords in ECLIPSE, these defaults can be changed to more iterations or relaxed tolerance to the convergence criteria [44]. Such modification is not recommended unless necessary and must be done with caution.

5.4.2 Shortening the Requested Time-Step between Injection Cycles:

An alternative solution is to request very small time steps where the saturation direction is changed. This would force the solver to take small steps and converge easier when the saturation and pressure are changing drastically. To illustrate the usefulness of this solution, three different time-step scenarios were tested using the model described in section 5.3.1. The time-step scenarios are summarised in table x:

Table 5-5: Summary of the three different time-step scenarios tested using the reservoir-scale simulation model

Case	Time-step per Cycle	Cycles	# Problems
Base Case	12*15 /	W1-G2-W3	728
Case 1	36*5 /	W1-G2-W3	451
Case 2	**Gas Cycle [G2]** 100*0.01 / 4*1 / 35*5 / **Water Cycle [W3]** 1000*0.1 / 800*0.1 /	W1-G2-W3	8

As illustrated by Table 5-5 and Figure 5-24, the shorter time-steps significantly reduced the number of non-linear convergence failures in the numerical simulation. The number of problems dropped from 728 to 8 by shortening the requested time-step, especially during three-phase water injection.

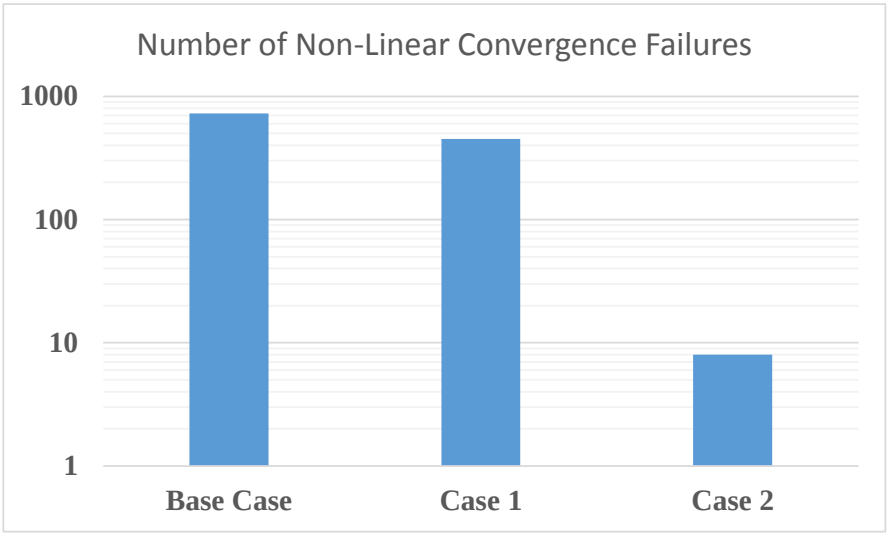

Figure 5-24: the number of non-linear convergence failures for each time-step scenario (logarithmic-scale)

Resolving the issue of non-linear convergence failures should improve numerical-simulation stability and allows for faster simulation runs. In the next section, the application of the suggested methodology in section 4.2 will be demonstrated on a reservoir-scale simulation model.

5.5 Application of the Suggested Methodology on a Reservoir-Scale Simulation Model:

The main objective of numerical simulation of WAG injection is to optimise its field application. As demonstrated in previous chapters, WAG injection behaviour changes for the later cycles due to the cyclic hysteresis. The suggested methodology to update the WAG-HYST parameters can be applied to reservoir-scale as well as core-scale simulation. To demonstrate the applicability and the usefulness of such a method, a reservoir sector-model was utilized to run a WAG injection scenario.

The same reservoir sector-model described in section 5.3.1 was used, with some modifications, to evaluate the applicability of the suggested method [Figure 5-7]. The WAG injection scenario modelled here started with waterflooding for 10 years then WAG injection cycles every six months were applied.

As suggested in section 4.2, the proper cyclic hysteresis requires an update to the WAG-HYST parameters after the third cycle W3. Therefore, the first run with initial hysteresis parameters was used for W1, G2 and W3. Then, different hysteresis parameters were used for the second simulation run which covers the later cycles as shown in Table 5-6:

Table 5-6: Summary of the WAG-HYST input parameters used in the reservoir sector-model

Injection Cycles	STONE1 Exponent (η)	Land's Parameter (C)	Reduction Exponent (α)
W1-G2-W3	6.5	2.00	0.45
G4-W5-G6 …	0.9	0.81	1.20

As part of the hysteresis model, the krw^{3ph} can be used to model the expected reduction in water mobility during the three-phase water injection cycles. Therefore, the water-relative permeability was reduced to capture a reasonable drop in water relative permeability in the three-phase zone [Figure 5-25]:

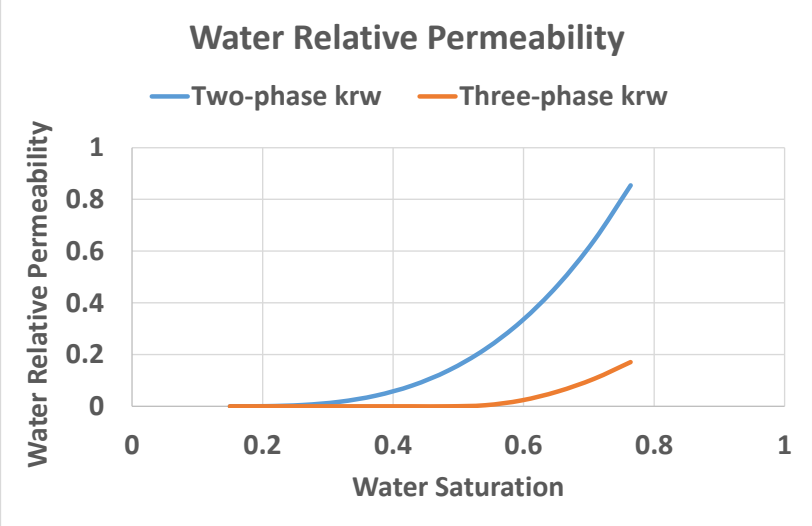

Figure 5-25: Two-phase and three-phase water-relative permeability for the reservoir sector-model

The simulation results of such WAG injection scenario by applying the suggested methodology showed a clear difference in oil production rate as shown in Figure 5-26:

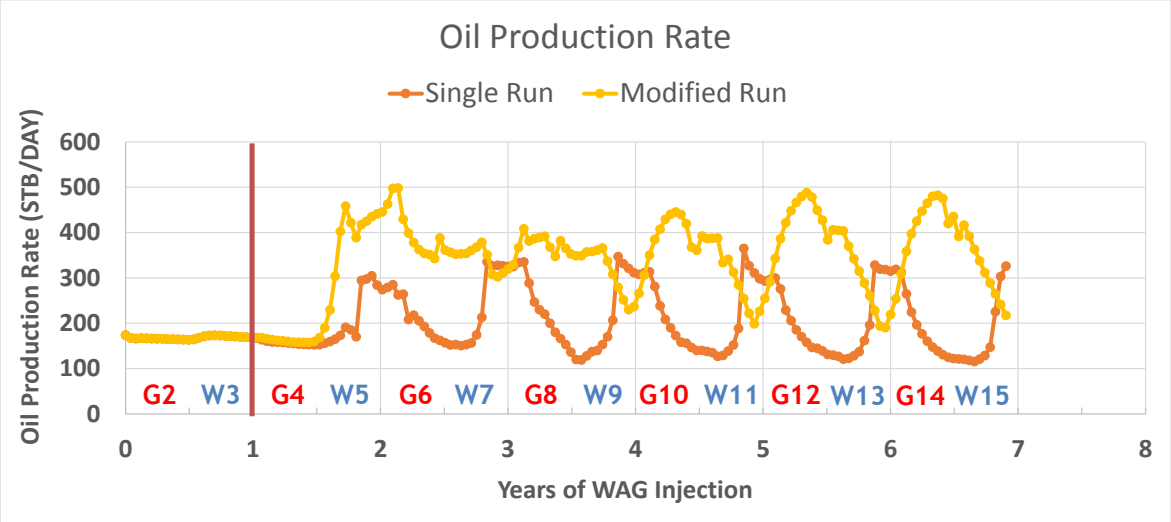

Figure 5-26: Oil production rate versus years of WAG injection predicted by the reservoir sector-model. (Orange line) shows the oil production rate by the single run. (Yellow line) shows the oil production rate by the modified run

The results of both simulations run started to differ after 18 months of WAG injection. The average oil production rate predicted by the modified run is significantly higher than the predicted oil rate by the single run. This difference in oil rate resulted in a 4 per cent higher oil recovery after 7 years of WAG injection as shown in Figure 5-27:

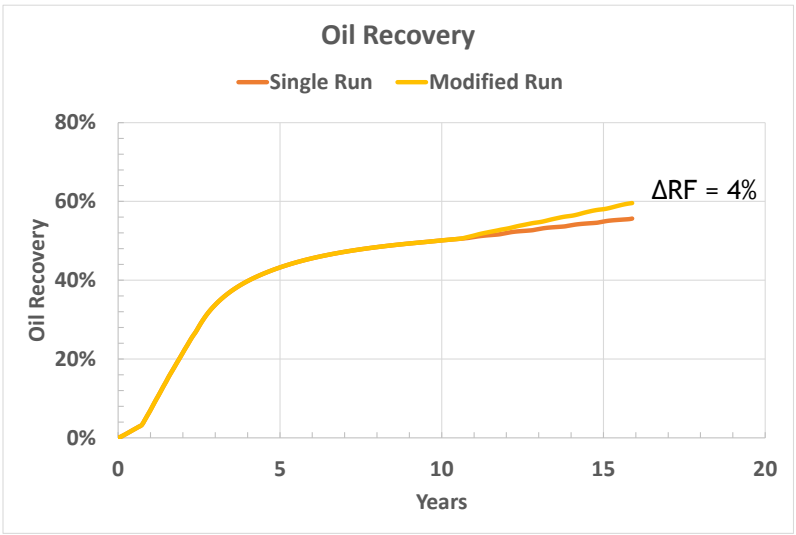

Figure 5-27: Oil recovery versus years of WAG injection predicted by the reservoir sector-model. (Orange line) shows the oil recovery by the single run. (Yellow line) shows the oil recovery by the modified run

Properly modelling the process of cyclic hysteresis would lead to a better prediction of oil recovery. The three-phase water imbibition would trap more gas in the three-phase zone which would result in mobilising some of the residual oil saturation [Equation 2-6]. Figure 5-28 shows the model cross-section with oil saturation to illustrate the difference in oil saturation in the three-phase zone between the two runs:

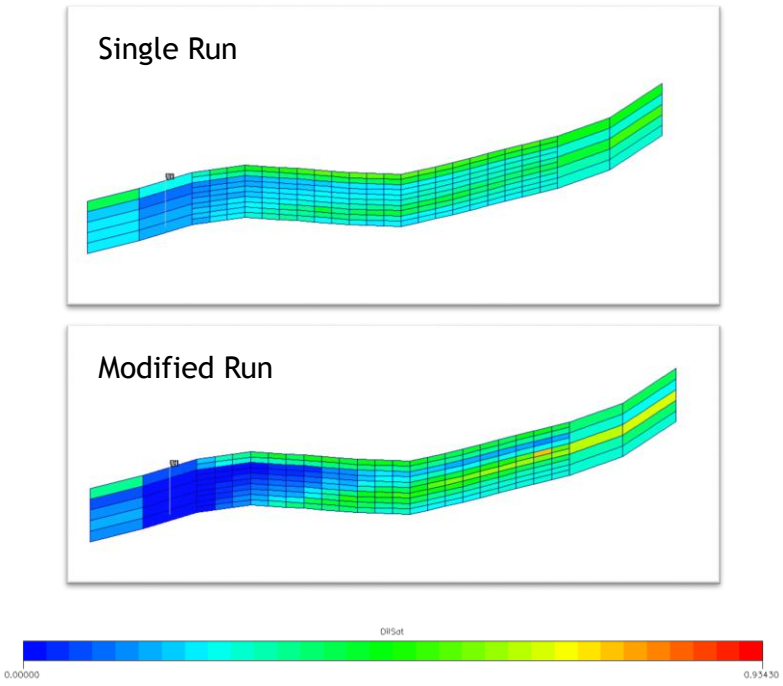

Figure 5-28: Cross sections from the reservoir sector-model illustrating the oil saturation in the three-phase zone after 7 years of WAG injection. Top cross section shows the oil saturation predicted by the single run. Bottom cross section shows the oil saturation predicted by the modified run.

The predicted oil saturation by the modified run in the three-phase zone after 7 years of WAG injection was less than 0.06. This very low residual oil saturation is due to the process of cyclic hysteresis. Such behaviour is expected to happen in real reservoirs under WAG injection; therefore, the suggested methodology should help in minimising the error in WAG injection simulation.

5.6 Conclusion

Oil reservoirs might need EOR at some point after waterflooding to maximise oil recovery. WAG injection is one of the proven EOR methods nowadays. However, WAG injection simulation is more complex and must be done properly to plan and predict WAG injection performance. Reservoir heterogeneity and anisotropy, as well as the gravity effect, make the simulation of WAG injection at reservoir scale more challenging. Capturing all the variation in geology and the hysteresis behaviour for each rock type in a very fine grid model would require huge computational power and long run time.

The most important parameter to model the multiphase flow in reservoir simulation is the flow functions (kr and Pc). Also, the current three-phase models use the input two-phase flow functions to empirically calculate three-phase kr and Pc. Therefore, kr and Pc should influence the performance of WAG injection. In this chapter, the effect of these two

functions was evaluated by a two-dimensional cross-section simulation model with homogenous properties. The results from this study confirmed that misrepresenting the flow function at reservoir-scale simulation could lead to significant differences in oil recovery and oil production plateau length.

Since WAG injection involves the injection of gas into the reservoir, the vertical permeability is expected to be of high importance. The common understanding in the industry is that vertical permeability is usually lower than horizontal permeability. Also, the rule of thumb that most engineers would use is that vertical permeability is almost 10 per cent of horizontal permeability. However, this is far from accurate in most cases, especially with fine-grid models. Therefore, in this chapter, a sensitivity study was conducted to understand the role of vertical permeability in WAG injection performance compared to waterflooding, and a quarter five-spot pattern with the reasonable resolution was utilised to understand the effect of vertical permeability on WAG injection performance. When refining the grid cells for simulating the WAG injection process, the vertical permeability assigned to the cells were often kept the same as the coarser model. It was demonstrated in this study that for WAG injection, the kv/kh ratio plays a more significant role in the prediction of oil recovery compared to the waterflood. The results from this sensitivity study showed that the predicted oil recovery factor can vary by 7 per cent due to the vertical-to-horizontal permeability ratio (kv/kh) alone.

Moreover, various rock types can exist in a small volume of the reservoir rock. Therefore, when gridding the rock section to make a numerical simulation model, often more than one rock type must be represented in each grid cell. Geologists usually work on averaging static properties and distributing them along the geological model grids. However, for the dynamic simulation model, sometimes only one average set of relative permeability could be used due to the lack of such data in most reservoirs, which could have a severe effect on WAG injection performance, as shown in this chapter.

The cyclic injection of water and gas into an oil reservoir would cause three-phase relative permeability hysteresis, which, however, is often ignored or misrepresented in reservoir-scale simulation studies of WAG injection. Thus, in this chapter, the effect of cyclic hysteresis on WAG injection performance was studied, and the results showed that not accounting for this factor would cause inaccurate predictions of:

- first three-phase oil bank arrival time

- the average oil production rate after WAG injection
- the total additional oil recovery by WAG injection
- the breakthrough time and the cumulative production of the gas phase

Therefore, it is vital to account for cyclic hysteresis in reservoir-scale simulations, and chapter 6 discusses some tips on how to best do so.

Chapter 6—WAG Injection Simulation Best Practices

The ultimate goal for reservoir engineers and managers is to maximise oil recovery and minimise cost. Utilising numerical simulation to achieve this goal has proven successful given that the simulation model is fit-for-purpose and as accurate as possible. Currently, there is no agreed guideline for WAG injection simulation. Alternatively, there are multiple efforts to bridge the gap in modelling accuracy of this EOR method ([21, 25, 48]. However, the cyclic-hysteresis process during WAG injection complicates the oil recovery process, which makes simulating this technique a challenge.

This thesis focusses on two main areas: the required data to model the WAG injection process into numerical simulation and the modelling process to capture the essential behaviour of oil recovery through this process. In this chapter, a systematic guideline is suggested for acquiring the relevant data for the analysis and simulation process. The first part of the chapter is about the ideal set of experiments to collect enough data to build the simulation model. Then a workflow is introduced to analyse the experimental data and extract information on cyclic hysteresis. Finally, the procedure to input the core-scale data into the reservoir-scale simulation model is discussed. This guideline should help the industry unify the approach to evaluating WAG injection projects and improve the outcomes of such a technique.

6.1 The Ideal Set of Experiments

An accurate and complete set of experiments is essential to formulate the input for the WAG injection simulation model. The minimum required experiments must be relevant to the simulation objective. The common method to simulate three-phase flow behaviour is to use the three-phase empirical models (section 2.1) to estimate kr and Pc from the input-two phase data. Therefore, the two-phase kr data must be as accurate as possible and cover a wide range of valid two-phase saturation ranges.

6.1.1 Two-Phase Displacement Experiments

Two-phase kr and Pc are the input functions for a numerical simulation to describe the simultaneous flow of two phases in the porous media. They can be estimated with the help of numerical simulation by matching the data from SS or USS displacement experiments. Water and oil flow functions (kr and Pc) can be obtained from a water-

displacing-oil experiment, whilst the gas and oil flow functions can be acquired from a gas-displacing-oil experiment at initial water saturation (Swi). The following two-phase displacement experiments are essential to estimate the required input for the numerical simulation:

- water-oil imbibition experiment
- gas-oil drainage experiment
- oil-gas imbibition experiment

More details about the conditions of these experiments can be found in section 3.1.

6.1.2 Three-Phase WAG Injection Experiments

The WAG injection is a three-phase process. Injecting different cycles (gas and water) into the rock/fluid system creates cyclic hysteresis, where kr and Pc should be adjusted. To understand the hysteresis behaviour and obtain the WAG-HYST parameters, WAG injection experiments should be performed, starting with either the water (WAG) or gas (GAW) cycle. The following experiments are recommended to obtain the full range of data to simulate the WAG injection process:

- three-phase water primary imbibition [Sw = Swc] experiment
- three-phase water secondary imbibition [Sw > Swc] experiment
- three-phase gas primary-drainage [Sgi = 0] experiment
- three-phase gas secondary-drainage [Sgi ≥ Sgt] experiment

More details about the conditions necessary for these experiments can be found in section 3.1.

6.2 Guideline for WAG Injection Simulation

The guideline for WAG injection simulation is the suggested procedure to prepare and analyse a set of experimental data to generate enough information to perform this process.

6.2.1 Basic Input Data

The usual procedure is to start WAG injection after an extended water-injection period. Therefore, enough information about the two-phase flow behaviour should be collected. The basic input for the three-phase numerical simulation consists of the two-phase flow

functions, saturations, and pressure. In this guideline, the requested input data for the first step are:

- the connate water saturation **(Swc),** which is the immobile saturation of water
- the residual oil saturation by water **(Sorw),** which is the saturation of oil remaining after an extended water injection
- the pressure drop **(DP)** at the end of two-phase water injection (**DPw^{2ph})**
- the two-phase water-oil imbibition relative permeability [**krw (Sw), krow (Sw)**]
- the critical gas saturation (**Sgc),** which is the saturation when the gas starts to move
- the residual oil saturation by gas (**Sorg),** which is the saturation of oil remaining after an extended gas injection
- the DP at the end of two-phase gas injection (**DPg^{2ph})**
- the two-phase gas-oil drainage relative permeability **[krg (Sg), krog (Sg)]**

6.2.2 Three-Phase Input Data

The collected three-phase data from the WAG injection experiments (section 6.1) can be used to estimate the input parameters for a WAG-HYST model in the numerical simulation. This tool would require the three-phase data to be entered in a table format, as in the following:

- **First column:** time in hours
- **Second column:** cumulative oil production in cubic centimetres.
- **Third column:** the average water saturation in fraction
- **Fourth column:** the average gas saturation in fraction
- **Fifth column:** the average oil saturation in fraction
- **Sixth column:** the DP in psi

Based on the information obtained in this thesis, the recommended three-phase data should be collected from the following experiments.

6.2.2.1 Three-Phase Water Primary Imbibition (Swi = Swc)

The three-phase primary-imbibition process means injecting water into a system containing movable oil and gas at initial connate water saturation (Swc) to reach the minimum possible residual oil saturation (Som). This situation represents any of the following scenarios:

- An oil reservoir undergoing gas injection before the start of WAG injection process

- Depleted oil reservoir with an expanded gas cap before the start of WAG injection process

Water injection starting into oil reservoirs with either these conditions should follow the three-phase water primary imbibition process. The assumption is that the water saturation in most of the reservoir is still at the connate water saturation. However, since the gas phase is present, then the water-relative permeability would most likely drop due to the existence of gas.

The three-phase water-relative permeability required for the WAG-HYST model is at the maximum gas saturation (the lowest water-relative permeability). If the gas saturation in the system is less than the maximum gas saturation, then the simulator would interpolate between two- and three-phase water-relative permeability.

The current numerical simulators would not automatically alter the input imbibition water-relative permeability unless the WAG-HYST model is activated and the three-phase imbibition water-relative permeability is inputted by the user. Thereafter, the data collected from this experiment would be used to estimate the three-phase water imbibition relative permeability (krw^{3ph}), which would be inputted into Table 6-1:

Table 6-1: Experimental data from the three-phase water primary imbibition (Swi = Swc)

Table 1: The three-phase water primary imbibition (Swi = Swc)					
Column 1	Column 2	Column 3	Column 4	Column 5	Column 6
Time (hours)	Cumulative oil (cc)	Sw (fraction)	Sg (fraction)	So (fraction)	DP (psi)

6.2.2.2 Three-Phase Water Secondary Imbibition (Swi > Swc)

The three-phase water-secondary imbibition process involves injecting water into a system containing movable oil, gas, and water saturation that is higher than the connate water saturation to reach the minimum possible residual oil saturation (Sorm). In most oil reservoirs where waterflooding was applied for a very long time, the remaining water saturation in most of the reservoir after three-phase gas injection is higher than the connate water saturation. Thus, starting a WAG injection there means that the three-phase water injection after the gas injection would be applied to an oil reservoir where most of the average water saturation is higher than the connate water saturation. The kr of the water in this situation should be different than the two-phase water-imbibition kr and

probably also different from the three-phase water primary imbibition, where Sw is equal to the Swc.

The current WAG-HYST model in numerical simulators would not differentiate between three-phase water primary imbibition and secondary imbibition. Therefore, the data collected from this experiment would be used to estimate the three-phase water imbibition relative permeability [krw^{3ph}] and compare it with that from the three-phase water primary imbibition. The data from this experiment should be inputted into Table 6-2:

Table 6-2: Experimental data from the three-phase water secondary imbibition (Swi > Swc)

Table 2: The three-phase water secondary imbibition (Swi > Swc)					
Column 1	Column 2	Column 3	Column 4	Column 5	Column 6
Time (hours)	Cumulative oil (cc)	Sw (fraction)	Sg (fraction)	So (fraction)	DP (psi)

6.2.2.3 Three-Phase Gas Primary Drainage (Sgi=0)

The three-phase gas primary drainage involves injecting gas for the first time into a system containing movable oil and water (Sw > Swc) until the minimum residual oil saturation (Sorm) is reached. This drainage process starts with gas injection into reservoirs as part of the WAG injection process after an extended period of waterflooding. The kr of the gas in this situation does not follow the same behaviour as in the two-phase primary drainage due to the presence of free water saturation. Also, this gas drainage process may not follow the same behaviour as the three-phase gas secondary drainage process where Sg is higher than zero (Sg=Sgt). The current WAG-HYST model in numerical simulators would not differentiate between this three-phase gas primary and secondary drainage (discussed next). The data collected from this experiment [G2], used to estimate the gas secondary drainage reduction exponent [α] and compared to the reduction exponent obtained from the secondary drainage, should be inputted into Table 6-3.

Table 6-3: Experimental data from the three-phase gas primary drainage (Sgi=0)

Table 3: The three-phase gas primary drainage (Sgi=0)					
Column 1	Column 2	Column 3	Column 4	Column 5	Column 6
Time (hours)	Cumulative oil (cc)	Sw (fraction)	Sg (fraction)	So (fraction)	DP (psi)

6.2.2.4 Three-Phase Gas Secondary Drainage (Sg > Sgt)

The three-phase gas secondary drainage process starts by injecting gas into a system containing movable oil, water, and gas, where the gas saturation is greater than zero (Sg > Sgt), to reach Sorm. This process represents the situation where the oil reservoir went through an extended gas injection followed by an extended water injection, and gas is being injected into the same areas of the reservoir. The best situation here is where the oil reservoir was initially flooded by water, and then WAG injection started. This process is the [G4] cycle of the WAG injection process (per the convention suggested in this thesis). The data from this experiment should be inputted into Table 6-4.

Table 6-4: Experimental data from the three-phase gas secondary drainage (Sg > Sgt)

Table 4: The three-phase gas secondary drainage (Sg > Sgt)					
Column 1	Column 2	Column 3	Column 4	Column 5	Column 6
Time (hours)	Cumulative oil (cc)	Sw (fraction)	Sg (fraction)	So (fraction)	DP (psi)

6.2.3 Logical Operations

Based on the input data from the previous sections, the following logical operations can be used to extract more information.

6.2.3.1 DP during Three-Phase Water Imbibition (DP_w^{3ph})

There are two definitions of the three-phase water imbibition, as discussed earlier:

1. **<u>Three-phase water primary imbibition:</u>** The water here is injected into a system that has the initial water saturation equal to the connate water saturation. If the DP during this injection cycle is higher than that during two-phase water injection,

then the three-phase water imbibition relative permeability [krw^{3ph}] must be lowered. This information can be extracted from [W2] in the GAW experiment.

2. **<u>Three-phase water secondary imbibition:</u>** The water here is injected into a system that has water saturation initially higher than the connate water saturation. If the DP during this injection cycle is higher than that during two-phase water injection, then the three-phase water imbibition relative permeability [krw^{3ph}] must be lowered. This information can be extracted from [W4] in the GAW experiment.

Therefore, the logical operations to record DP during three-phase water imbibition [$DP_w{}^{3ph}$] are as follow:

- $DP_{W2}{}^{3ph}$ = maximum (DP; Table 1 [column 6])
- $DP_{W4}{}^{3ph}$ = maximum (DP; Table 2 [column 6])
- **$DP_W{}^{3ph}$ = maximum ($DP_{W2}{}^{3ph}$, $DP_{W4}{}^{3ph}$)**

6.2.3.2 DP during Three-Phase Gas Drainage ($DP_g{}^{3ph}$)

There are two different definitions of three-phase gas drainage, as suggested earlier:

1. **<u>Three-phase gas primary drainage:</u>** This gas is injected into a system that initially has zero gas saturation. If the DP during this injection cycle is higher than that during two-phase gas injection, then the three-phase gas drainage relative permeability [$krg_{PD}{}^{3ph}$] must be lowered using the reduction exponent [α]. This information can be extracted from [G2] in the WAG experiment.
2. **<u>Three-phase gas secondary imbibition:</u>** This gas is injected into a system that initially has gas saturation higher than the trapped-gas saturation [Sgt]. If the DP during this injection cycle is higher than that during two-phase gas injection, then the three-phase gas secondary drainage relative permeability [$krg_{SD}{}^{3ph}$] must be lowered by [α]. This information can be extracted from [G4] in the WAG experiment.

Therefore, the logical operations to record the DP during three-phase gas drainage [$DP_g{}^{3ph}$] are as follow:

- $DP_{G2}{}^{3ph}$ = maximum (DP; Table 3 [column 6])
- $DP_{G4}{}^{3ph}$ = maximum (DP; Table 4 [column 6])
- **$DP_g{}^{3ph}$ = maximum ($DP_{G2}{}^{3ph}$, $DP_{G4}{}^{3ph}$)**

6.2.3.3 Trapped-Gas Saturation (Sgt)

It has been established that during three-phase water injection, the process of three-phase water imbibition will trap some of the free gas in the system. However, based on the information collected in this thesis, the amount of trapped gas from three-phase water primary imbibition is different than the water secondary imbibition. Therefore, the following logical operations to record Sgt are suggested:

- Sgt' (W2) = minimum (Sg; Table 1 [column 4])
- Sgm' (W2) = maximum (Sg; Table 1 [column 4]
- Sgt'' (W4) = minimum (Sg; Table 2 [column 4])
- Sgm'' (W4) = maximum (Sg; Table 2 [column 4]

6.2.3.4 Minimum Two-Phase Residual Oil Saturation (Sorm)

In the two-phase system, there is only one residual oil saturation: Sorg or Sorw. However, in the three-phase system, the residual oil saturation is assigned by one of two methods:

1. **No Hysteresis:** In this case, the three-phase residual oil saturation is the minimum of the two residual oil saturations.
    - Sorm = minimum (Sorw, Sorg).
2. **WAG Hysteresis:** In this case, the minimum residual oil saturation (Sorm) is modified based on the Sgt.
    - Som = Sorm – aSgt

The logical operations to be considered here to allow for estimation of a-factor (the residual oil modification factor) are:

- Sorm = minimum (Sorw, Sorg)
- Som = minimum (So; Table 2 [column 5])

6.2.4 Cyclic Hysteresis Systematic Check

As established in the previous chapters, WAG injections usually exhibit a strong cyclic-hysteresis effect. However, this may not always be the case or be significant. The analysis of several WAG core-flood experiments in section 4.3 showed that cyclic-hysteresis effects can be extracted from the WAG injection experimental data, but to make the process of detecting it more systematic, the following criteria are suggested to decide whether WAG hysteresis is essential or not.

6.2.4.1 Water Model

If the DP during a three-phase water injection cycle (DPw^{3ph}) is higher than that during a two-phase cycle (DPw^{2ph}), then cyclic hysteresis is essential. In another form, if $DPw^{3ph} / DPw^{2ph} > 1.0$, then three-phase water relative permeability [krw^{3ph}] is essential. In this case, the water model in the WAG-HYST must be activated. The logical process to do so is illustrated in Figure 6-1:

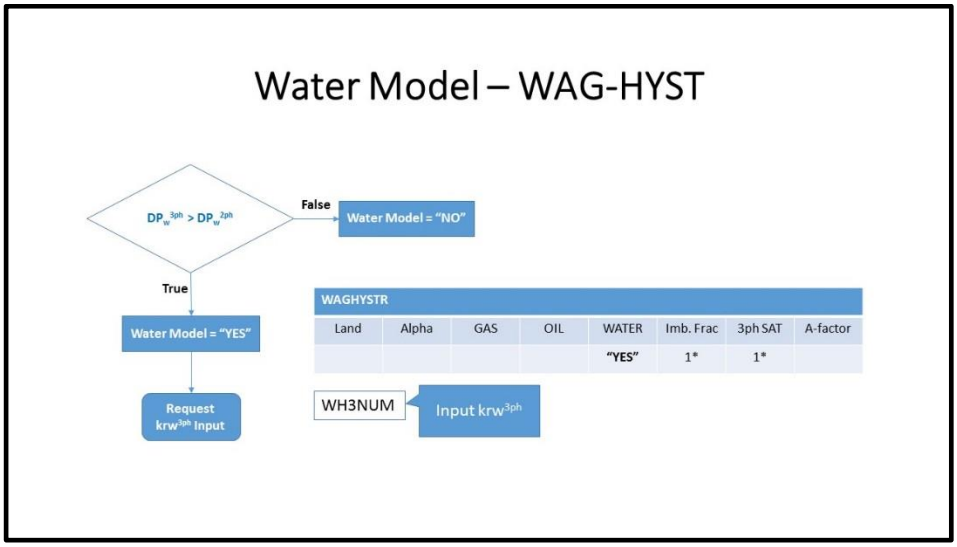

Figure 6-1: The logical process to activate the water model in the WAG-HYST model

6.2.4.2 Gas Model

If the DP during a three-phase gas injection cycle (DPg^{3ph}) is higher than that during a two-phase cycle (DPg^{3ph}), then cyclic hysteresis is essential. In another form, if $DPg^{3ph}/DPg^{2ph} > 1.0$, then the gas secondary-drainage reduction exponent [α] is essential. Also, if the Sgt is higher than zero, then accounting for cyclic hysteresis is essential. In another form, if Sgt > 0.001, then Land's gas-trapping parameter [C] is essential. In any of these cases, the gas model in the WAG-HYST must be activated. The logical process to do so is illustrated in Figure 6-2:

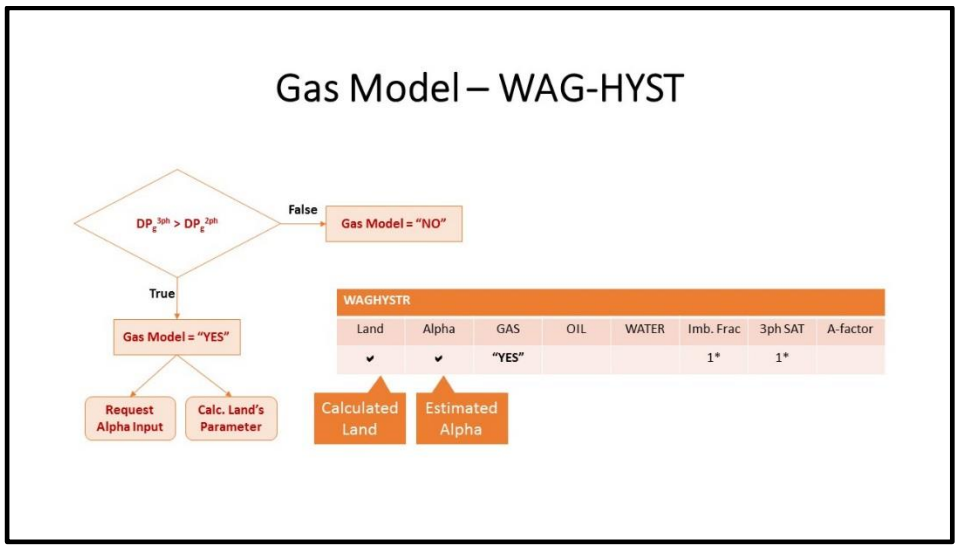

Figure 6-2: The logical process to activate the gas model in the WAG-HYST model

6.2.4.3 Oil Model

If the minimum residual oil saturation after a three-phase WAG injection is less than that after a two-phase injection, then cyclic hysteresis is essential. In another form, if Som < Sorm, then the residual oil modification factor [a] is essential.

- In this case, the oil model in the WAG-HYST must be activated.
- The STONE 1 three-phase oil-relative permeability model must be used.
- The STONE 1 Exponent model can be used to adjust the way the STONE 1 model predicts the three-phase oil relative permeability (section 2.1.5).

The logical process to activate the oil model is illustrated in Figure 6-3:

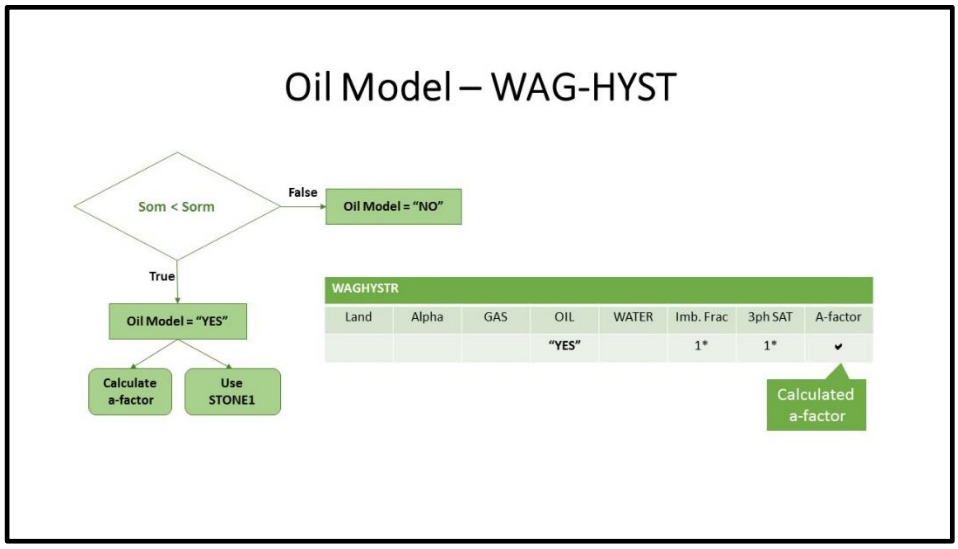

Figure 6-3: The logical process to activate the oil model in the WAG-HYST model

6.2.5 Calculated Data

By using the information collected from the basic input data and the logical operations, several calculations can be performed. The calculated data are below.

6.2.5.1 Land's Gas-Trapping Parameter [C]

As established previously, gas-trapping behaviour is different from the three-phase water primary imbibition and secondary imbibition. Therefore, Land's gas-trapping parameter will be different for each definition below.

1. Land's gas-trapping parameter from three-phase water primary imbibition [C']
   - $C' = \frac{1}{Sgt'} - \frac{1}{Sgm'}$
2. Land's gas-trapping parameter from three-phase water secondary imbibition [C'']
   - $C'' = \frac{1}{Sgt''} - \frac{1}{Sgm''}$

6.2.5.2 Residual Oil Saturation Modification Factor [a]

Since the gas-trapping behaviour is different, then the residual oil modification factor [a] should be different as well. The following calculations are suggested:

1. The residual oil saturation modification factor from three-phase water primary imbibition [a']
   - $a' = \frac{Sorm - Som}{Sgt'}$
2. The residual oil saturation modification factor from three-phase water primary imbibition [a'']
   - $a'' = \frac{Sorm - Som}{Sgt''}$

6.3 Activating the WAG Hysteresis Model

If three-phase cyclic-hysteresis behaviour is observed from the core-flood results, then accounting for a proper hysteresis model is required at any scale. At core scale, the whole core is assumed to be at three-phase zone, and hysteresis is affecting the whole core. However, at reservoir scale, the three-phase zone is only formed in parts of the reservoir. Only within the three-phase zone is cyclic hysteresis behaviour essential. Therefore, in the reservoir-scale simulation, both two-phase and three-phase models should be defined.

The current available WAG-HYST model can be activated in Eclipse by the actions summarised in Table 6-5 (other simulators might have different set-up and keywords):

Table 6-5: Summary of the required keywords to activate WAG-HYSTR model in Eclipse-100

Section	Keyword	Input Specification	Comments
RUNSPEC	SATOPTS	'HYSTER'	To activate hysteresis
	TABDIMS	NTSFUN = 2 or 4	**For simple core-scale:** Table 1: two-phase kr Table 2: three-phase kr **For reservoir-scale:** Table 1: Drainage kr Table 2: Imbibition kr Table 3: two-phase krwo Table 4: three-phase krwo
PROPS	WAGHYSTR	Land's parameter, C	Gas-trapping parameter input
		The secondary drainage reduction factor, α	The exponent to reduce primary drainage gas relative permeability. The default is 0.0
		Gas model flag	YES or NO
		Residual oil flag	YES or NO
		Water model flag	YES or NO
		Imbibition curve linear fraction	The default is 0.1
		Three-phase model threshold saturation	The default is 0.001
		Residual oil modification fraction, a	The default is 1.0
	STONE1		Stone 1 three-phase oil kr.
	STONE1EX	Values 0.01 – 100.0	Refer to section 2.1.5
REGIONS	SATNUM	#grids*1	Drainage kr for (all grids)
	IMBNUM	#grids*2	Imbibition kr (all grids)
	WH2NUM	#grids*3	Two-phase krw (all grids)
	WH3NUM	#grids*4	Three-phase krw (all grids)

6.4 Suggested Methodology to Simulate WAG Injection Process

Two important steps must be done correctly before simulating the WAG injection process. First is to collect the required data for the simulation model (Chapter 3) and, second, to analyse the data and extract the input data for simulating the WAG injection process (section 3.5). If the cyclic-hysteresis behaviour is essential, then the following procedures to simulate the WAG injection process are suggested:

6.4.1 For Oil Reservoirs Started with Waterflooding

1. Set up the simulation to allow for flexible restart (section 4.1.4).
2. Ensure that the number and size of the grids are enough to minimise numerical dispersion (section 4.1.1).
3. Ensure that the time-step length is proper to have a stable numerical simulation (section 4.1.2).
4. Activate WAG hysteresis in the model (section 6.3).
5. Run the simulation model using the first set of hysteresis parameters until the end of **W3,** and then stop the run (**W1-G2-W3**).
6. Use the restart file to run the second part of the process (**G4-W5-G6-W7**...etc.) with the second set of hysteresis parameters.

6.4.2 For Oil Reservoirs Started with Gas Flooding

1. Set up the simulation to allow for flexible restart (section 4.1.4).
2. Ensure that the number and size of the grids are enough to minimise numerical dispersion (section 4.1.1).
3. Ensure that the time-step length is proper to have a stable numerical simulation (section 4.1.2).
4. Activate WAG hysteresis in the model (section 6.3).
5. Run the simulation model using the first set of hysteresis parameters until the end of **G3**, and then stop the run **(G1-W2-G3).**
6. Use the restart file to run the second part of the process **(W4-G5-W6-G7... etc.)** with the second set of hysteresis parameters.

These procedures can be very useful in history matching the observed data from the field as well as predicting the performance of WAG injection.

6.5 Conclusion

This chapter suggested a systematic workflow to acquire the relevant data and analyse it to generate the input data for WAG injection simulation. The first part focussed on the ideal set of experiments to collect enough data to build the simulation model. Then a sequence of actions to analyse the experimental data and extract information on cyclic hysteresis was discussed. Finally, the procedure to simulate the WAG injection process in a reservoir-scale model was introduced.

The recommended two-phase displacement experiments to estimate the required input data to the numerical simulation was suggested in section 3.1. Also, the three-phase WAG injection experiments required to obtain the full range of WAG-HYST parameters were discussed in section 3.4.

The three-phase water imbibition can be either a primary or secondary imbibition. Therefore, the logical operation to record the DP during three-phase water imbibition [DP_w^{3ph}] was specified.

Likewise, the three-phase gas drainage can be either primary or secondary. Therefore, the logical operation to record the DP during three-phase gas drainage [DP_g^{3ph}] was stated as well.

Based on the information collected in this thesis, the amount of trapped gas from three-phase water primary imbibition is different than secondary imbibition. Therefore, some logical operations to record Sgt were suggested.

Land's gas-trapping parameter will be different for each definition. For three-phase water primary imbibition [C'], it should be calculated as:

- $C' = \frac{1}{Sgt'} - \frac{1}{Sgm'}$

However, for three-phase water secondary imbibition [C''], it should be calculated as:

- $C'' = \frac{1}{Sgt''} - \frac{1}{Sgm''}$

Since the gas-trapping behaviour is different, then the residual oil modification factor [a] should be different as well. For three-phase water primary imbibition [a'], it should be calculated as:

- $a' = \frac{Sorm - Som}{Sgt'}$

For three-phase water secondary imbibition [a''], it should be calculated as:

- $a'' = \frac{Sorm - Som}{Sgt''}$

The logical process of the WAG-HYST model is illustrated in the following figure:

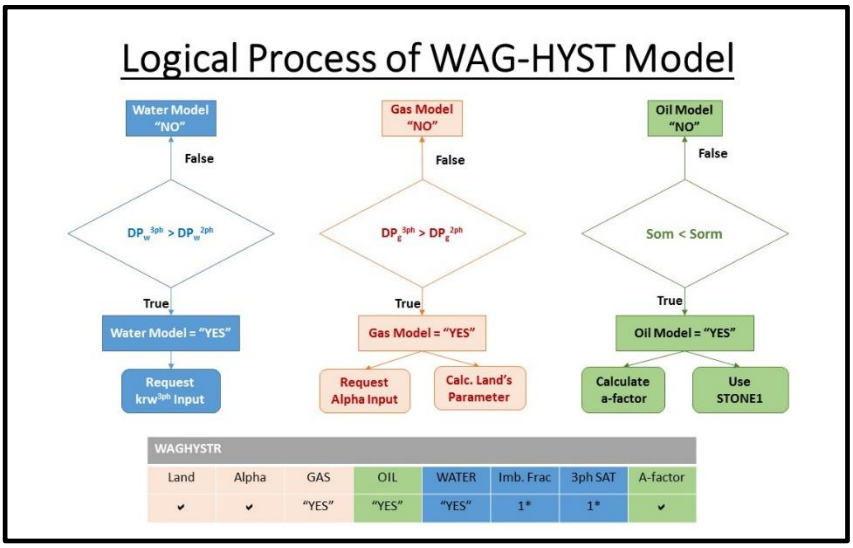

Figure 6-4: The logical process of the WAG-HYST model

With this guideline, the simulation outcome of WAG injection projects can be improved. This systematic workflow provided a step-by-step guide to collect the relevant data and run a simulation of WAG injection. The next chapter will conclude this thesis and highlight some recommendations and future work.

Chapter 7—Conclusions and Recommendations

Water-Alternating-Gas (WAG) injection is a promising EOR technique to unlock some of the remaining oil in the partially depleted reservoirs. WAG injection is a proven technology, which was applied in several oil fields; yet, it is complex and expensive calling for careful planning and efficient development. Currently, numerical reservoir simulation is the most applicable tool to guide reservoir engineers and managers to determine the optimum means for maximising oil recovery. Having three different phases flowing in the reservoir at the same time complicates the physics of oil recovery. The current capabilities of reservoir simulators are not sufficient, unless modified, to model the key mechanisms of oil recovery by WAG [21, 25-27].

Any WAG injection project needs extensive reservoir simulation studies to optimize the field development plan and predict reservoir performance. Therefore, accurate numerical simulation is needed to guide future field implementations of WAG-EOR. This thesis provides a guideline for a more reliable WAG injection simulation. The guideline was defined by reviewing the historical evolution of the published literature about the three-phase relative permeability and hysteresis models and simulating several WAG injection experiments. Each chapter in this thesis has discussed part of the guideline. The conclusions and recommendations of each chapter are discussed in the next sections:

7.1 Conclusions

7.1.1 Conclusions of the Required Data for WAG Injection [Chapter 3]:

As petroleum reservoirs are located hundreds of meters underground, there are limitations of the information to be collected from these reservoirs. Some information can be obtained by logging multiple sections of the reservoir, flowing some wells and recording pressure responses, or collecting core samples to perform various laboratory experiments. Most of the data collected by these methods need to be processed and analysed before making complete sense.

In this chapter, the process of obtaining, processing and analysing rock-fluid properties such as relative permeability (kr), capillary pressure (Pc), and cyclic-hysteresis [WAG-HYST] parameters were discussed. These properties are usually estimated from core-scale data with the help of numerical simulation.

Since hydrocarbon's recovery is greatly controlled by both kr and Pc, their accuracy is crucial in any multi-phase flow simulation. Two-phase kr and Pc are often numerically estimated from history-matching Steady-State (SS) or Unsteady-State (USS) coreflood experiments. As shown in Chapter 3, providing capillary pressure (experimentally obtained) is essential in estimating relative permeability for the same rock system. Failing to use the proper flow functions could lead to inaccurate results at two-phase and three-phase flow simulation.

WAG injection is a three-phase process; therefore, the appropriate choice of the three-phase relative permeability and cyclic-hysteresis models are essential to accurately predict WAG injection performance at any scale. Currently, the oil and gas industry are accepting the use of core-scale experimental data to decide the proper three-phase model and hysteresis parameters. In this chapter, the suggested experiments to collect enough data for WAG injection were suggested. Also, the procedure to obtain WAG-HYST parameters were discussed. However, the demonstration of the process of obtaining such parameters from the experimental data will be discussed in more details in Chapter 4.

The WAG injection experiments used in this thesis were introduced in section 3.6. A series of USS WAG injection experiments performed at water-wet and mixed-wet conditions were used in this study. All experiments were conducted at near miscible conditions with low gas/oil interfacial tension (IFT) of 0.04 mN/m. The analysis and the WAG-HYST parameters for these experiments were discussed in Chapter 4.

7.1.2 Conclusions of the Core-Scale WAG Injection Simulation [Chapter 4]:

The process of obtaining the WAG-HYST parameters from the various WAG injection experiments [chapter 3] was discussed in this chapter. As widely published in the literature, there is usually a mismatch between WAG injection experimental data and the simulation results. The reason for the mismatch suggested in this chapter is that the WAG-HYST model suggested by Larsen and Skauge is based on limited cycles WAG (G-W-G and W-G-W). Therefore, the current WAG-HYST model needs to be extended to match further WAG cycles.

As discussed in section 3.5.1, Land's gas-trapping parameter [C] could be different for each hysteresis cycle. This observation became obvious as more WAG cycles are

implemented beyond a single hysteresis loop. The variable gas-trapping behaviour has been confirmed by several authors since 2003 [47]. Therefore, a new approach to manipulate the simulation and update WAG-HYST parameters were suggested [section 4.2]. The suggested procedure to update gas trapping parameter in the simulation is:

1) Set up the simulation model in a way to allow flexible restart after each hysteresis cycle.
2) Ensure that the number of grids used in the model is sufficient to minimize numerical dispersion (100 grids was enough for this study).
3) Activate Hysteresis option and use proper three-phase relative permeability model then run first hysteresis cycle (W1-G2-W3 or G1-W2-G3) and stop the run to write a restart file.
4) When a reasonable match is achieved from the first run, use the restart file to run the second part of the experiment (G4-W5-G6 or W4-G5-W6) with a new calculated gas trapping parameter [C].

The results obtained from the simulation of the five different WAG injection experiments discussed in this chapter confirmed that updating the gas-trapping parameter significantly improves the ability of the simulation to match WAG experimental results. As the Land's gas-trapping parameter changes, the other parameters might need to be adjusted as well. For example, in some cases, the STONE1EX parameter must be adjusted as oil saturation goes from higher to lower values, and as a result, the gas secondary drainage reduction exponent [α] must be modified. Table 4-8 summarises the obtained hysteresis parameters for all five experiments:

Table 7-1: summary of the obtained WAG-HYST parameters from the five experiments

Experiment	Injection Modes	STONE1 Exponent (η)	Land's Parameter (C)	Reduction Exponent (α)
65mD, Water-Wet, WAG	W1-G2-W3	6.5	2.00	0.45
	G4-W5-G6	0.9	0.81	1.20
65mD, Mixed-Wet, WAG	W1-G2-W3	1.50	8.9	0.08
	G4-W5-G6	0.90	5.9	0.08
65mD, Water-Wet, GAW	G1-W2-G3	8.5	18.1	0.85
	W4-G5-W6-G7-W8	6.5	5.3	0.85
40mD, Mixed-Wet, WAG	W1-G2-W3	3.0	3.5	2.0
	G4-W5-G6	3.0	3.1	1.8
40mD, Mixed-Wet, GAW	G1-W2-G3	0.7	38.8	2.10
	W4-G5-W6-G7	0.1	4.4	2.25

In almost all experiments, except the 40mD, Water-Wet, WAG experiment, η had to be adjusted to match the oil recovery. Further investigation is still needed to understand the relationship between oil saturation and the need to adjust η; however, these results highlighted the role of η in WAG injection simulation.

The calculated C for the first run had to be reduced for the second run in all simulated experiments. However, the amount of reduction in the GAW experiments is more significant than the WAG experiments. The reason for such difference is due to the different trapping behaviour between W2 and W3 (section 3.5.1).

The estimated α for the first run and the second run is almost the same for most cases except the 65mD, Water-Wet, WAG experiment. Further investigation is still needed to understand the behaviour of this exponent during cyclic hysteresis. However, the exponent α can be used to improve the match of DP_g^{3ph}.

7.1.3 Conclusions of the Reservoir-Scale WAG Injection Simulation [Chapter 5]:

Most oil reservoirs would need EOR at some point after waterflooding injection is one of the proven methods for this. However, WAG injection simulation is more complex and must be done properly to plan and predict WAG injection performance. Reservoir heterogeneity and anisotropy, as well as the gravity effect, make the simulation of WAG injection at reservoir scale more challenging. Capturing all the variation in geology and the hysteresis behaviour for each rock type in a very fine grid model would require huge computational power and long run time.

Multiphase flow in reservoir simulation is represented by flow functions (kr and Pc). Also, the current three-phase models use the input two-phase flow functions to empirically calculate three-phase kr and Pc. Therefore, kr and Pc should influence the performance of WAG injection. In this chapter, the effect of these two functions was evaluated by a two-dimensional cross-section simulation model with homogenous properties. Three scenarios were tested at this reservoir scale, and the conclusions are as follow:

- In the model where the input kr and Pc were properly estimated (section 3.2.3), the oil production plateau length was 3,360 days with a recovery factor of 51 per cent at 5,400 days.
- In the model where the input kr was estimated by ignoring Pc (section 3.2.2), the oil production plateau length was 2,950 days with a recovery factor of 48 per cent at 5,400 days.
- Ignoring Pc would result in unphysical behaviour of the waterflood front, which could underestimate oil recovery by waterflooding.
- Misrepresenting the flow function at reservoir-scale simulation could lead to significant differences in oil recovery and oil production plateau length.

Since WAG injection involves the injection of gas into the reservoir, the vertical permeability is expected to be of high importance. The common understanding in the industry is that vertical permeability is usually lower than horizontal permeability. Also, the rule of thumb that most engineers would use is that vertical permeability is almost 10 per cent of horizontal permeability. However, this is far from accurate in most cases, especially with fine-grid models. Therefore, in this chapter, a sensitivity study was conducted to understand the role of vertical permeability in WAG injection performance compared to waterflooding, and a quarter five-spot pattern with the reasonable resolution was utilised to understand the effect of vertical permeability on WAG injection

performance. When refining the grid cells for simulating the WAG injection process, the vertical permeability assigned to the cells were often kept the same as the coarser model. It was demonstrated in this study that for WAG injection, the kv/kh ratio plays a more significant role in the prediction of oil recovery compared to the waterflood. The results from this sensitivity study showed that the predicted oil recovery factor can vary by 7 per cent due to the vertical-to-horizontal permeability ratio (kv/kh) alone.

Moreover, various rock types can exist in a small volume of reservoir rock. Therefore, when gridding the rock section to make a numerical simulation model, often more than one rock type must be represented in each grid cell. Geologists usually work on averaging static properties and distributing them along the geological model grids. However, for the dynamic simulation model, sometimes only one average set of relative permeability could be used due to the lack of such data in most reservoirs, which could have a severe effect on WAG injection performance, as shown in this chapter.

The cyclic injection of water and gas into an oil reservoir would cause three-phase relative permeability hysteresis, which, however, is often ignored or misrepresented in reservoir-scale simulation studies of WAG injection. Thus, in this chapter, the effect of cyclic hysteresis on WAG injection performance was studied, and the results showed that not accounting for this factor would cause inaccurate predictions of:

- first three-phase oil bank arrival time
- the average oil production rate after WAG injection
- the total additional oil recovery by WAG injection
- the breakthrough time and the cumulative production of the gas phase

Therefore, it is vital to account for cyclic hysteresis in reservoir-scale simulations, and chapter 6 discusses some tips on how to best do so.

7.1.4 Conclusions of the WAG Injection Simulation – Best Practices [Chapter 6]:

This chapter suggested a systematic workflow to acquire the relevant data and analyse it to generate the input data for WAG injection simulation. The first part focussed on the ideal set of experiments to collect enough data to build the simulation model. Then a sequence of actions to analyse the experimental data and extract information on cyclic

hysteresis was discussed. Finally, the procedure to simulate the WAG injection process in a reservoir-scale model was introduced.

The recommended two-phase displacement experiments to estimate the required input data to the numerical simulation are:

- water-oil imbibition experiment
- gas-oil drainage experiment
- oil-gas imbibition experiment

The following experiments are recommended to obtain the full range of three-phase data to simulate the WAG injection process:

- three-phase water primary imbibition [Sw = Swc] experiment (Table 1)
- three-phase water secondary imbibition [Sw > Swc] experiment (Table 2)
- three-phase gas primary drainage [Sgi = 0] experiment (Table 3)
- three-phase gas secondary drainage [Sgi ≥ Sgt] experiment (Table 4)

The basic data requested at the first step are:

- connate water saturation (Swc)
- residual oil saturation by water (Sorw)
- DP at the end of two-phase water injection (DPw^{2ph})
- critical gas saturation (Sgc)
- residual oil saturation by gas (Sorg)
- DP at the end of two-phase gas injection (DPg^{2ph})
- two-phase water-oil imbibition and gas-oil drainage relative permeability [krw (Sw), krow (Sw); krg (Sg), krog (Sg)]

The three-phase water imbibition can be either a primary or secondary imbibition. Therefore, the logical operation to record the DP during three-phase water imbibition [DP_w^{3ph}] is:

- DP_{W2}^{3ph} = maximum (DP; Table1 [column 6])
- DP_{W4}^{3ph} = maximum (DP; Table2 [column 6])
- **DP_W^{3ph} = maximum (DP_{W2}^{3ph}, DP_{W4}^{3ph})**

Likewise, the three-phase gas drainage can be either primary or secondary. Therefore, the logical operation to record the DP during three-phase gas drainage [DP_g^{3ph}] is:

- DP_{G2}^{3ph} = maximum (DP; Table3 [column 6])
- DP_{G4}^{3ph} = maximum (DP; Table4 [column 6])
- **DP_g^{3ph} = maximum (DP_{G2}^{3ph}, DP_{G4}^{3ph})**

Based on the information collected in this thesis, the amount of trapped gas from three-phase water primary imbibition is different than secondary imbibition. Therefore, the following logical operations to record Sgt are suggested:

- Sgt' (W2) = minimum (Sg; Table 1 [column 4])
- Sgm' (W2) = maximum (Sg; Table 1 [column 4]
- Sgt'' (W4) = minimum (Sg; Table 2 [column 4])
- Sgm'' (W4) = maximum (Sg; Table 2 [column 4]

Land's gas-trapping parameter will be different for each definition. For three-phase water primary imbibition [C'], it should be calculated as:

- $C' = \frac{1}{Sgt'} - \frac{1}{Sgm'}$

However, for three-phase water secondary imbibition [C''], it should be calculated as:

- $C'' = \frac{1}{Sgt''} - \frac{1}{Sgm''}$

Since the gas-trapping behaviour is different, then the residual oil modification factor [a] should be different as well. For three-phase water primary imbibition [a'], it should be calculated as:

- $a' = \frac{Sorm - Som}{Sgt'}$

For three-phase water secondary imbibition [a''], it should be calculated as:

- $a'' = \frac{Sorm - Som}{Sgt''}$

The logical process of the WAG-HYST model is illustrated in Figure 6-4. This guideline should help the industry to unify the approach to evaluating WAG injection projects and improve the outcome from such a technique.

7.2 Recommendations for Future Work

1. This research focused on the near-miscible WAG injection with the assumption that the hysteresis behaviour would be similar for the immiscible and fully

miscible cases. More investigation is recommended to ensure that the suggested methodology can improve the simulation accuracy for iWAG and mWAG injection processes.

2. The methodology suggested in this research could be converted into an advanced formulation within the simulator to avoid the restart process. The advanced formulation would automatically detect the primary and secondary three-phase cycles and update the WAG-HYST parameters accordingly.
3. The reservoir-scale simulation in this thesis was based on theoretical understanding. It is recommended to check the findings discussed in Chapter 5 with actual reservoir-scale WAG injection data.
4. The simulation work discussed in this thesis used ECLIPSE-100 black-oil models. It is recommended to test the suggested methodology using different black-oil simulators as well as compositional simulators (if required).

References:

1. Outlook, B.E., *Edition, Outlook to 2035*. 2016.
2. Labastie, A., *En Route: Increasing Recovery Factors: A Necessity.* Journal of Petroleum Technology, 2011. **63**(08): p. 12-13.
3. Christensen, J.R., E.H. Stenby, and A. Skauge, *Review of WAG Field Experience*, in *International Petroleum Conference and Exhibition of Mexico*. 1998, Society of Petroleum Engineers: Villahermosa, Mexico. p. 14.
4. Meyer, J.P., *Summary of carbon dioxide enhanced oil recovery (CO2EOR) injection well technology.* American Petroleum Institute, Washington, DC, 2007.
5. Sohrabi, M., D. Tehrani, and M. Al-Abri. *Performance of near-miscible gas and swag injection in a mixed-wet core*. in *International Symposium of the Society of Core Analysts*. 2007.
6. Sohrabi, M. and S.M. Fatemi. *Experimental investigation of oil recovery by different injection scenarios under low oil/gas IFT and mixed-wet condition: Water-flood, gas injection, WAG and SWAG injection*. in *Abu Dhabi International Petroleum Conference and Exhibition*. 2012. Society of Petroleum Engineers.
7. Fatemi, M., O. Shahrokhi, M. Sohrabi, R. Vieira, and K. Ahmed. *Experimental Investigation of Oil Recovery from Carbonate Reservoir Rocks Under Oil-Wet Condition: Waterflood, Gas Injection, SWAG and WAG Injections*. in *Abu Dhabi International Petroleum Exhibition and Conference*. 2015. Society of Petroleum Engineers.
8. Alzayer, H., A. Jahanbakhsh, and M. Sohrabi. *New Methodology for Numerical Simulation of Water-Alternating-Gas (WAG) Injection*. in *IOR 2017-19th European Symposium on Improved Oil Recovery*. 2017.
9. Alzayer, H. and M. Sohrabi. *Water-Alternating-Gas Injection Simulation-Best Practices*. in *SPE EOR Conference at Oil and Gas West Asia*. 2018. Society of Petroleum Engineers.
10. Alkhazmi, B., S.A. Farzaneh, M. Sohrabi, and A. Sisson. *An Experimental Investigation of WAG Injection Performance under Near-Miscible Conditions in Carbonate Rock and Comparison with Sandstone*. in *SPE Western Regional Meeting*. 2018. Society of Petroleum Engineers.
11. Skauge, A. and K. Sorbie, *Status of Fluid Flow Mechanisms for Miscible and Immiscible WAG*, in *SPE EOR Conference at Oil and Gas West Asia*. 2014, Society of Petroleum Engineers: Muscat, Oman. p. 15.
12. Sohrabi, M., A. Danesh, and D.H. Tehrani, *Oil Recovery by Near-Miscible SWAG Injection*, in *SPE Europec/EAGE Annual Conference*. 2005, Society of Petroleum Engineers: Madrid, Spain. p. 12.
13. Sohrabi, M., D.H. Tehrani, A. Danesh, and G.D. Henderson, *Visualization of Oil Recovery by Water-Alternating-Gas Injection Using High-Pressure Micromodels.* SPE Journal, 2004. **9**(03): p. 290-301.
14. van Dijke, M.I.J., M. Lorentzen, M. Sohrabi, and K.S. Sorbie, *Pore-Scale Simulation of WAG Floods in Mixed-wet Micromodels*, in *SPE Symposium on Improved Oil Recovery*. 2008, Society of Petroleum Engineers: Tulsa, Oklahoma, USA. p. 14.
15. van Dijke, M.I.J., M. Lorentzen, M. Sohrabi, and K.S. Sorbie, *Pore-Scale Simulation of WAG Floods in Mixed-Wet Micromodels.* SPE Journal, 2010. **15**(01): p. 238-247.
16. Holm, L.W., *Miscibility and Miscible Displacement.* Journal of Petroleum Technology, 1986. **38**(08): p. 817-818.
17. Sohrabi, M., G.D. Henderson, D.H. Tehrani, and A. Danesh, *Visualisation of Oil Recovery by Water Alternating Gas (WAG) Injection Using High Pressure*

Micromodels - Water-Wet System, in *SPE Annual Technical Conference and Exhibition*. 2000, Society of Petroleum Engineers: Dallas, Texas. p. 8.
18. Fatemi, S.M. and M. Sohrabi, *Cyclic Hysteresis of Three-Phase Relative Permeability Applicable to WAG Injection: Water-Wet and Mixed-Wet Systems under Low Gas/Oil IFT*, in *SPE Annual Technical Conference and Exhibition*. 2012, Society of Petroleum Engineers: San Antonio, Texas, USA. p. 21.
19. Alkhazmi, B., S.A. Farzaneh, M. Sohrabi, and J. Buckman, *A Comprehensive and Comparative Experimental Study of the Effect of Wettability on the Performance of Near Miscible WAG Injection in Sandstone Rock*, in *SPE Annual Technical Conference and Exhibition*. 2018, Society of Petroleum Engineers: Dallas, Texas, USA. p. 26.
20. Arogundade, O.A., H.-R. Shahverdi, and M. Sohrabi. *A study of three phase relative permeability and hysteresis in water alternating gas (WAG) injection*. in *SPE Enhanced Oil Recovery Conference*. 2013. Society of Petroleum Engineers.
21. Duchenne, S., R. de Loubens, M. Petitfrere, and T. Joubert, *Modeling and Simultaneous History-Matching of Multiple WAG Coreflood Experiments at Reservoir Conditions*, in *Abu Dhabi International Petroleum Exhibition and Conference*. 2015, Society of Petroleum Engineers: Abu Dhabi, UAE. p. 23.
22. Masalmeh, S.K. and L. Wei, *Impact of Relative Permeability Hysteresis, IFT dependent and Three Phase Models on the Performance of Gas Based EOR Processes*, in *Abu Dhabi International Petroleum Exhibition and Conference*. 2010, Society of Petroleum Engineers: Abu Dhabi, UAE. p. 20.
23. Spiteri, E.J. and R. Juanes, *Impact of relative permeability hysteresis on the numerical simulation of WAG injection.* Journal of Petroleum Science and Engineering, 2006. **50**(2): p. 115-139.
24. Manrique, E.J., C.P. Thomas, R. Ravikiran, M. Izadi Kamouei, M. Lantz, J.L. Romero, and V. Alvarado, *EOR: Current Status and Opportunities*, in *SPE Improved Oil Recovery Symposium*. 2010, Society of Petroleum Engineers: Tulsa, Oklahoma, USA. p. 21.
25. Mahzari, P. and M. Sohrabi, *A Robust Methodology To Simulate Water-Alternating-Gas Experiments at Different Scenarios Under Near-Miscible Conditions.* SPE Journal, 2017. **22**(05): p. 1,506-1,518.
26. Shahrokhi, O., M. Fatemi, M. Sohrabi, S. Ireland, and K. Ahmed, *Assessment of Three Phase Relative Permeability and Hysteresis Models for Simulation of Water-Alternating-Gas (WAG) Injection in Water-wet and Mixed-wet Systems*, in *SPE Improved Oil Recovery Symposium*. 2014, Society of Petroleum Engineers: Tulsa, Oklahoma, USA. p. 20.
27. Shahverdi, H. and M. Sohrabi, *Relative permeability characterization for water-alternating-gas injection in oil reservoirs.* SPE Journal, 2016. **21**(03): p. 799-808.
28. Land, C.S., *Calculation of imbibition relative permeability for two-and three-phase flow from rock properties.* Society of Petroleum Engineers Journal, 1968. **8**(02): p. 149-156.
29. Larsen, J. and A. Skauge, *Methodology for numerical simulation with cycle-dependent relative permeabilities.* SPE Journal, 1998. **3**(02): p. 163-173.
30. Blunt, M.J., *An empirical model for three-phase relative permeability.* Spe Journal, 2000. **5**(04): p. 435-445.
31. Beygi, M.R., M. Delshad, V.S. Pudugramam, G.A. Pope, and M.F. Wheeler, *Novel three-phase compositional relative permeability and three-phase hysteresis models.* SPE Journal, 2015. **20**(01): p. 21-34.
32. Stone, H., *Probability model for estimating three-phase relative permeability.* Journal of Petroleum Technology, 1970. **22**(02): p. 214-218.

33. Stone, H., *Estimation of three-phase relative permeability and residual oil data.* Journal of Canadian Petroleum Technology, 1973. **12**(04).
34. Aziz, K., *settari, A.* Petroleum reservoir simulation, 1979.
35. Dietrich, J.K. and P.L. Bondor. *Three-phase oil relative permeability models*. in *SPE Annual Fall Technical Conference and Exhibition*. 1976. Society of Petroleum Engineers.
36. Fayers, F. and J. Matthews, *Evaluation of normalized Stone's methods for estimating three-phase relative permeabilities.* Society of Petroleum Engineers Journal, 1984. **24**(02): p. 224-232.
37. Killough, J.E., *Reservoir Simulation With History-Dependent Saturation Functions.* Society of Petroleum Engineers Journal, 1976. **16**(01): p. 37-48.
38. Carlson, F.M., *Simulation of Relative Permeability Hysteresis to the Nonwetting Phase*, in *SPE Annual Technical Conference and Exhibition*. 1981, Society of Petroleum Engineers: San Antonio, Texas. p. 9.
39. Baker, L.E., *Three-Phase Relative Permeability Correlations*, in *SPE Enhanced Oil Recovery Symposium*. 1988, Society of Petroleum Engineers: Tulsa, Oklahoma.
40. Hustad, O.S. and T. Holt. *Gravity stable displacement of oil by hydrocarbon gas after waterflooding*. in *SPE/DOE Enhanced Oil Recovery Symposium*. 1992. Society of Petroleum Engineers.
41. Jerauld, G., *General three-phase relative permeability model for Prudhoe Bay.* SPE reservoir Engineering, 1997. **12**(04): p. 255-263.
42. Skauge, A. and J. Alex Larsen, *Three-Phase Relative Permeabilities and Trapped Gas Measurements Related to WAG Processes*. Vol. 9421. 1994.
43. Shahrokhi, O., M. Fatemi, M. Sohrabi, S. Ireland, and K. Ahmed. *Assessment of three phase relative permeability and hysteresis models for simulation of water-alternating-gas (WAG) injection in water-wet and mixed-wet systems*. in *SPE Improved Oil Recovery Symposium*. 2014. Society of Petroleum Engineers.
44. Schlumberger, <*EclipseTechnicalDescription.pdf*>. 2015.
45. Blunt, M.J., *An Empirical Model for Three-Phase Relative Permeability*, in *SPE Annual Technical Conference and Exhibition*. 1999, Society of Petroleum Engineers: Houston, Texas. p. 14.
46. DiCarlo, D.A., S. Akshay, and M. Blunt, *Three-phase relative permeability of water-wet, oil-wet, and mixed-wet sandpacks.* SPE Journal, 2000. **5**(01): p. 82-91.
47. Element, D., J. Masters, N. Sargent, A. Jayasekera, and S. Goodyear. *Assessment of three-phase relative permeability models using laboratory hysteresis data*. in *SPE International Improved Oil Recovery Conference in Asia Pacific*. 2003. Society of Petroleum Engineers.
48. Duchenne, S., R. de Loubens, and T. Joubert. *Extended Three-Phase Relative Permeability Formulation and its Application to the History-Matching of Multiple WAG Corefloods Under Mixed-Wet Conditions*. in *Abu Dhabi International Petroleum Exhibition & Conference*. 2016. Society of Petroleum Engineers.
49. Neshat, S.S. and G.A. Pope, *Three-Phase Relative Permeability and Capillary Pressure Models With Hysteresis and Compositional Consistency.* SPE Journal, 2018. **Preprint**(Preprint): p. 15.
50. Spiteri, E.J. and R. Juanes, *Impact of Relative Permeability Hysteresis on the Numerical Simulation of WAG Injection*, in *SPE Annual Technical Conference and Exhibition*. 2004, Society of Petroleum Engineers: Houston, Texas. p. 18.
51. Skauge, A. and E.I. Dale, *Progress in Immiscible WAG Modelling*, in *SPE/EAGE Reservoir Characterization and Simulation Conference*. 2007, Society of Petroleum Engineers: Abu Dhabi, UAE. p. 6.

52. Zuo, L., Y. Chen, Z. Dengen, and J. Kamath, *Three-Phase Relative Permeability Modeling in the Simulation of WAG Injection.* SPE Reservoir Evaluation & Engineering, 2014. **17**(03): p. 326-339.
53. Fatemi, S.M., M. Sohrabi, S. Ireland, and M. Jamiolahmady, *Recovery Mechanisms and Relative Permeability for Oil/Gas System at Near-miscible Conditions: Effects of Immobile Water Saturation, Wettability, Hysteresis and Permeability*, in *SPE Improved Oil Recovery Symposium*. 2012, Society of Petroleum Engineers: Tulsa, Oklahoma, USA. p. 28.
54. Agnia, A., H.A. Algdamsi, and M.I. Al-Mossawy, *Oil -Water Relative Permeability Data for Reservoir Simulation Input, Part-I: Systematic Quality Assessment and Consistency Evaluation*, in *International Petroleum Technology Conference*. 2014, International Petroleum Technology Conference: Kuala Lumpur, Malaysia. p. 33.
55. Helset, H.M., J.E. Nordtvedt, S.M. Skjaeveland, and G.A. Virnovsky, *Three-Phase Relative Permeabilities from Displacement Experiments with Full Account for Capillary Pressure.* SPE Reservoir Evaluation & Engineering, 1998. **1**(02): p. 92-98.
56. Jahanbakhsh, A. and M. Sohrabi, *A New Approach for Simultaneous Estimation of Relative Permeability and Capillary Pressure from Coreflood Experiments*, in *SPE Annual Technical Conference and Exhibition*. 2015, Society of Petroleum Engineers: Houston, Texas, USA. p. 13.
57. Egermann, P., J.-M.N. Lombard, C. Fichen, E. Rosenberg, E. Tachet, and R. Lenormand, *A New Experimental Method To Determine Interval of Confidence for Capillary Pressure and Relative-Permeability Curves*, in *SPE Annual Technical Conference and Exhibition*. 2005, Society of Petroleum Engineers: Dallas, Texas. p. 9.
58. Wang, X. and V. Alvarado, *Effects of Low-Salinity Waterflooding on Capillary Pressure Hysteresis*, in *SPE Improved Oil Recovery Conference*. 2016, Society of Petroleum Engineers: Tulsa, Oklahoma, USA. p. 16.
59. Abdallah, W., J.S. Buckley, A. Carnegie, J. Edwards, B. Herold, E. Fordham, A. Graue, T. Habashy, N. Seleznev, C. Signer, H. Hussain, B. Montaron, and M. Ziauddin, *Fundamentals of Wettability.* Oilfield Review, 2007: p. 44-61.
60. Huang, D.D. and M.M. Honarpour, *Capillary end effects in coreflood calculations.* Journal of Petroleum Science and Engineering, 1998. **19**(1-2): p. 103-117.
61. Chardaire-Riviere, C., G. Chavent, J. Jaffre, J. Liu, and B.J. Bourbiaux, *Simultaneous estimation of relative permeabilities and capillary pressure.* SPE Formation Evaluation, 1992. **7**(04): p. 283-289.
62. Holm, R., R. Kaufmann, E.I. Dale, S. Aanonsen, G.E. Fladmark, M. Espedal, and A. Skauge, *Constructing three-phase capillary pressure functions by parameter matching using a modified ensemble Kalman filter.* Communications in Computational Physics, 2009. **6**(1): p. 24.
63. Ypma, T.J., *Historical development of the Newton–Raphson method.* SIAM review, 1995. **37**(4): p. 531-551.
64. Suzuki, K. and T.A. Hewett, *Sequential Scale-Up of Relative Permeabilities*, in *SPE Asia Pacific Conference on Integrated Modelling for Asset Management*. 2000, Society of Petroleum Engineers: Yokohama, Japan. p. 11.
65. Stone, H.L., *Rigorous Black Oil Pseudo Functions*, in *SPE Symposium on Reservoir Simulation*. 1991, Society of Petroleum Engineers: Anaheim, California. p. 12.

66. Hewett, T.A. and R.A. Archer, *Scale-Averaged Effective Flow Properties for Coarse-Grid Reservoir Simulation*, in *SPE Reservoir Simulation Symposium*. 1997, Society of Petroleum Engineers: Dallas, Texas. p. 9.
67. Kossack, C.A., J.O. Aasen, and S.T. Opdal, *Scaling Up Heterogeneities With Pseudofunctions.* SPE Formation Evaluation, 1990. **5**(03): p. 226-232.
68. Lasseter, T.J., J.R. Waggoner, and L.W. Lake, *Reservoir heterogeneities and their influence on ultimate recovery*, in *Reservoir characterization*. 1986, Elsevier. p. 545-559.